Taylor & Francis
Taylor & Francis Group

Journal of Macromolecular Science, Part A
Pure and Applied Chemistry

ISSN: 1060-1325 (Print) 1520-5738 (Online) Journal homepage: www.tandfonline.com/journals/lmsa20

Catalytic activity of biodegradable polymeric colloidal particles in ground water remediation: recent progress and challenges

Mouli Sarkar, Chandrani Sarkar & Sampa Saha

To cite this article: Mouli Sarkar, Chandrani Sarkar & Sampa Saha (17 Sep 2025): Catalytic activity of biodegradable polymeric colloidal particles in ground water remediation: recent progress and challenges, Journal of Macromolecular Science, Part A, DOI: 10.1080/10601325.2025.2560078

To link to this article: https://doi.org/10.1080/10601325.2025.2560078

JOURNAL OF MACROMOLECULAR SCIENCE, PART A: PURE AND APPLIED CHEMISTRY
https://doi.org/10.1080/10601325.2025.2560078

Taylor & Francis
Taylor & Francis Group

REVIEW ARTICLE

Catalytic activity of biodegradable polymeric colloidal particles in ground water remediation: recent progress and challenges

Mouli Sarkar[a], Chandrani Sarkar[a,b], and Sampa Saha[a]

[a]Department of Materials Science & Engineering, Indian Institute of Technology Delhi, Hauz Khas, New Delhi, India;
[b]Present address: Eledrogen Pvt. Ltd, Naktala, Kolkata, West Bengal, India

ABSTRACT

Applications of colloid science in ground water remediation enable the selective targeting of the contaminants while minimizing the environmental side effects. When the waste reaches the ground water level, the subsurface becomes unreachable for extraction of the contaminants, thereby restricting the efficacy of conventional remediation processes. Particularly hydrophobic contaminants such as non-aqueous phase liquid (NAPLs) accumulate under the subsurface of the aquifer and create a contaminant plume which is very difficult to extract. Pristine nanoparticles show versatile catalytic activities to decontaminate the ground water, but they face difficulty in reaching the targeted zone due to their tendency to form agglomerates, thereby compromising the subsurface mobility. This encourages the study of biodegradable polymeric coating to the active nanoparticles acting as remediation catalyst. Hence, these micro-to-nano-sized polymeric colloid materials are only viable options for the *in-situ* ground water remediation. This particular study reviews the catalytic activity of various metal and carbonaceous nanoparticles for the removal of contaminants, and their biodegradable polymeric coating, which ensures their environmental compatibility, transportability and enhances the efficacy of nanoparticles to remove chlorinated solvents, dyes and heavy metals from contaminated groundwater. Advances in nanotechnology-integrated eco-friendly formulations are explored to address their limitations, emphasizing the need for further research and development to optimize their deployment in diverse environmental settings.

GRAPHICAL ABSTRACT

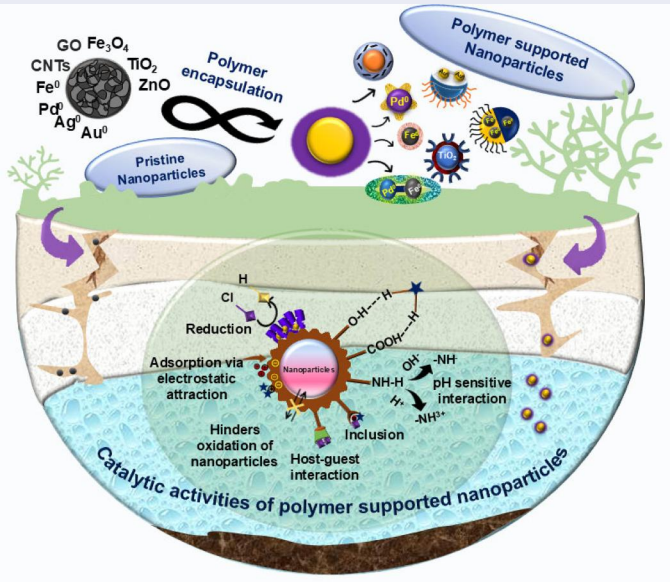

ARTICLE HISTORY
Received July 2025
Accepted September 2025

KEYWORDS
Ground water remediation; colloid particles; metal nanoparticles; catalysis; biodegradable polymer; recyclability

1. Introduction

The primary supply of freshwater usually comes from the ground water, and it also serves as the natural reservoir for the essential resource of drinking water, agriculture, and industrial sectors. According to Water facts (2020 data), 71% portion of the Earth is covered with water; predominantly saline water (96.5%); and the rest 3.5% of water is drinkable. Whereas a major portion of this freshwater

CONTACT Sampa Saha ssaha@mse.iitd.ac.in Department of Materials Science & Engineering, Indian Institute of Technology Delhi, Hauz Khas, New Delhi 110016, India.

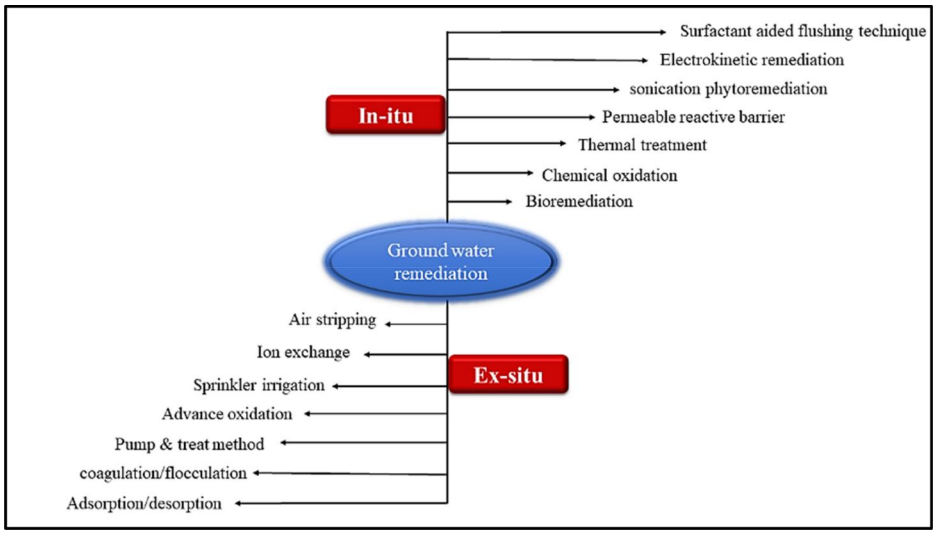

Figure 1. The *in-situ* and *ex-situ* ground water remediation methodologies.

(30.1%) is locked in groundwater.[1,2] Among this available fresh water, 72% of water are used by agriculture, 16% by industries and 12% by municipalities and household purpose (according to water facts 2025).[2] Nowadays, an emerging population started misusing this major resource. Instead of following rules and regulations, industries show negligence for purification of water before discharge to avoid the extra expenditure for the waste removal step. Among various contaminants found in ground water, hydrocarbons, chlorinated contaminants include- perchloroethylene (PCE), tetrachloroethylene (TCE), carbon tetrachloride, cis- and trans-dichloroethylene (DCE), harmful dyes, agricultural wastes, pesticides and moreover heavy metals are the most toxic elements which emerge from textile industries, gasoline fuel stations, underwater storage tanks, pipeline leaks including agricultural runoff flows directly to the ground water and floats onto it.[3–5] This practice causes severe health problems to human and other living being and creates an imbalance toward the aquatic system. Specially, the halogenated hydrocarbons, oils and dyes remain immiscible in water. Due to this immiscibility, these hydrocarbons generate a physical interface with water and remain suspended inside the aquifer which creates organic plume, and these are collectively known as non-aqueous phase liquid (NAPL). These contaminants are known by- light non-aqueous phase liquid (LNAPL) and dense non-aqueous phase liquid (DNAPL). The terms, light and dense signify the relative specific gravity between the hydrocarbons and water. The transport of the non-aqueous fluids from the industries or underground storage tanks through the subsurface of the ground water is a very complex phenomenon. The main challenge of this contamination occurs due to slower movement of the contaminants inside the aquifer. The complex geological structure of subsurface further complicates the remediation process. Hence, the critical water purity level is compromised. Thus, researchers desperately look for systems, which can cover a large hydraulic window for the ground water remediation. Depending on the water remediation and the energy requirement there are two routes, i.e., 1. *Ex-situ* and 2. *In-situ* (Figure 1).

Earlier, due to lack of studies, people used to excavate the soil or pumping out the NAPL pool from the ground water, treat them outside and re-pump again. Besides, air stripping, membrane-based adsorption and ion exchange, and coagulation-flocculation are another ex-situ systems which requires higher energy and cost, maintenance, longer operation time.[6–8] To deal with these disadvantages, scientists developed more sustainable and minimally invasive techniques which mainly focused on thi*n-situ* technologies like permeable reactive barrier, bioremediation, chemical oxidation, chemical flushing, biosorption, enhanced bio restoration for their energy efficient water remediation etc.[9] The bioremediation requires the introduction of a microbial population inside the contaminants which assist the conversion of the pollutant into degraded products but simultaneously enhances the amount of microbes in the water body under anaerobic condition which is envisaged to contaminate the ground water further.[10] Whereas the *in-situ* chemical oxidation (ISCO) is more popular as it can oxidize the organic contaminants in the ground water, but sometimes it fails to reach to the lower impermeable barrier of the aquifer where the contaminant remains at lower temperature (12 °C–15 °C).[11] Another approach is the application of sustained released materials (SRMs).[12] Materials that can be released slowly, reduces large number of vulnerable by-products and thus the synthesis of these materials are gaining top-notch research in the scientific world.

Nanoparticles bearing the properties of sustained release have shown significant results for facilitating catalytic dehalogenation. In this respect, zero valent iron (ZVI), iron oxides (Fe_2O_3/Fe_3O_4), Titanium dioxide (TiO_2), Palladium (Pd), Silver (Ag), and Ceria-Trititanate, nanoparticles were well studied systems, which effectively dechlorinate ground water as discussed below.[12–14] However, challenges such as their stability still remain an issue, which can be partly handled by coating these particles with surface active agents (SAA) i.e. surfactants or inorganic substance or polymers.

A typical SAA wrapped nanoparticles system consists of two major components-

1. A reactive site, which catalytically removes the contaminants from the ground water; and
2. A stabilizing agent having diverse functionalities that can immobilize the reactive centers, adsorb the contaminants and help to stabilize the reactive center for prolonged time.

For a successful stabilizer the materials must have the following characteristics, (i) mobile through sand particles, (ii) cost-effective, (iii) should not produce any vulnerable by-products, (iv) environment friendly, and (v) easily tunable. The surfactants try to minimize the interfacial tension between NAPL/water due to a hydrophilic and a hydrophobic part, which controls a hydrophile-lipophile balance (HLB) when dispersed in oil/water phases. Commonly, surfactants are categorized into cationic (contains quaternary ammonium group),[15] anionic (contains carboxylate groups),[16] nonionic (polypeptide, sugars, and some polymers),[17] gemini (contains more than one hydrophilic or hydrophobic groups),[18] and zwitterionic (contains both the cationic and anionic part).[19] The surfactant enhanced stabilization is a concentration dependent term (requires much higher concentration to create emulsion). This factor provides the particles with extensive stability to the emulsions, as clearly reviewed by Bernard *et al.*[20] However, if we put a general comparison, the synthetic surfactants can be toxic toward the ground water if overdosed; simultaneously, these generate large amount of foam which may further enhance the stabilization of contaminants rather than remediating. Also, surfactants can prevent the nanoparticles' mobility before reaching toward ground water by adsorbing onto soil, thereby reducing the long-term effectiveness of the active agents.[21] In this review, we focused on the comparatively nontoxic, biodegradable, eco-friendly polymers which provide the nanoparticles to produce a stable suspension, improved mobility through subsurface as well as prolonged catalytic activity inside the aquifer. Natural polymers like carboxymethyl cellulose (CMC), starch, lignin, alginate, chitosan, cyclodextrin, and hydroxyapatite (containing -OH, -COOH, -NH_2 groups) get adsorbed onto the nanoparticles and prevent them from aggregation by creating a physical barrier, host-guest interaction or steric factors. Moreover, the charged polymers such as carboxymethyl cellulose (CMC), chitosan, alginate carry charge and stabilize the nanoparticles from getting agglomerated *via* electrostatic repulsion. Whereas, synthetic polymers such as polyvinylpyrrolidone (PVP), polyethylene glycol (PEG), polyethyleneglycol diacrylate (PEGDA), polyacrylic acid (PAA), polylactic acid (PLA), poly (hexamethylene 2,3-O-isopropylidenetartarate) (PE), poly(2-acrylamido-2-methylpropanesulfonic acid) (PAMPS), and block copolymers like Carboxymethyl-β-cyclodextrin (CM-β-CD) offers better chelation, amphiphilicity, serves as a protective layer around the nanoparticles, thereby providing sustained transportability of the system toward the targeted application inside ground water. The role of different polymers in encapsulating the nanoparticles is discussed in Table 3 in detail. Another advantage of using such polymers is their tunable surface properties. Depending on the application, surface of such polymers can be easily modified *via* functionalizable groups (-OH, -COOH, -NH_2 etc.). Moreover, after application, these systems do not leave harmful residues, thus creating a sustainable way of water remediation. Hence, colloidal transport becomes a topic of interest nowadays for the application of *in-situ* ground water remediation as the polymer stabilized particles have the less tendency to agglomerate due to Brownian motion. Typically, the size of the colloid particles ranges between 1 nm to 1000 nm. Colloids are often expanded into a wide range of particles owing to their size (nano to micro range), shapes, compositional anisotropy and properties.[47–51] These polymer-coated nanoparticles are termed as colloidal particles.[52–56] The morphology of the polymeric colloidal particles can be engineered in such a way so that the particles with a unique chemical and physical property may achieve specific targeted applications.[57,58]

This review summarizes the catalytic activities of various nanoparticles for remediating groundwater and simultaneously discussed the advance techniques for the synthesis of the polymeric colloidal particles with various shapes as well as various compositions to create effective colloid facilitating their transport through the subsurface for the remediation of the ground water contaminants. This review as well provides a scope to discuss about the mechanistic insights of the polymeric colloidal particles in hydrogeological conditions, the interaction parameters with the sand particles, and environmental impact after remediation. In addition, this study motivates to review about the recent progresses in the designing of surface-functionalized nano-engineered polymeric colloidal particles and their near-future developments toward the real-world problem.

2. Catalytic activity of nanoparticles in ground water remediation

Nanoparticles are the most powerful agents which provide promising results when applied in the field of water remediation. Due to its high surface area to volume ratio, high reactivity and ease of removal, injection of SRMs is gaining popularity in research field. Specifically, if we consider the ground water remediation applications, the nanomaterial must be sustainable, cost-effective, and recyclable as well as stable inside the adverse geological condition beneath the subsurface. This section mainly focuses on the catalytic activity of nanoparticles which directly relates with metallic nanoparticles and carbonaceous nanoparticles.

2.1. Metallic nanoparticles (MNPs)

Nowadays, MNPs are most studied system among researchers for its remarkable catalytic effect. MNPs use their redox capability to enable the unreachable contaminants' degradation inside the aquifer. Moreover, the surface of the MNPs is easily tunable which further enhances the properties for

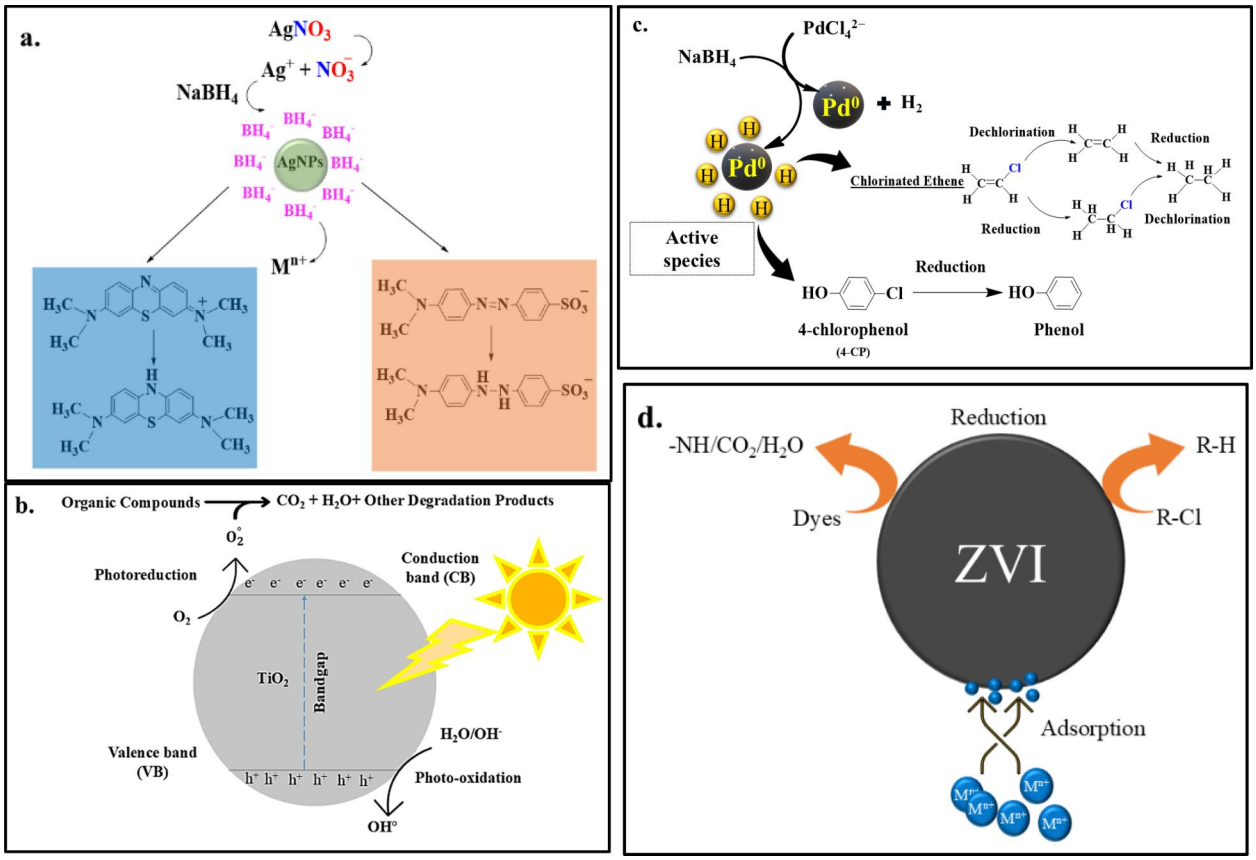

Figure 2. (a) Mechanism for the synthesis of Ag nanoparticles and simultaneous adsorption of metal ions and reduction of methylene blue (blue) and methyl orange (Orange). (b) Mechanism of photocatalytic degradation of TiO_2 (Inspired from Ref. [62]). (c) Mechanism of catalytic reactions of Pd. (d) Reduction and adsorption of ZVI.

the effective dechlorination, heavy metals, and textile effluent or pharmaceuticals' removal from the ground water. While some scientists utilized single metal as the reducing agent, others incorporated dual metal system for enhancing the reducing capability of the first one. Depending on the MNPs' catalytic activity, MNPs are classified in two categories- mono-metallic and bi-metallic nanoparticles.

2.1.1. Mono-metallic nanoparticles (MMNPS)

MMNPs exhibit exclusive catalytic effects for the *in-situ* ground water remediation. Fe, Ag, Pd are the most studied monometallic moieties which show redox reactivity or adsorption capability toward contaminants' degradation. These nanoparticles are generally synthesized *via* top down or bottom up method or greener method.[59] For instance, Ag nanoparticles (AgNPs) showed excellent catalytic effect for the removal of Co^{2+}, Pb^{2+} and methylene blue.[60,61] Due to its cost effectiveness, biocompatibility, thermal conductivity and antimicrobial nature, higher catalytic activity, and stability, AgNPs are profoundly utilized for ground water remediation.[52] The basic catalytic mechanism of Ag follows adsorption followed by electron transfer to the metal or dye molecules, hence degradation happens quickly. It was well established that in absence of AgNPs, the electron donating ability of $NaBH_4$ is very slow and it is thermodynamically favored, but in presence of AgNPs, the electron donation becomes kinetically favored and happens quickly. This mechanism is termed as electron relay system which was monitored by spectrophotometrically (Figure 2a).[61]

Another class of effective noble metallic nanoparticle is Palladium nanoparticles (PdNPs) which are well known catalyst used in organic reactions. Scientists used PdNPsfor ground water remediation to dechlorinate the 4-chlorophenol(4-CP)[53] or degradation of phenol red dye.[54] Since Pd has higher affinity toward hydrogen, PdNPs act as active agents that induce faster hydrolysis of $NaBH_4$ and by adsorbing $H_2$to form an activated (Pd-H) species which is active intermediate during dechlorination process.[55] This study demonstrates the contribution of the presence of such nanoreactors enhance the capability of $NaBH_4$ through breaking down of 4-CP into comparatively less hazardous chemical phenol. A plausible mechanism is provided in Figure 2(c) through which the dechlorination or hydrogenation reactions usually occurs.

Similarly, zero valent iron (ZVI) is one such nanoparticles which are widely studied for water remediation. As discussed above, the major components of ground water contaminants include halogenated substances which are difficult to remove by any conventional ways. The chlorinated contaminants (NAPLs) which are mostly recovered by ZVI inside the ground water.[56,63] ZVI shows multifunctionality (adsorption, reduction) routes to decontaminate ground water (Figure 2d). When ZVI come in contact with organic pollutants (such as DNAPL), it immediately degrades the chlorinated hydrocarbons to gaseous hydrocarbons and gets

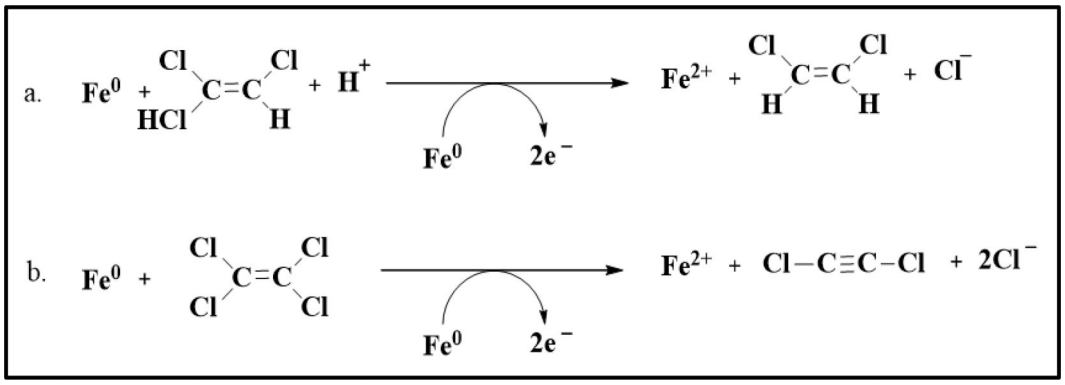

Scheme 1. Path (a) hydrogenolysis; Path (b) reductive β-elimination.

oxidized itself to Fe_2O_3/Fe_3O_4 (component of earth crust)[64] leaving no further residuals in water but can be easily recovered due to their magnetic property.

The dechlorination routes of ZVIs happen *via* two major ways: hydrogenolysis and reductive β-elimination. Basically, in the former process, one chlorine atom is replaced by one hydrogen atom and the latter one grabs two chlorine atoms adjacent to the carbons creating one bond in between them (Scheme 1). One of the advanced oxidation procedures (AOP) enables sulfidated-ZVI where ZVI can activate the persulfate to generate radicals which is able to degrade a common pesticide such as atrazine.[63]

Besides, research showed Pt, Pd, Ni, Cu, and Ag provide further support to the ZVIs to enhance the rate of hydrogenation by formation of bimetallic moieties which will be discussed in next section.

Apart from the ZVI, the ores of iron such as maghemite (?-Fe_2O_3), hematite (α-hematite), and magnetite (Fe_3O_4) nanoparticles also show applicability in the separation of heavy metals based on their magnetic properties. In general, the iron oxide nanoparticles (IONPs) decontaminate the ground water *via* three major routes, adsorption, redox reaction, and magnetic separation.[65–67] IONPs create permeable reactive barrier (PRB) which captures the heavy metals *via* adsorption and simultaneous reduction happens onto their surface. Besides, IONPs can be recovered easily *via* magnetic separation. One such study was reported for the degradation study of TCE by iron oxide in presence of H_2O_2.[68] The ferrous ion [Fe(II)]reacts with H_2O_2 to yield OH. radical under acidic (pH = 3) condition *via* several intermediates. This OH. radical further reacts with organic contaminants like TCE and generates hydrochloric acid, formic acid and carbon dioxide.

Apart from these, Titanium oxide (TiO_2) nanoparticles too show photocatalytic properties that can be exploited for the degradation of contaminants. The absorption of UV light accelerates the electron transfer from valence band (VB) to conduction band (CB) of TiO_2. This conduction creates hole-pairs over the surface of the nanoparticles. The excited electrons then react with oxygen to produce superoxide anions which further bind with H^+ ions to produce $OH^·$ radicals. Also, the holes react with water present in the medium and yield the same hydroxyl radicals. Finally, these hydroxyl radicals are responsible for converting most of the organic dyes present in water to carbon dioxide or water (Figure 2b).[69]

2.1.2. Bi-metallic nanoparticles (BMNPS)

BMNPs are composed of two metals which plays synergistic effect to each other for better performance than MMNPs. Although the above study represents the better catalytic effect of single metal nanoparticles, but sometime single metals are unable to achieve 100% efficiency for the required application due to higher aggregation. The presence of a secondary metal enhances the catalytic ability of the other by providing enhanced stability and reduced aggregation. For example, Fe-Pd moiety undergoes98% dechlorination of 2,4-dichlorophenol(2,4-DCP) and monochloroacetic acid (MCAA) under acidic conditions.[70] The performance of bimetals is similar as that of mono-metals, but the increased reactivity can be attributed to the generation of H_2 *via* corrosion of the ZVI under acidic conditions,[71] and immediate adsorption of H_2 by Pd, which generated Pd-H. This activated H species leading to the dechlorination of 2,4-DCP to 2-chlorophenol(2-CP) and finally phenol.[72] Furthermore, Fe-Pd shows prolonged activity, greater catalytic activity at lower doses within shorter time period and better resistant to surface fouling than ZVI (Scheme 2).

Another similar bimetallic, Cu-Fe nanoparticle was explored for the complete dechlorination of hexachlorobenzene (HCB) to tetra-, tri- and dichlorobenzenes (TeCB, TCB, and DCB) within 48 h. One advantage of using Cu is that it is cheaper than Pd. The key mechanism can be explained by similar approach as Pd-Fe; i.e. the H_2 production *via* ZVI corrosion under acidic condition and simultaneous reduction of HCB by the active hydrogen, which is catalytically generated by Cu. Moreover, the dissolved O_2 and water generate an oxide layer entrapping Cu inside. This creates an additional adsorption site where HCB molecules can easily diffuse inside the oxide film and undergo sequential dechlorination.[73]

Several group of scientists studied another set of silver based BMNPs such as Au-Ag, Ag-Cu, and Ag-Zn, for the catalytic reduction of 4-nitrophenol, photocatalytic degradation of MB, and removal of trihalomethanes, respectively. Au-Ag induce the hydrogenation of 4-nitrophenol by strongly binding with the nitrophenolate. This mechanism follows a pseudo first order kinetics. On the other hand, Ali

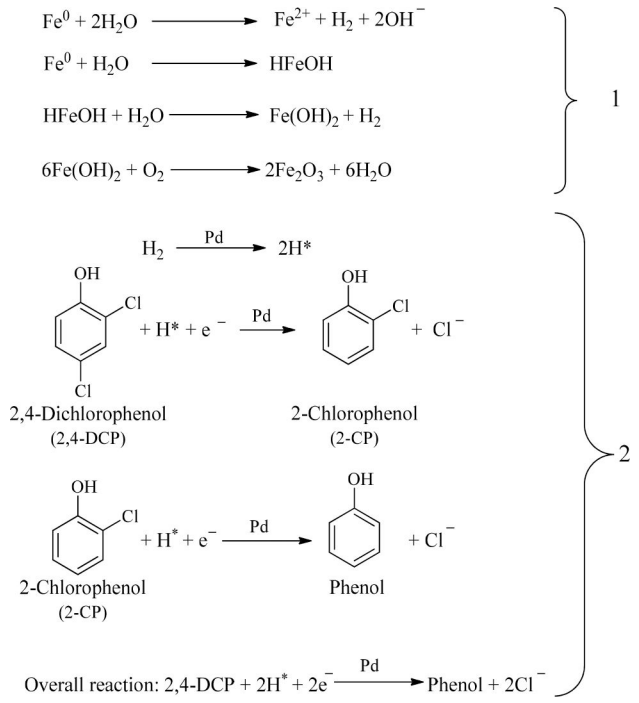

Scheme 2. The corrosion behavior of Fe(0) (stepwise presented by (1) and catalytic degradation of 2,4-DCP (stepwise presented by (2)) (Adapted from Refs. [71,72]).

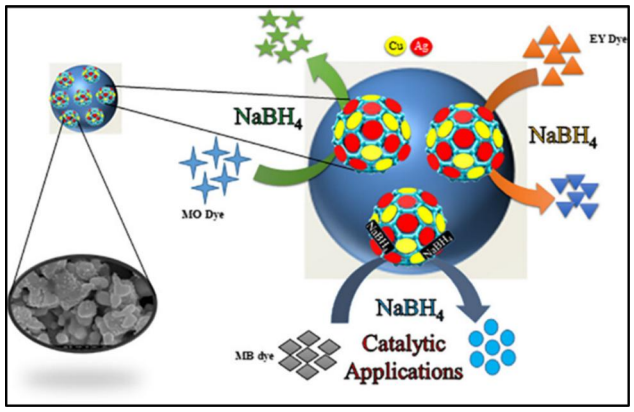

Figure 3. Catalytic degradation of methylene blue (MB), Methyl orange(MO) and Eosin-Y(EY) dye by the synergistic mechanism of Ag-Cu bimetal (Adapted with permission from Ref. [74]).

et al. carried out a study to remove azo dyes (methylene blue (MB), Methyl orange (MO) and Eosin-Y(EY)) *via* Ag-Cu BMNPs. This study highlighted the catalytic activity of Ag-Cu *via* their surface plasmon resonance (SPR) effect in presence of a reductant, i.e., $NaBH_4$ (Figure 3).[74–76]

To investigate about BMNPs, scientists discovered one such lanthanide-based metal nanoparticles which has stronger affinity toward fluoride ions. Also, due to their multivalent states and Lewis acid character, cerium (Ce), lanthanum (La), neodymium (Nd), gadolinium (Gd), and Titanium (Ti) are able to form strong complex with fluorides.[77,78] One such system is porous CeO_2–ZrO_2 nanocages, designed to act as adsorbent. The oxide bed produces hydroxyl groups on the surface of the nanocages upon reacting with water. These hydroxyl groups act as the adsorption sites.[79] The adsorption site is largely dependent on pH of the medium. For instance, at mild acidic conditions (pH < 7.5) surface gets positively charged and attracts the fluoride ions, whereas, above pH 7.5 the surface gets negatively charged which repels the F^- ions. A similar approach was attributed to another system, such as Ceria and Trititanate Nanotubes composite (CTNC). It exhibits a highly effective fluoride adsorption mechanism primarily driven by ion exchange between fluoride ions (F^-) in water and the surface hydroxyl groups (–OH) on CTNC.[80] [≡M–OH+F−→≡M–F + OH−].

2.2. Carbonaceous nanoparticles (CNPS)

Carbon is naturally derived, well abundant material in earth. It was well documented that the micron sized activated carbons are less efficient than nanoscale carbonaceous materials (Figure 4) like- carbon nanotube, graphene and its oxides. Also, activated carbon can facilitate decontamination *via* adsorption only whereas, latter materials adsorb, disinfect and simultaneously generate fewer toxic by-products.[83] The physicochemical properties of CNPs like- higher surface area, greater thermal, electrical and mechanical stability, cost-effectiveness, higher sorption/desorption capability, hydrophobicity, corrosion-resistance, and most importantly easy derivation from fossil fuels make them excellent advance materials for catalytic degradation. Carbon nanotubes (CNT) and graphene oxide (GO) are the various form of CNPs which perform multifaceted approach for ground water remediation *via* adsorption, photocatalytic degradation and catalytic routes. We will discuss the catalytic activity of these advanced CNTs below.

2.2.1. Carbon nanotubes (CNTS)

It is a cylindrical hollow nanostructure comprised of rolled-up hexagonal graphene sheets. This is the one-dimensional allotrope of carbon that has length to diameter ratio of 100000. Depending on the position of graphene sheets, CNTs can be divided into two groups—single-walled CNT (SwCNT) (where folding occurs with a single graphene layer) and multi-walled CNT (MwCNT) (where folding occurs with concentric multiple graphene layers) (Figure 4a). Recent studies confirm that the pristine CNT shows their catalytic ability *via* oxidative dehydrogenation(ODH) (conversion of ethyl benzene to styrene; n-butane to butene to 1,2-butadiene),[84,85] wet air oxidation (WAO) of phenol,[86] cumene to cumene hydroperoxide,[87] and aerobic liquid phase oxidation (ALPO) (ethylbenzene to acetophenone or benzyl alcohol to benzaldehyde).[88,89] The basic catalysis mechanism (Figure 5a,b) of first two steps is similar, i.e. pre oxidation but the second step varies. The ODH majorly targets the pretreatment of CNT surface with oxidants (like HNO_3) which generates active oxygenated species such as electrophilic (superoxide O_2^-, peroxide O_2^{2-}) and nucleophilic oxide (O^{2-}). Among them, the electrophilic oxide species are the secondary intermediates which lead to combustion of the hydrocarbons, whereas the actual intermediate i.e., nucleophilic species (C=O) tries to react with electron deficient saturated molecules (C-H bond of butane) to yield more stable alkenes *via* dehydrogenation

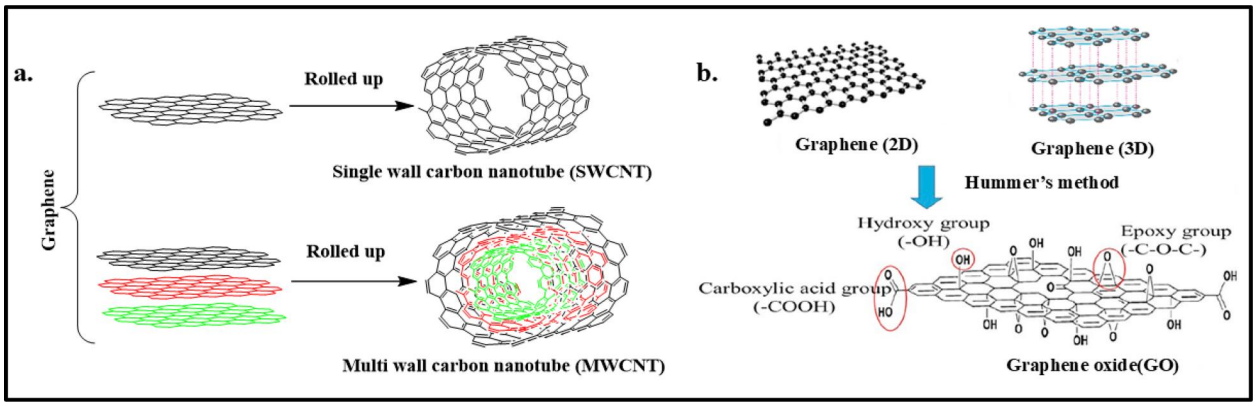

Figure 4. The structure of (a) Carbon Nanotube(CNT) and (b) Graphene oxide (GO) (Redrawn and adapted with permission from Refs. [81,82]).

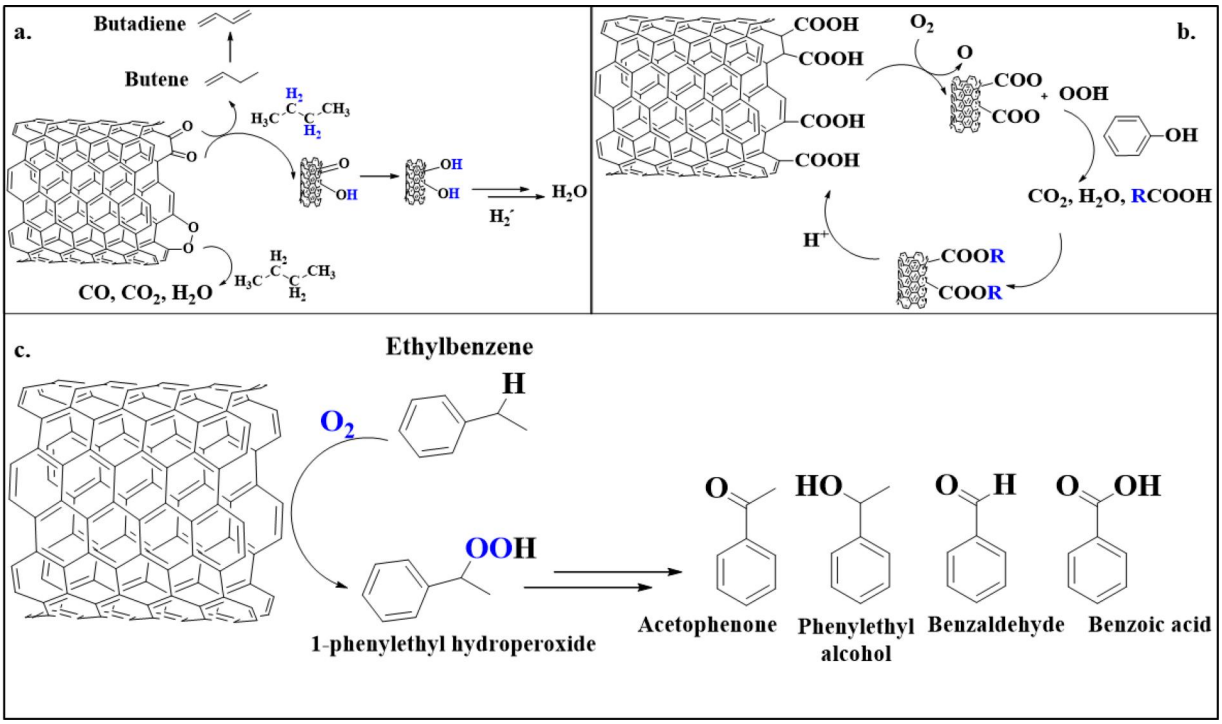

Figure 5. Mechanism of catalytic activity of CNTs *via*- (a) oxidative dehydrogenation (ODH), (b) wet air oxidation(WAO), and (c) aerobic liquid phase oxidation(ALPO) (Inspired & redrawn and from Refs. [85,86,89]).

(Figure 5a). Ultimately, the surrounding H_2 acts as a quencher of the catalytic cycle by forming H_2O. On the other hand, the WAO method facilitates generation of -COOH groups onto the CNT surface followed by reaction with air/oxygen to generate hydroperoxyl radical (-$HOO^{\cdot}$). This highly reactive oxygenated species degrades phenolic compounds to small chain acids (maleic/formic/acetic/oxalic acids-RCOOH) which further react with carboxylic groups to form innocuous by-products like esters. These esters can reform the carboxylic containing NT surface *via* hydrolysis at higher temperature. Unlike the other two mechanisms, the route ALPO proceeds *via* electron transfer between the substrate and CNT layers followed by the generation of active species, i.e., either peroxyl radical or nitric oxide. This method is suitable for degrading the non-polar contaminants like ethylbenzene. Upon immobilization of liquid phase like ethyl benzene, there occurs a strong π-π interaction between CNT layers and phenyl group of ethyl benzene. This follows the formation of highly reactive peroxy phenyl radical which further reacts to yield multiple side products like acetophenone, benzoic acid, phenyl ethyl alcohol, benzaldehyde etc. It has been seen from the study that if in ALPO, the surface of the CNT is pretreated (by introducing hydrophilic groups) like the previous methods, the outcome is negative, majorly due to hydrophilic-hydrophobic interaction between CNT surface and ethylbenzene. Hence, direct immobilization and stabilization through aerobic oxidation is the essential criteria for the ALPO method (Figure 5c).

2.2.2. Graphene oxide derivatives (GOS)

Graphene is the 2D allotrope of carbon exhibiting excellent thermal and electrical properties. The pristine graphene itself is hydrophobic in nature, hence, for water remediation, it would not be the ideal candidate due to higher agglomeration rate. Similarly, oxidation of graphene sheets under

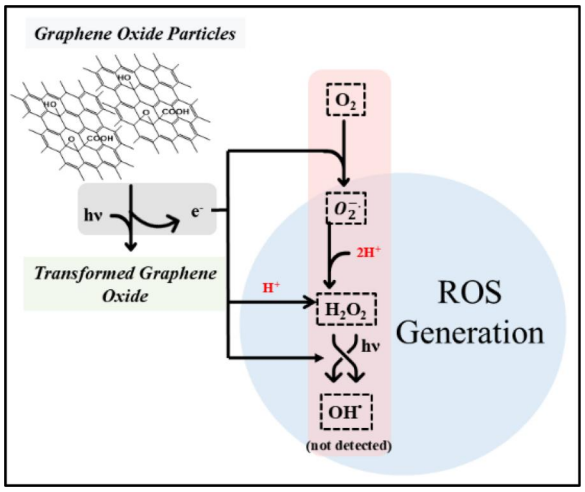

Figure 6. Pathway for production of ROS by GO upon absorbing light (Inspired & redrawn from Ref. [94]).

highly acidic conditions and in presence of strong oxidants, induce hydrophilic OH, C = O or COOH groups, which make the surface of graphene oxide hydrophilic (Figure 4b). These functional groups provide better dispersibility in water and also possess active sites which facilitate adsorption, redox or photocatalytic degradation of heavy metals or dyes. Generally, the mechanism follows *via* adsorption of heavy metals such as Pb(II), Cu(II), Pd(II), and Pt(II).[90–92] The oxygen moieties bind with the metal ions *via* coordination or electrostatic interaction and this interaction tends to deform the layer like structure of GO. For instance, immediate stacking and wrinkling happened to the GO sheets upon adsorbing Cu^{2+}. This might be the result of reducing polar groups which engage in coordinating metal ions, thereby reducing the electrostatic repulsion between the polar groups.[93] Another route is the photocatalytic degradation by which GO layers produce reactive oxygen species (ROS) in presence of solar/UV light (Figure 6). However, several literatures provided different notions about the generation of ROS. For example, Matsumoto *et al.* demonstrated the formation of CO_2 *via* degradation of carbon of GO and -COOH groups, when irradiated with light (280 nm).[95] Whereas another group hypothesized the removal of HO· radical and formation of extended conjugated π bonds at the layers.[96] But Zhao *et al.* provided a clear idea about the ROS production, when GO is irradiated with light and yield highly reactive O_2^- which simultaneously disproportionate into H_2O_2.[94] The H_2O_2 upon extracting another electron from GO, generate HO· radical. This ROS is effective to interact with several contaminants present in water.

Below we summarize the Table 1 where the contaminants' removal capacity of different metals is discussed, though these nanoparticles still suffer from few limitations/challenges for their applicability ed in ground water remediation.

3. Limitations of metallic/carbonaceous nanoparticles in ground water remediation

Nanoparticles can be easily delivered to the impermeable zone as well as effectively interact with large number of contaminants inside the ground water. But the major issue with the nanoparticles is their high aggregation rate. The nanoparticles with higher surface area to volume ratio always try to minimize the surface chemical potential with rapid aggregation. More the aggregation, lesser the surface to volume ratio and more will be the size of the aggregated cluster (size can range from micro to millimetre). Under these circumstances, particles remain undelivered to the target site through sand and huge number of free nanoparticles are required to inject inside the aquifer to meet the targeted application inside the aquifer.[107] This further enhances the cost and simultaneously potential toxicity to the aquatic environment. For example, ZVIs are prone to agglomeration due to higher surface area while transportation *via* soil or aquifer. In fact, due to their negative reduction potential, these zero valent nanoparticles get easily oxidized. Moreover, the separation of GO, CNT and other non-magnetic metals from ground water after usage, is challenging. A group of researchers proved the reduction of toxicity happened when Ag nanoparticles are coated with polymers.[108,109] Hence, researchers started finding ways to provide support to the nanoparticles either by inorganic compounds or by using polymeric materials.[110–112] There are multiple literatures reported for the inorganic materials which efficiently support the metal nanoparticles, but these further increases the total metal count and left harmful unreacted inorganic chelates inside the aquifer, thereby further intoxicating the ground water.[113,114] Whereas, among polymers, biodegradable polymers are more preferred as it can circumvent this problem of potential hazard by minimizing direct leaching of free nanoparticles into aqueous environment which ensures a sustainable greener approach, lowers the risk of secondary contamination and controls the injection of free nanoparticles not beyond limit. Also, biodegradable polymers fulfill almost all the criteria for a perfect stabilizing agent as they are less hazardous, environmentally benign and easily tunable.[115] However, this polymer supported metal/carbonaceous nanoparticles may also increase the potential risk factor for leaving the pristine nanoparticles after decomposition of polymers; but there are some scenarios which governs the fate of the nanoparticles. For instance, iron-based nanoparticles are highly investigated active agents which are easily encapsulated inside polymers and post treatment, they can be easily recovered *via* magnetic separation which enhances its reusability, mitigating the secondary pollution. Also, iron nanoparticles can be deposited *via* sedimentation as earth core and hence pose no further risk as ground water contaminants. In case of the non-magnetic nanoparticles, research is still confined in the laboratory and yet to be discoverable in the real-world applications. Colloidal filtration theory (CFT) suggests this occurs because colloidal particles remain stable due to their Brownian motion and the Van der Waals force hindering them to self-aggregate.[116,117] This is why the biodegradable polymer encapsulated nanoparticles act like colloidal particles and provide a sustainable approach for the removal of contaminants. We have discussed the detailed mechanism, synthetic routes and the role of different polymers for

Table 1. Various metallic nanoparticles and their removal capacity.

Metallic nanoparticles	Size	Removal capacity	Method of operation	Refs.
Silver (Ag)	20 nm	24% for cobalt and 77% for lead	Reduction	[60]
Zero valent iron(ZVI)	40-60 nm	Degradation of 87% tetrachloroethylene (PCE), 97% of trichloroethylene (TCE), 94% of *cis*-dichloroethylene (*cis*-DCE), and 99% of *trans*-dichloroethylene (*trans*-DCE)	Reduction	[97,98]
Titanium dioxide(TiO_2)	20 nm	Inhibition of the bacterial growth on activated sludge	Photocatalytic deflocculation	[99,100]
γ-Fe_2O_3	7-12 nm	As(III)- 74.83 mg/g and As(V)- 105.25 mg/g at 50 °C	Adsorption	[101]
Ironoxide (Fe_2O_3/Fe_3O_4)		Fe_2O_3 shows 1250 μg/g for As(III) and 4600 μg/g for As(V) ; Fe_3O_4 shows 8196 μg/g for As(III) and 6711 μg/g for As(V)	Adsorption	[102]
Zinc Oxide(ZnO)	10 nm	156.74 for Cd(II), 194.93 for Pd(II), 67.93 for Co(II), 115.47 for methylene blue, 62.19 for congo red, 14.54 for Pb(II), and 47.5 for Cu(II) (all in mg/g unit)	Adsorption	[103]
Palladium (Pd)	38 nm	Phenol red-dye degradation	Photocatalytic degradation	[54]
Bio-Pd	1. nm2)2-12 nm	1)Methyl orange removal 2)reduction of 200 mg/L Cr(VI)	Reduction	[104]
Graphene oxide (GO)	400 nm–2 μm	46.6 mg/g Cu(II), 842 mg/g Pb(II), 108.3 mg/g Au(III), 106.3 mg/g Cd(II)	Adsorption	[90–92]
Reduced graphene oxide (RGO)	–	158 mg g^{-1} of methylene blue	Adsorption	[105]
Ceria-incorporated trititanate nanotube composite (CTNC)	average length-95 nm, average diameter-9 nm	Fluoride ions adsorption capacity 65.37 mg/g	Adsorption *via* anion exchange	[80]
CeO_2–ZrO_2 nanocages	80-100 nm	Fluoride ions adsorption capacity 111.6 mg/g	Adsorption *via* anion exchange	[79]
Fe-Pd	47 ± 11.5 nm	Dechlorination of monochlorocetic acid	Reduction	[70]
Gold-silver (Au-Ag) alloy	<10 nm	Catalytic degradation of 4-nitrophenol	Reduction	[76]
Copper-Iron(Cu-Fe)	63.6 nm	Dechlorination of hexachlorobenzene (HCB)	Reduction	[73]
Ag-Zn	–	Degradation of trihalomethanes	Reduction	[75]
Ag-Cu	114 nm	95.21% MO, 98.57% MB, and 96.65% Eosin-Y(EY), removal	Adsorption	[74]
Fe-Ni	60-85 nm	Removal of triclosan and Cu(II)	Adsorption followed by reduction of Cu(II) and reductive dichlorination of triclosan	[106]

effective encapsulation of colloidal particles in the subsequent sections.

4. Polymer wrapped metal nanoparticles for ground water remediation

The role of biodegradable polymers for supporting the active agents is very crucial in terms of environmental benignity, long term effectiveness, easy tunability, and better mobility through the subsurface. The polymer wrapped nanoparticles are often termed as colloids. In general, colloids are known as the nano to micrometre sized suspension of solid particles in water or oil medium. Milk, blood, and ink paints are the practical examples of suspensions in water. Inside water, the colloidal surfactants are stabilized by creating emulsion which is also called Pickering emulsion-based system, named after "Pickering" which creates a rigid or semi-rigid barrier around the emulsion droplet and through a steric barrier prevents the particles coalescence. The wettability is highly controlled by the contact angle and most importantly it does not require higher concentration like surfactant to create a robust barrier for the droplets. Also, the colloidal particles are having customizable functional groups over the surface which can provide extensive mechanical stability. The exceptional stability of colloidal suspension in aqueous media is regulated by the surface charges, pH and ionic strength (IS) of the solution. Generally, the organic colloids possess a negative surface charge density due to the presence of -COOH, and -OH groups. The negative charges repel each other, and this electrostatic repulsion helps the colloidal particles for better transportability and suspension stability by preventing unwanted agglomeration.[118] the detailed structure of biodegradable polymers and their mode of action is discussed below (Table 2).

Structural aspect is also a controlling parameter for water remediation applications. The spherical particles contain the least surface energy and easy to synthesize. However, recent studies include various shapes like ellipsoid, rods, disks, worm like, cubic, cylinders, cups etc. other than spheres, that can be designed depending on the nature of the compounds and the synthesis methodology,[128–131] while the compositional anisotropy can be seen in Janus type colloid particles.[132] Besides, researchers from the past two decades have been trying to optimize various shapes of such colloids which ranges from vesicular structures to capsules, mesoporous structures, metal organic framework, liposomes (containing enzymes or virus) etc.[133] (Figure 7). Higher surface area and dense functional groups on the surface aid the particles to adsorb the contaminants like heavy metals, organic dyes, trace elements, NAPL etc. which are abundant in the ground water.[134] Organic contaminants are commonly

Table 2. A generalized polymer toolbox with their functional properties.

Classification	Polymer	Chemical structure	Functional properties	Refs.
Natural polymers	Starch	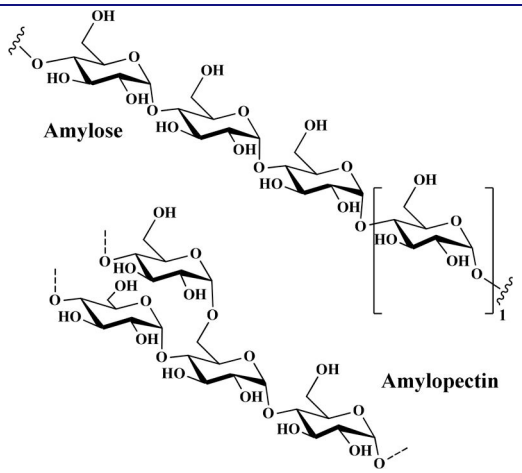	Hydrophilicity, biodegradability, multi-hydroxyl functionality, nontoxic, higher availability, and higher adsorption capability.	[119]
	Carboxy methyl cellulose (CMC)	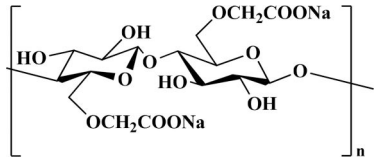	Water solubility, Biodegradability, film-forming ability, nontoxic, adsorption ability.	[120]
	Chitosan	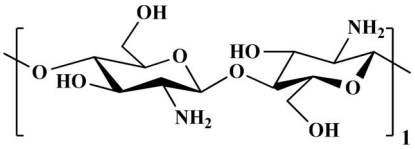	Biodegradability, biocompatibility, nontoxic, antimicrobial property, active functionality (-NH_2 group),	[121]
	Lignin	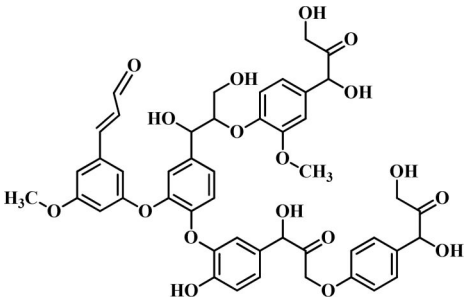	Biodegradability, nontoxic, multi-functionalities (hydroxyl, carbonyl, methoxy, carboxylic) for adsorption and chelation of metal ions, rigidity.	[122]
	Alginate	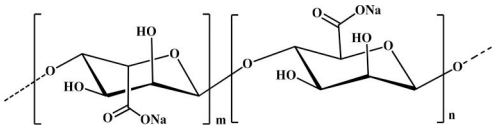	Biocompatibility, biodegradability, higher gelation ability, super hydrophilicity, higher adsorption capability.	[123]
	Cyclodextrin	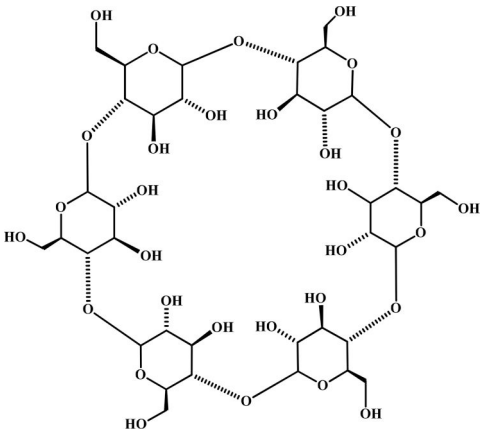	Biodegradability, nontoxic, the hydrophilic exterior and hydrophobic interior, encapsulates metals *via* host-guest inclusion complex formation, stability in harsh conditions (pH ranges from 3–12 and temperature up to 250 ^{0}C)	[124]

(*continued*)

Table 2. Continued.

Classification	Polymer	Chemical structure	Functional properties	Refs.
Synthetic polymers	PLA	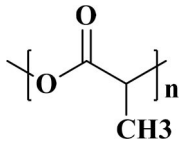	Water insoluble but hydrolyzes in moisture rich conditions, biodegradable, nontoxic, brittle, adsorption capability.	[125]
	Polyethylene glycol (PEG)	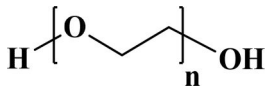	Biodegradability, molecular weight tunability, hydrophilicity, nontoxic.	[36]
	Polyethylene glycol diacrylate (PEGDA)	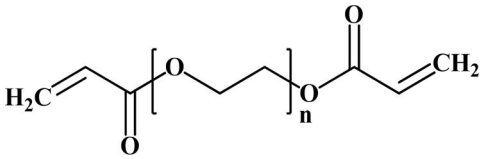	Hydrophilicity, non-biodegradable but environment friendly, higher mechanical rigidity, ability to form 3D network when crosslinked, nontoxic.	[126]
	Polyacrylic acid (PAA)	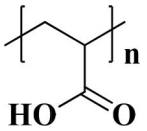	Anionic polymer which has ability to chelate metal ions and selective organic dyes, generate active radical for advanced oxidation processes. Superabsorbent ability.	[28]
	Poly (hexamethylene 2,3-O-isopropylidenetartarate) (PE),	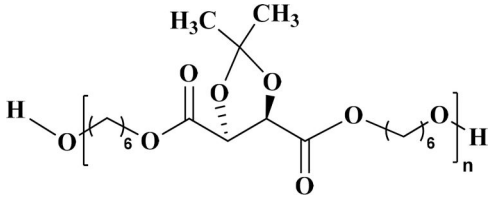	Biodegradable, stimuli-responsive nature; hydrophobic to hydrophilic transformation ability under acidic media or presence of UV. Chelation property, nontoxic.	[45]
	Poly(2-acrylamido-2-methylpropanesulfonic acid) (PAMPS)	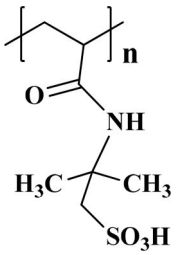	Biodegradable, water solubility, superabsorbent, zwitterionic in nature, tunable mechanical properties.	[127]

removed through adsorption or breakdown *via* redox reactions, whereas heavy metals and metalloids are typically immobilized by adsorption and precipitation processes. The similar concept is drawn toward the synthesizing colloidal particles in nano to micro level for various applications.

4.1. Mechanistic insights of transportation of colloids through subsurface to reach ground water

In order to know the mechanism of the colloidal transport through the soil media, we need to understand the nature of the transportation media (soil particles) where the migration and interaction of the colloidal particles happen.

Soil is the essential support for the agriculture, livelihood, and raising livestock. This is the material that covers the major portion of the terrestrial part of the Earth and consist of organic matter, weathered rocks, minerals, water, and air. Depending on the air-water content, soil subsurface are divided into three segments- vadose, capillary and saturated zone (Figure 8a). Vadose zone is considered to be adjacent to the ground surface and reaching toward the aquifer level, whereas saturated zone is extended from the top of the groundwater to the rock layer where the level of saturation of soil is 1. The capillary zone is exactly at the intermediate of above two zones which maintain the capillary pressure of the ground water. There is a primary difference between the local environment of vadose and saturated zone. Mostly, the pores of soil in the vadose zone consist of air but the pore in saturated zone contains water. The vadose zone contains comparatively higher organic matter and higher microbial activity due to presence of oxygen content than the saturated zone; the contaminants' transportation in the vadose zone is mainly horizontal which resides exactly opposite of the saturated zone. Also, the chemical nature of the vadose zone differs significantly which remains invariable in the

saturated zone. So, it is important to design the colloid system which can bind with the suitable contaminants present in either the immobile aquifer or bind with the particulate matters present in the ground water.[135,136]

The application of colloidal particles or surfactants in groundwater remediation operates through several key mechanisms, including micelle formation, adsorption, and emulsification. Surfactants can form micelles which encapsulate hydrophobic contaminants effectively by increasing their aqueous solubility and facilitating their removal whereas, the amphiphilic colloidal particles or surfactants remain stable inside the soil during transportation due to the electrostatic repulsion between the soil particles and can bind with the hydrophobic contaminants in the vadose zone and desorbing bound contaminants into the aqueous phase through electrostatic interaction, Van der Waals force, complexation or any chemical linkage which is effective for addressing non-aqueous phase liquids (NAPLs) and other persistent organic pollutants that are challenging to remediate by the conventional methods. The halogenated or non-halogenated hydrocarbons migrate through the soil vertically due to chemical spillage as waste under the forces of gravity and soil capillary.[17] While migrating, DNAPL reaches to a certain limit where some proportion of it reach to the ground water and some part differentiate from the continuous phase of the DNAPL and retain in the porous soil media as isolated globules. The latter one is termed as residual saturation which appears in the unsaturated zone (vadose zone). With time, the residual DNAPL globules invades to the ground water through the vadose zone and gets solubilized by the hydrocarbon parts and reaches to the lower permeable zone where the pressure depletes and starts flowing laterally with the ground water[137,138] (Figure 8b,c).

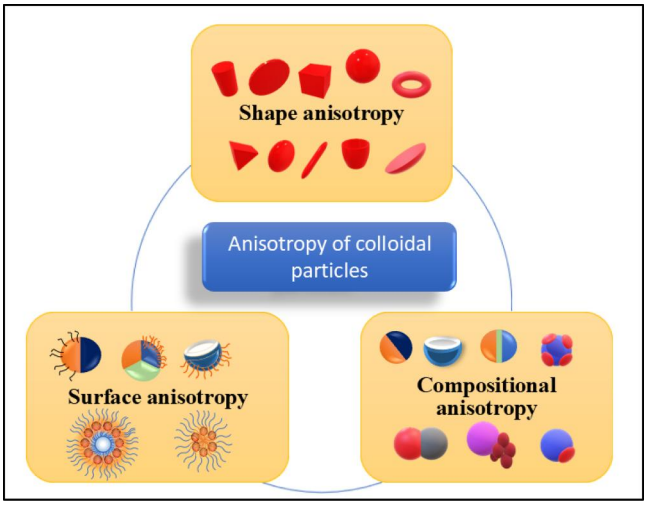

Figure 7. Categorization of different shaped particles (Inspired and redrawn from Refs. [132,133]).

Extensive investigation suggest that the *in-situ* mobilization is the effective way to disperse and transport the colloid particles inside the aquifer and adsorb onto the porous subsurface. The transportation of the colloidal particles through sands is dependent on few crucial factors: (1) the chemical composition of the colloids, (2) porosity of the sand, (3) the composition of the minerals present in sand, (4) chemicals present in aqueous media, (5) the sticking coefficient (6) the hydraulic flow, and (7) the alteration of ground water quality due to heavy rain/drought.[136] The ionic strength (IS) of soil keeps changing due to the alteration of the weather which changes the soil quality by repeated wetting/drying.[139] pH promotes the mobility and encapsulation of charged species. For instance, high pH makes the surface of a specific type of colloid negatively charged which can absorb metal ion contaminants.[140,141]

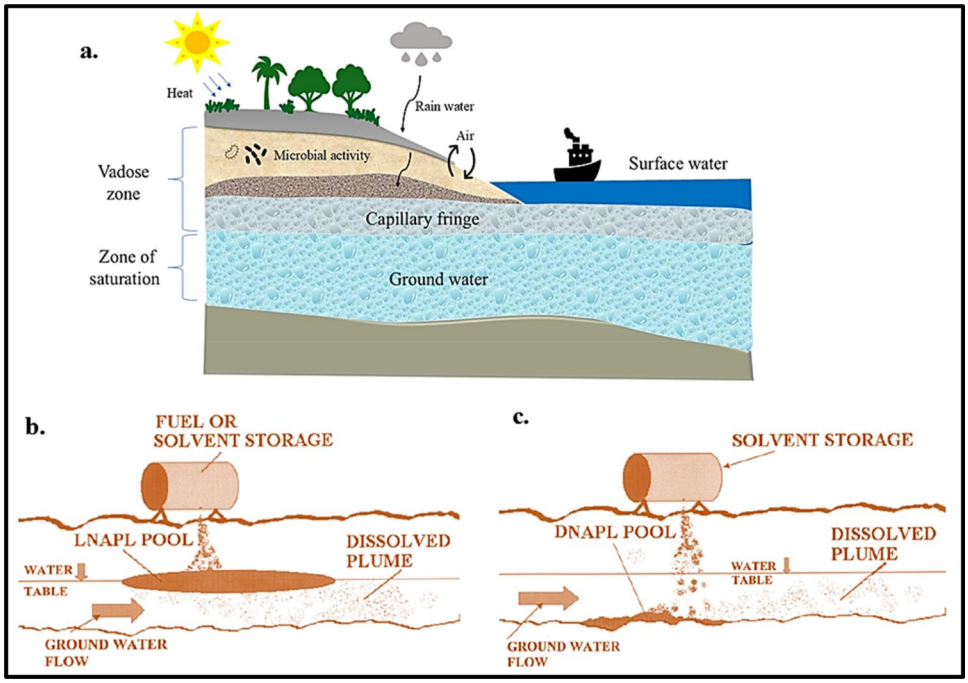

Figure 8. (a) Soil subsurface division- vadose zone, capillary zone and saturated zone, and ground water contamination by (b) LNAPL and(c) DNAPL pool (Adapted with permission from Ref. [17]).

The transport of the metal ions is facilitated by the support of polymers. Biodegradable polymers are excellent support systems for the immobilization of colloidal particles. According to the classical colloidal theory, colloidal particles can be transported within the range of meters although the major factors, the particle size and the type of sand control the mobility of the particles which are based upon several well studied models.[142–144] Research has been carried out with the transport of ZVI and the different polymer coatings which gives the colloidal particles stability during the column transport study. The performance of nanoparticles incorporated colloidal polymeric particles is mainly based on their shape, size and surface charge. All these properties can be tailorable by choosing specific synthetic method. In the next section, the synthetic methods which are commonly used for the preparation of nanoparticles incorporated colloidal polymeric particles are discussed.

4.2. Synthetic strategies of nanoparticles incorporated colloidal polymeric particles for ground water remediation

There are several synthetic routes for the formation of the colloidal particles investigated for last two decades. Researchers adopted some selective synthetic approaches based on the morphology of the particles. Scientists have been using emulsion-based, self-assembly driven, *in-situ* chemical reduction, microfluidics, and electro hydrodynamic co-jetting (EHDC) method. A brief discussion on each has been stated below.

4.2.1. Emulsion-based synthesis

This is one of the earliest low energy-based synthesis methods for the colloidal nanoparticles' synthesis, since it does not require any specialized instruments but only depend on the nature of emulsifier, oil or water media and the reaction conditions. An emulsion is such a system which consists of two immiscible liquids (one is dispersed in the other); the dispersed systems are either inorganic particles or polymers. These systems are termed as colloidal capsules or colloidosomes. The typical synthetic route for the colloidosome synthesis follows three steps: (a) the dispersion of the colloidal particles in either oil or water phase of the emulsion, (b) the adsorption of the colloidal particles at the interface of the emulsion droplets, and (c) the transfer of the stabilized emulsion droplets to a continuous phase. The techniques which focus on the strengthening of the shell of the colloidosomes are- (a) dialysis,[145] (b) solvent evaporation,[146] (c) ultrasonication,[147] (d) salting out,[148] and (e) nanoprecipitation,[149–153] (Figure 9).

Apart from these, other advanced techniques of the shell reinforcement consists (a) thermal annealing, (b) covalent crosslinking, (c) polyelectrolyte complexation, and (d) gel trapping.[157] Dinsmore *et al.* first demonstrated the term "colloidosome" where carboxylated polystyrene latex based emulsion droplets were formed followed by sintering the monolayer of shell made of latex at 105 °C.[158] The similar approach was adopted later by a group of scientists as the route provides annealed-shell structures to the emulsion which lock in the cargos inside the shell. But it was noticed that the inter particles fusion happening along with the intra particles' accumulation.[159,160] In general, most of the polysaccharides, PLA, PLGA, PEG, cellulose, chitosan, lignin, dextran, etc.[161–163] are efficient to form stable microemulsion while encapsulating nanoparticles. For example, microemulsion of lignin significantly reduces the size of Ag nanoparticles to 153 ± 4 nm from 227 ± 3 nm which was the size from direct reduction of Ag salts.[164] However, later the Ag particles' size became smaller (25–50 nm) when chitosan was employed as the stabilizing agent for pesticide removal.[165] Besides, amphiphilic block co-polymers like PLA-PEG also encapsulated the nanoparticles effectively *via* emulsion method. This system is ideal for remediating effluents of textile or cosmetic industries where dyes and chlorinated organic components are predominantly present. Recently, ultrasonication becomes one of the easy routes for synthesis of the polymeric colloidal particles. In this method, both the active agent (like GO or CNTs) and polymer (polyacrylic acid, chitosan) must have the ability to sustain strong forces due to sonication.[166] For example, Shan *et al.* synthesized Fe-Mn encapsulated in graphene oxide-chitosan moiety for effective removal of As from ground water. The Fe-Mn system was embedded into chitosan *via* ultrasonication.[41] Moreover, another study found that, cadmium sulfide (CdS) based nanocomposite was synthesized with microcrystalline cellulose (MCC) *via* ultrasonication and this photocatalyst effectively degrades MB from wastewater.[167] This method provides the polymers to be the excellent protective layer to the active materials inside and hence, can be used in capturing heavy metals and degradation of dyes from textile industrial effluents; however, these methods possess few disadvantages too due to usage of high amount of surfactant, followed by their purification. Also, phase separation poses a negative effect, which sometimes create difficulty in the formation of multilayered particles.

4.2.2. In-situ *chemical reduction*

One of the captivating colloidosome syntheses occurred *via* chemical reduction. Generally, the size of the metal nanoparticles cannot be controlled when the MNPs precursors are reduced *via* conventional co-precipitation due to rapid nucleation. Also, they get easily aggregated and settled down in chunks during reaction. That's why a novel approach to avoid this problem is to embed the nanoparticles into a three-dimensional rigid moiety such as polymers *in-situ* and further to study the contaminants' adsorption in large scale. The general steps of these methods are: (a) reduction of metal precursor either pre-encapsulation or *in-situ*, (b) encapsulation the zero valent metal ions in a support of either inorganic[168–172] or organic compounds,[173–177] and (c) surface functionalization, although the last step is optional depending on the application (Figure 10). Mostly, encapsulation by polymers and reduction of the MNP precursors happen in one-pot

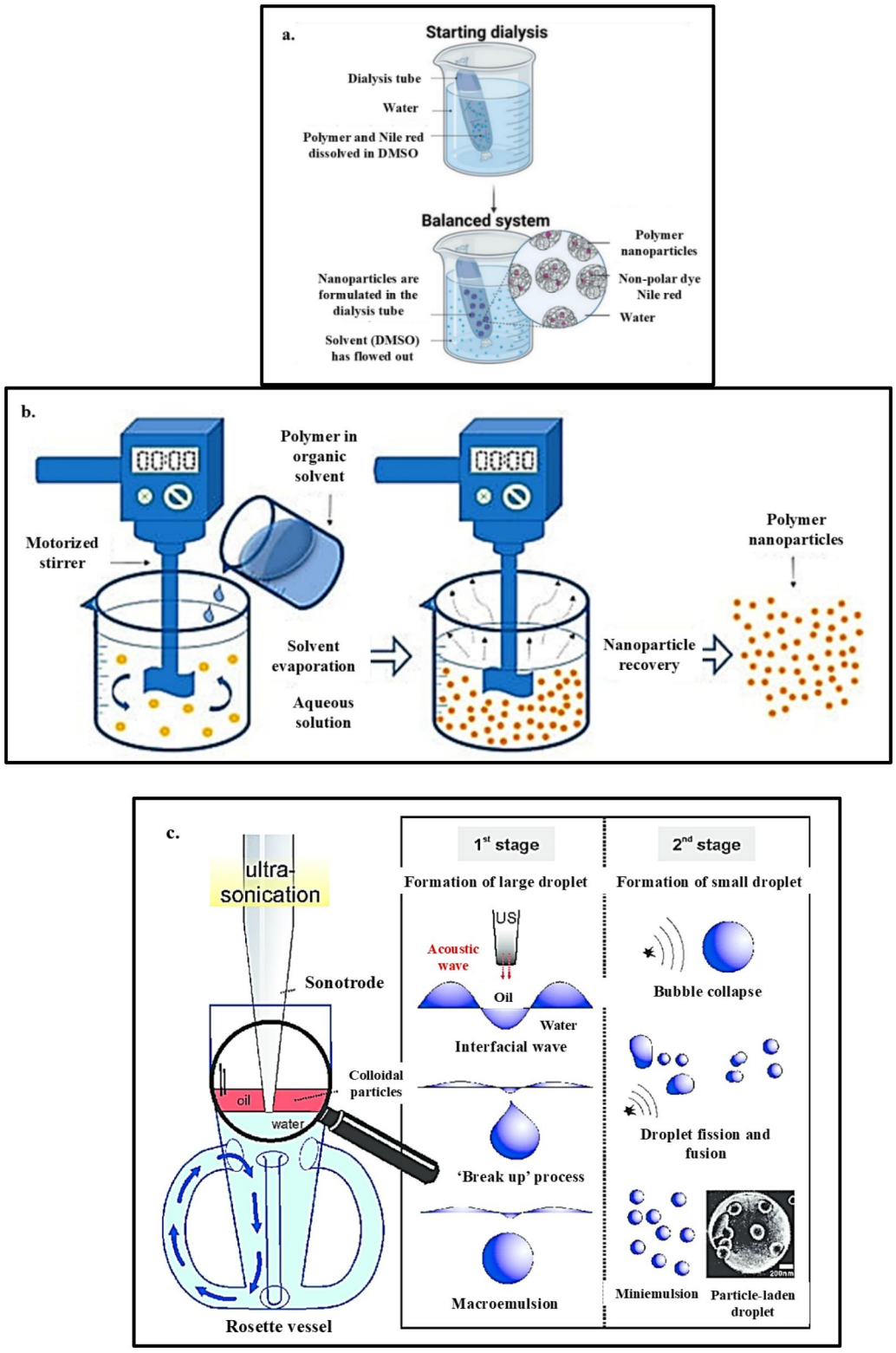

Figure 9. Emulsification techniques (a) dialysis, (b) solvent evaporation, (c) ultrasonication, (d) salting out, and (e) nanoprecipitation (Adapted from [154–156]).

to get the better yield of the colloidal particles. Moreover, the polymers not only play significant role in stabilizing, but also, control the reactivity of the suspended metal nanoparticles in varying physiological conditions (pH and ionic strength) and also creating more adsorption sites. Several polymers like carboxy methyl cellulose (CMC), starch, cyclodextrin, starch, chitosan etc. Stabilize zero valent nanoparticles like Pd, Fe, Fe-Mn, Fe-Ni etc. which are briefly summarized in Table 3. The abundant functional groups effectively chelate the metal ions and provide support for freshly formed nanoparticles which becomes well dispersed in the aqueous media, thereby removing the chlorinated hydrocarbons, heavy metals which are largely found in the industrial wastewaters.

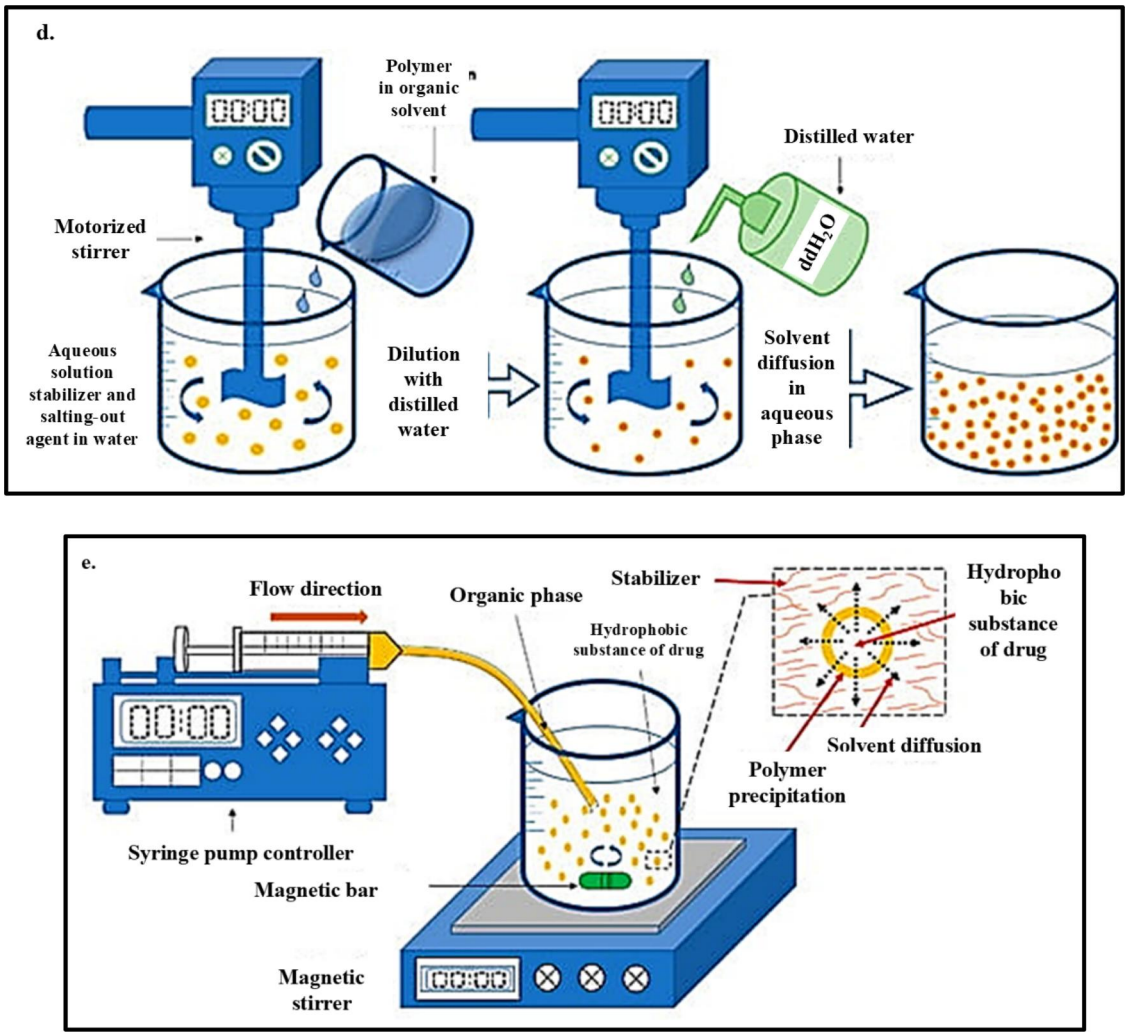

Figure 9. Continued

Recently major investigations are carried out by ZVI [Fe(0)]in the water remediation. The simplest way to encapsulate zero valent nanoparticles is by treating the nanoparticles' precursors in presence of reducing agent and the encapsulating agents (like polymers or metal supports) in one-pot system.[178] Kim *et al.* and Gong *et al.* carried out a similar kind of stabilization-reduction by synthesizing sulphidated ZVI and carboxymethyl cellulose stabilized ZVI, respectively, by dripping the mixture of $Na_2S_2O_4$/carboxy methylcellulose and $NaBH_4$ solution into $FeCl_3.6H_2O$ solution.[179,180] Whereas, Kumari *et al.* prepared sodium alginate encapsulated ZVI particles for removal of the Chromium from polluted water.[175] Another interesting strategy to prepare stabilized colloids in the oil-water interface is to functionalize the colloid surface *via*" grafting-to" and "grafting-from" approach. The "grafting-to" approach requires the attachment of polymers onto the reactive surface (either film or particles) and the "grafting-from" approach is the *in-situ* polymerization of the monomers onto the macro initiators (particles' surface previously anchored with the reactive groups). Among these two routes the latter one provides dense functionality on the nanoparticles' surface, mostly accomplished by surface-initiated atom transfer radical polymerization (SI-ATRP).[181,182] SI-ATRP provides dense, but controlled brush density onto the active nanoparticles. Similar studies were carried out by Berger *et al.* who designed a Janus nanoparticle (Jp) covered with stimuli-responsive polymers on each hemisphere. On one side, they have conducted surface initiated ATRP (SIATRP) for the growth of brush like polymer chains from one hemisphere of Si particles using "grafting from" approach, while the other side was simply attached with reactive terminating group of a polymer *via* "grafting to" approach. This unique design provides an excellent outcome which enlarges the possibilities of desirable fabrication methods of Jps.[183]

4.2.3. Self-assembly

Self-assembly is the process where colloidal particles organize themselves spontaneously by some interactive forces such as Vander Waals, electrostatic, dipole-dipole, depletion force, hydrogen bonding, π- π stacking etc. and the driving forces for the aggregation are thermodynamic and kinetic parameters.[184] Amphiphilic polymers (PEG-PLA or PEG-

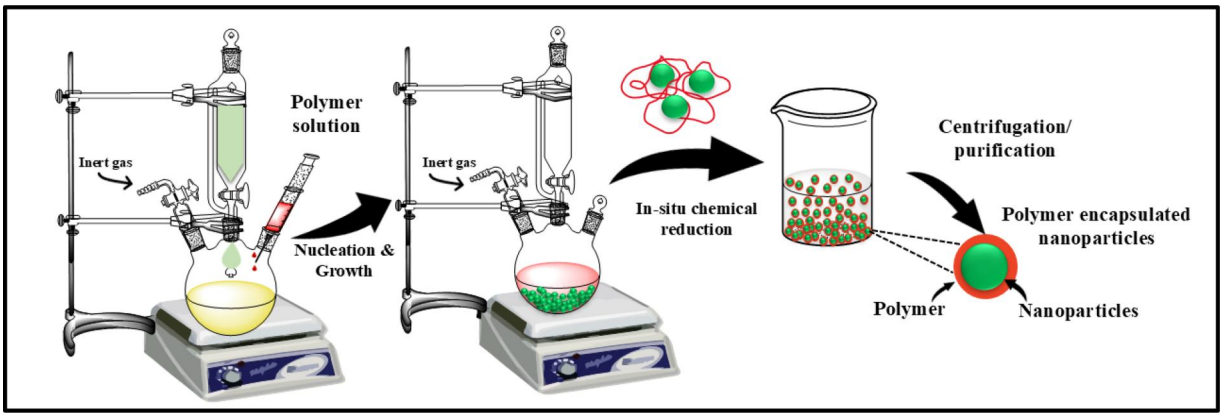

Figure 10. *In situ* chemical reduction method for the synthesis of encapsulated nanoparticles.

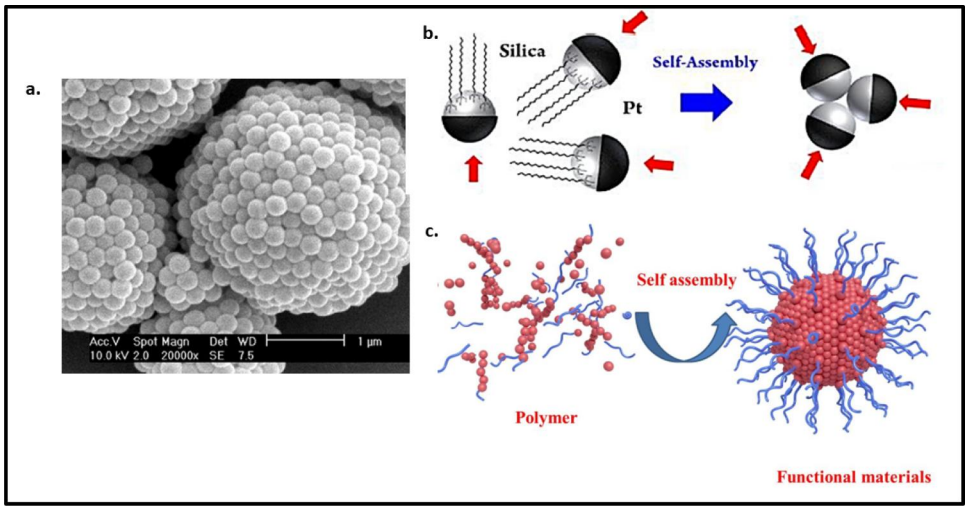

Figure 11. (a) Scanning electron micrograph of supraball of the polystyrene nanobeads. (b) Mechanism of self-assembly of the Jps. (c) Self-assembly of polymers *via* attractive hydrophobic interactions (Adapted with permission from Refs. [186,187,190]).

PCL block co-polymers) or natural polymers like starch tend to aggregate in a particular solvent (either aqueous or non-polar solvent) and arrange themselves in micellar or vesicular structures allowing the encapsulation of various hydrophilic and hydrophobic cargos.[185] The synthesis of colloidal particles is controlled by several factors such as nature of solvents, concentration of the polymer, temperature and pH of the medium.[186] Evaporation-based technique is ruling the self-assembly; as the solvent evaporates, separated particles get assembled and lead to aggregated structure. Self-assembly can create ordered arrangements such as crystalline or liquid crystalline phases. The process is highly sensitive to factors such as particle size uniformity (monodispersity), shape, and the nature of inter-particle forces like electrostatic and Vander Waals interactions. For example, spherical colloids can transition from a disordered liquid phase to an ordered crystalline phase when the particle concentration increases, driven by the system's entropy maximizing its vibrational freedom.[187] Similarly, rod-shaped colloids exhibit unique self-assembled phases like nematic (orientationally ordered) and smectic (layered) structures due to their anisotropic shapes. The additional attractive interactions, such as depletion forces, further broaden the range of self-assembled structures, enabling the formation of complex configurations like tactoids, twisted ribbons, and colloidal membranes[188,189] (Figure 11).

The process of nucleation and growth also plays a critical role in the self-assembly of colloidal particles, as outlined in Sacanna *et al.*'s work. In this case, the polymerizable oil drops form on some preexisting polymeric seed at the beginning of the nucleation and it follows the growth stage which facilitates the expansion of the droplet size and ensures uniformity. By modifying conditions such as seed concentration and the addition of secondary monomers, it is possible to create various geometries, including monodisperse dumbbells and multi-lobed particles. These stages of nucleation and growth are observed and controlled using advanced microscopy techniques, ensuring precision in particle size and morphologies.[191] These assemblies not only provide insights into natural systems, such as biological membranes, but also hold immense potential for nanotechnology, where designer particles and tailored interactions can create precise, functional structures. This approach as well is well suited for treating organic micropollutants, pesticides or pharmaceuticals from the industrial and agricultural wastewater.[192] Self-assembly thus represents a convergence

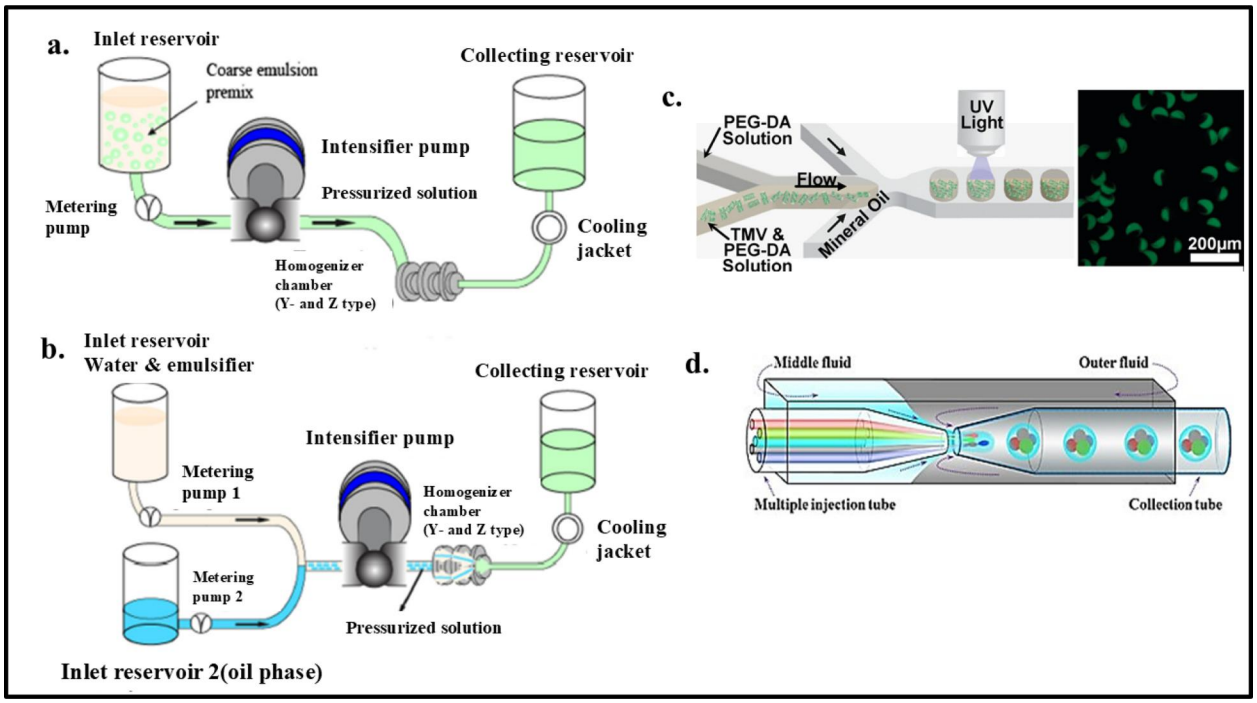

Figure 12. The schematic diagram of nano emulsions *via* (a) two-step single channel and (b) one-step dual channel micro fluidization. (c) Microfluidic technique to synthesize fluorescent labeled tobacco mosaic virus (TMV) and Pd based Janus nanoparticles. (d) a schematic presentation of the capillary microfluidic device where multiple injection channels (red, green, blue, and gray) used for the generation of the multiple core double emulsions (Adapted with permission from Refs. [196–198]).

of fundamental science and practical innovation, showcasing nature's ability to achieve order through inherent forces.[193] However, there are limited studies done for the colloidal particles' synthesis for ground water remediation *via* self-assembly.

4.2.4. Microfluidic

This is the top-down approach for synthesizing uniform size droplets by using certain mechanical forces of shear, cavitation or turbulence. Highly intensive disruptive forces are required to create stress on the primary emulsion and breakdown to small sized droplets which are further stabilized by emulsifiers, thus this is classified in higher energy-based processes. The microfluidizer consists of two crucial parts-air driven pump, which is the source of the high pressure to split the crude liquid stream into two parts, and a fixed geometry interaction which is the center of the device directing the flows toward one another passing each half *via* a tiny aperture. The flow stream is guided through the microchannels toward the impingement area by the microfluidizer using high pressure (typically from 150 kPa to 150 MPa), which produces a very high shearing action that yields an incredibly fine emulsion.[194,195] Hence cavitation along with the shear force and the impact in the interaction chamber decreases the size of emulsion droplets. A conventional microfluidizer can produce nano emulsions via two different pathways. It is basically two different instrumentations either can be two-step single channel or one-step dual channel. The former technique needs the premixing of the oil and water in a single chamber to prepare the coarse emulsion which needs to be passed through a single channel for further processing. Whereas the later method feeds the oil and water separately toward the intensifier pump, which is substantially more effective than the former one in the perspective of energy, time and economy (Figure 12). However, the energy factor somehow misguides this method while in operation, due to "over-processing" which increases the size of the nano emulsions by recoalescence of the fine droplets, if not properly optimized.[199,200]

Recently, few more advanced microfluidic techniques have been reported by researchers for synthesizing core-shell microcapsules. Such methods include focused surface acoustic wave (FSAW),[201] glass capillary microfluidics with multiple injection channels (Figure 12d), 3D as well as 2D flow-focusing microfluidic devices etc. These are highly efficient processes which were elaborately discussed in a review written by Zhao *et al.*[196] Furthermore, scientists explored various facile methodologies for synthesizing metal nanoparticles loaded polymers for ground water remediation. A larger variety of polymers can be compatible with this approach. Among them PLA, PCL, photocurable polycaprolactone diacrylate (PCLDA), polyethylene glycol (PEG) were mostly chosen for treatment of organic contaminants, pharmaceuticals, dyes or heavy metal ions from the industrial, textile, agricultural base wastewater effluents.[197,198] For example, a group of scientists synthesized polyethylene glycol (PEG) loaded Pd nanoparticles which was modified with fluorescent labeled tobacco mosaic virus (TMV) templated Janus particles for Cr removal,[202] other group, on the other hand, have demonstrated the fabrication of polyethylene glycol diacrylate encapsulated titanium dioxide [TiO_2–

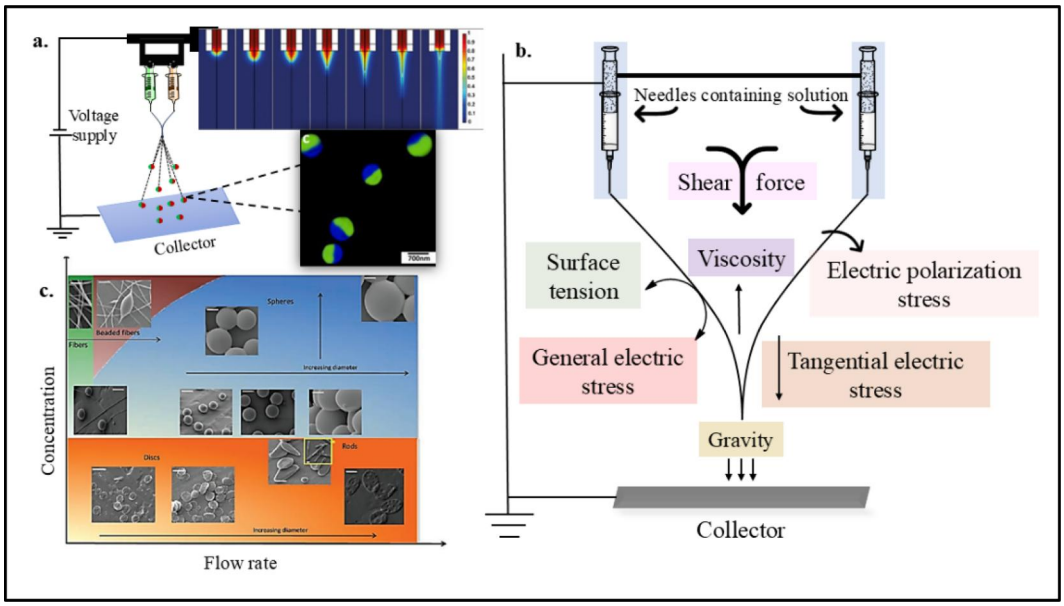

Figure 13. (a) Formation of Taylor cone in presence of electric field; the bipolar liquid forms a Taylor cone at the tip and flows toward the counter electrode. (b) The distribution of active forces within liquid cone-jets. (c) The generalized graph showing formation of particles is concentration and flow-rate dependent (Adapted and redrawn with permission from Refs. [45,204–206]).

P(EGDA)] and Ag[Ag–P(EGDA)]microgel *via* microfluidic route, which were employed to show photocatalytic degradation of methylene blue from waste water.[38,203]

4.2.5. Electro hydrodynamic co-jetting (EHDC)

It is a top-down process which needs high voltage as an energy factor. Liquid droplets of multiple compositions are produced by this technique, alike in a microfluidic reactor, but the difference is the collection of particles. Generally, polymer or any functional materials are loaded in syringes in presence of any conducting liquid and subjected to high voltage (5–15 kV) which controls the propagation of multicomponent droplets toward the collector. When the primary droplet leaves the needle tip, surface charge generates on the droplet under the electric field which begins to change its original shape and under certain voltage the electric force overcomes the surface tension of the liquid and get distorted to achieve a conical shape (termed as Taylor cone) which further migrates toward the collector in the form of jet sprays (secondary droplets) (Figure 13). Higher the voltage, the electrified jets tend to break into hundreds to millions of secondary droplets and collects in either aluminum foil (electrojetting), in a rolling device as fibers/mats (electrospinning) or in solution (electrospraying). Thus, the formation of either continuous fibers or discontinuous droplets is contingent upon the fluid's viscosity and surface tension, viscoelastic forces or the coulombic force. The applied electric field, the molecular weight and concentration of the polymer, the flow rate, the viscosity, and the conductivity are all significant factors controlling the fabrication of a wide range of particle sizes, shapes, and characteristics. Lahann *et al.* studied the effect of poly(lactic-co-glycolic acid) (PLGA) concentration and flow rate for generating various shapes as shown in Figure 13(c). Increased polymer concentration hinders the Taylor cone formation as well as jet becomes unstable and the probability of formation of the fibers happen at the lower flow rate. When the flow rate is increased, a transition from beaded fibers to spherical particles can be observed. On the other side, polymer with lower concentration with lower flow rate leads to discoid shaped particles due to rapid solvent evaporation during the transition from the droplet stage to solidified particles.[204] However, the surface charge and above-mentioned factors are not solely determining the shape of the particles, but the role of solvent is also a crucial factor. The optimum solvent choice is highly necessary for the homogenous solvent evaporation throughout the particles for smooth shape and spherical geometry. It has been seen by mixing nonvolatile solvents with the volatile one delays the solvent evaporation, in other terms, delays the phase separation between polymers and solvent, generating multiple geometries like sphere,[207] rods, core-shell, cup-shaped[128,208,209] particles, depending on the process parameters. Besides, multicomponent particles can also be synthesized (Janus particles) by this technique using multiple needles while jetting the polymeric solution.[204,210,211] In order to form a stable jet, PLA, PCL, PLGA, and polysaccharides like chitosan, starch, dextran derivatives etc. were employed to capture well dispersed nanoparticles which are compatible with those polymers. There are very few systems reported in the literatures by this process which are effective in removing organic contaminants like NAPLs and dyes from industrial wastewater. But a recent study performed by Pandey *et al.* which perfectly coordinates with the previous discussion, for the synthesis of the biphasic Janus nanoparticles encapsulated with ZVI and the shell made of biodegradable polymers for degradation of chlorinated contaminants (TCE). This work dealt with the fabrication of ZVI incorporated amphiphilic polymeric particles with Janus geometry using EHDC and their application in water remediation *in-situ*. Upon changing the polymer

concentration and simultaneous decrease in the flow rate, extensively reduced the size of colloidal particles from 18 μm to 700 nm so that the composite particles can be easily transported to the subsurface without compromising their water dispersibility, while maintaining the catalytic activity of ZVI nanoparticles. This particular example shows how Janus geometry achieved by EHDC may enhance the efficacy of the catalytic system by adsorbing at NAPL and removing both hydrophobic and hydrophilic contaminants.[45,212]

These are some of the common techniques for the synthesis of the colloidal particles with wide range of sizes as well as shapes; the fabrication requires the optimization of the concentration of the polymer, size of the metal nanoparticles, appropriate surfactants and its concentration, and suitable solvents. However, these polymers are also able to encapsulate metal nanoparticles through various ways, i.e.- biosynthesis, hydrothermal, sol-gel, ionic gelation, reverse micellar method, co-precipitation, spray drying, ball-mill, coacervation, microwave-assisted, gel trapping, covalent crosslinking etc. The ultimate goal is to design a wide range of pH, temperature, light or magnetic sensitive colloidal particles which offer sustainable application to remove contaminants from the ground water. Although this area is yet to gain popularity in terms of membrane-based water decontamination technology, but this could be an effective green method for the potential microencapsulation of the nanoparticles. Hence, to gain aconsiderable knowledge about the systems already developed, we should get some idea about subtle aspects of the contaminants which is summarized in below table.

4.3. The importance of nanoparticles entrapped biodegradable polymeric colloidal particles for ground water remediation

The recent advances in the biodegradable polymers encapsulating nanoparticles brought innumerable successful applications in the field of contaminants' removal. Since, biodegradable polymer leave nontoxic residue in the water in most cases, polymers provide functional support and tunable surface which accelerates the contaminants' adsorption and binding with the nanoparticles. Moreover, the crucial role of polymers is to create homogenous suspension in water, and better transportability *via* subsurface. Few examples elaborating on the role of biodegradable polymers in stabilizing the active nanoparticles are stated below in Table 3.

These stabilizers can vary from naturally obtained polysaccharide to commercially synthesized polymers. Hoch *et al.* synthesized ZVI impregnated onto carbon *via* carbothermal method which was able to convert toxic Cr(VI) to Cr(III). Subsequently they added CMC and polyacrylate (PAA) to these particles to examine their stability and received encouraging results. CMC modified nanoparticles was able to convert Cr(VI) for 7 days whereas, bare nanoparticles were stable only upto 3 days.[213] A group of researchers examined a lab-based study for the removal of nitrate and phosphate by the help of ZVI coated with polymers.[214] They used a variety of polymers such as polyacrylamide (PAA), carboxymethyl cellulose (CMC), Polyethylene sorbitan monolaurate (PSM) and polyvinylpyrrolidone (PVP) and assessed their removal efficiency. Simultaneously, field-based study was also performed with the polymer stabilized metal nanoparticles.[215,216] For instance, Moyo *et al.* demonstrated the removal of hexavalent Cr(VI) from wastewater using Pd nanoparticles embedded onto the Polyethylene imine (PEI) grafted macadamia nutshell (MNS) scaffold.[29] MNS is a type of biomass containing large amount of cellulose and lignin. The structure of raw MNS contains insufficient pores which can attach the nanoparticles' precursors due to presence of lignin moieties. Hence, lignin was removed through bleaching (upon treatment with NaOH and H_2O_2) from the raw MNS before being functionalized with PEI. On the other side, PEI possess lesser affinity toward the hydroxyl groups of delignified-MNS (D-MNS), so another cross linker such as glycidyl methacrylate (GMA) was added onto the surface of D-MNS through surface radical initiated addition polymerization. Hence, finally Pd nanoparticles' precursors were immobilized onto the scaffold *via* hydrazine mediated reduction to form Pd@PEI-MNS. There are three kinds of sites present in this scaffold (i) adjacent to the ligands and far from Pd nanoparticles; (ii) adjacent to both ligands and Pd nanoparticles; and (iii) adjacent to Pd nanoparticles and far from ligands. Further research was carried out to compare the Cr(VI) removal capacity between PEI-MNS and Pd@PEI-MNS in presence of formic acid(HCOOH) and found an exciting result which showed, in the first 120 mins of addition of the scaffold in the Cr(VI) solution, the removal of Cr(VI) is higher for PEI-MNS than the latter. The reason behind this was the presence of higher number of accessible ligands which facilitated the adsorption and reduction of the incoming Cr(VI) ions in the former scaffold whereas, in the Pd@PEI-MNS, only site (i) and (ii) were accessible, since most of the portion was occupied with Pd nanoparticles. But surprisingly, after 120 mins, the reverse phenomenon happened i.e. Pd@PEI-MNS showed higher removal capacity for the Cr(VI) ions due to sustained release of Pd nanoparticles (Figure 14a,b). This was the result of reduction capability of Pd nanoparticles in presence of HCOOH. It was hypothesized, Pd nanoparticles started reducing the Cr(VI) ions when the efficacy of ligands was exhausted; thus, this scaffold was a promising candidate for Cr(VI) removal from contaminated water for prolonged period (reusability achieved upto15 consecutive cycles). Similar Kind of work reported in another biomass of spent coffee ground (SCG) as a sustainable source for the encapsulation of Pd nanoparticles by Chan *et al.*[217] SCG is composed of cellulose, hemicellulose and lignin. In this work, they have first delignified the SCG by H_2O_2 to produce delignified SCG(D-SCG) and then reduced Pd-salt to Pd(0) *in-situ* followed by encapsulating Pd(0) inside the D-SCG cavity to produce Pd-D-SCG (Figure 14c). The main reason for delignification is to enhance the cavities for higher catalysis rate and also the hydrophilicity of the system for better immobilization.

Table 3. Role of biodegradable polymers on the nanoparticles and their various applications in removal of contaminants.

Nanoparticles	Encapsulating system	Method used for the synthesis of colloidal particles	Role of biodegradable polymers for encapsulating nanoparticles	Contaminants removed from ground water	Refs.
n-ZVI	Sodium carboxymethyl cellulose (CMC)	*In-situ* chemical reduction	Provides long term stability, dispersibility and sustained release of the nanoparticles.	Trichloroethylene degradation and removal of Congo red (CR) dye	[22,23]
n-ZVI	Cyclodextrin	*In-situ* chemical reduction	The rigid hydrophobic core and relatively loose hydrophilic surface provide higher mechanical strength to the polymer which produce extensive sorption activity toward the organic compounds *via* host-guest interaction.	Removal of p-nitrophenol	[24]
Ag	Starch	Microwave irradiation	Acts as biological reducing agent and protects the nanoparticles from agglomerating.	Methyl orange (MO) and Rhodamine B removal	[25]
Fe_3O_4	Poly(acrylic acid) (PAA)	Reduction of metal salts *via* hydrothermal method followed by sonication.	The acidic groups(-COOH) provides better chelation ability to the metal ions than bare Fe_3O_4 particles. Also, these acidic groups make the particles pH sensitive which accelerates the stability in different geological conditions.	Cu(II) and Cr(VI) ions and methylene blue (MB) dye removal	[26,27]
GO	PAA	*In-situ* polymerization	Presence of C = O groups in polymer aids the π-π interaction between phenol and GO and also helps GO to be dispersible in water for longer period of time.	Phenolic waste removal	[28]
Pd	Poly(ethylene imine) (PEI) grafted macadamia nutshell (MNS) scaffold	*In-situ* chemical reduction	The presence of nitrogen groups of PEI help anchoring the metal ions present in water and also provides better stability to the Pd nanomaterial.	Cr(VI) ions removal	[29]
Au	Carboxy methyl cashew gum (CMCG)	Microwave irradiation	This polymer also produces Au nanoparticles in-situ; and the presence of -OH and -COOH groups effectively chelates with metal ions and also bind with dyes.	Methyl red and $Hg2^+$ detection	[30]
Cu_2O/CuO	Chitosan	Ball-mill	Chitosan contains the functional groups of ($–NH_2$) and (–OH) having a strong ability for complexing with Cu^{2+} ions. Upon milling, the Cu^{2+} are adsorbed and/or captured onto Cs surface using ($–NH_2$) and (–OH) groups.	Removal of 4-nitrophenol, MB and MO.	[31]
TiO_2	Chitosan	Nanoprecipitation	The functional groups of the polymers enhance the chelation ability of As.	As(III) removal	[32]
$Ni_3Si_2O_5(OH)_4$ nanotubes	Poly(2-acrylamido-2-methylpropanesulfonic acid) (PAMPS)	SI-ATRP	Provides stability to the nanotubes and better adsorption ability toward the cations due to its higher isoelectric point.	Pb(II) removal	[26]
MwCNT	Hydroxyapatite	Ultrasonication	This polymer remains stable during water remediation for long time as well as produce ion-exchange capability with several anionic pollutants and the abundant OH groups show chelation ability toward the heavy metals.	Pb(II) andMB removal	[33]
TiO_2	Thiazolylazopyrimidine (TAP)	Ring opening reaction	TAP acts as light sensitizer which promotes the photocatalytic ability of TiO_2.	Cu(II) removal	[34]

(*continued*)

Table 3. Continued.

Nanoparticles	Encapsulating system	Method used for the synthesis of colloidal particles	Role of biodegradable polymers for encapsulating nanoparticles	Contaminants removed from ground water	Refs.
Fe_3O_4	Carboxymethyl-β-cyclodextrin (CM-β-CD)	Co-precipitation method	Multiple OH and COOH groups enable complexation with heavy metals and the cavity structure of β-cyclodextrin ensures the selective inclusion of organic molecules.	MB, bisphenol-A and resorcinol removal	[35]
Fe_3O_4 and MWCNTs	Poly(ethylene glycol) (PEG)	Co-precipitation followed by ultrasonication and heating	The amphiphilic character helps the polymer to attach with both metal ions and organic dyes. Also, helps the nanoparticles to be water soluble, biocompatible and dispersible in water for long time.	MO capture and removal of tracer amount of Cd(II) and Pb(II).	[36,37]
TiO_2	Poly(ethylene glycol diacrylate) (PEGDA)	Microfluidic	PEGDA enhances the binding ability of MB *via* van der Waals forces and H-bonding.	MB removal	[38]
Fe-Pd (palladized iron)	Starch	*In-situ* chemical reduction	The hydroxyl groups act as secondary support for effective redction of Fe(III) to Fe(0) and stabilization of the bi metallic nanoparticles for a longer period of time.	Dechlorination	[39]
Fe-Mn	Polysaccharide	*In-situ* chemical reduction	Stabilizing agents and enhancing the mobility of the bimetallic nanoparticles	Oxidation of As(III) and As(V)	[40]
Fe-Mn	Chitosan-GO	Ultrasonication	Stabilizing the bimetal system and anchoring the contaminant effectively.	Oxidation of As(III) and As(V)	[41]
Carbo-iron	CMC	Chemical reduction	Stabilizing agents and enhancing the mobility of the bimetallic nanoparticles	Dechlorination	[42]
Fe-Ag	Chitosan	*In-situ* chemical reduction	The cationic surface of chitosan provides the bimetal system an extensive stability *via* electrostatic repulsion.	Removal of BOD, COD, turbidity.	[43]
Co-Ni- Fe_3O_4	Chitosan	*In-situ* chemical reduction	Chitosan covers iron-based moiety and also the presence of functional groups enhances the attraction for the organic contaminants. Also, the functional groups hold Co-Ni metals by chelation for effective removal at ambient temperature.	Removal of MO (93.14%) and 2,4-D (95.50%)	[44]
n-ZVI	PLA and PE [poly (hexamethylene 2,3-O-isopropylidenetartarate)]	Electro hydrodynamic co-jetting	The presence of one hydrophobic part (PLA) and one hydrophilic part(PE) (which become OH containing moiety after deprotection) provides amphiphilicity to the particles which enhance the transportability of the particles for better suspension and catalytic activity of the ZVIs.	Dechlorination	[45]
GO	Chitosan	Electrospraying	The polymer provides a base for honeycomb cob-web like structure and entraps the GO inside it for adsorption of cationic and anioic dyes.	Adsorption of heavy metal ions of Pb(II), Cu(II), Cr(VI), and cationic dyes (MB and Rhodamine B), anionic dyes (MO and Eosin Y, and phenol.	[46]

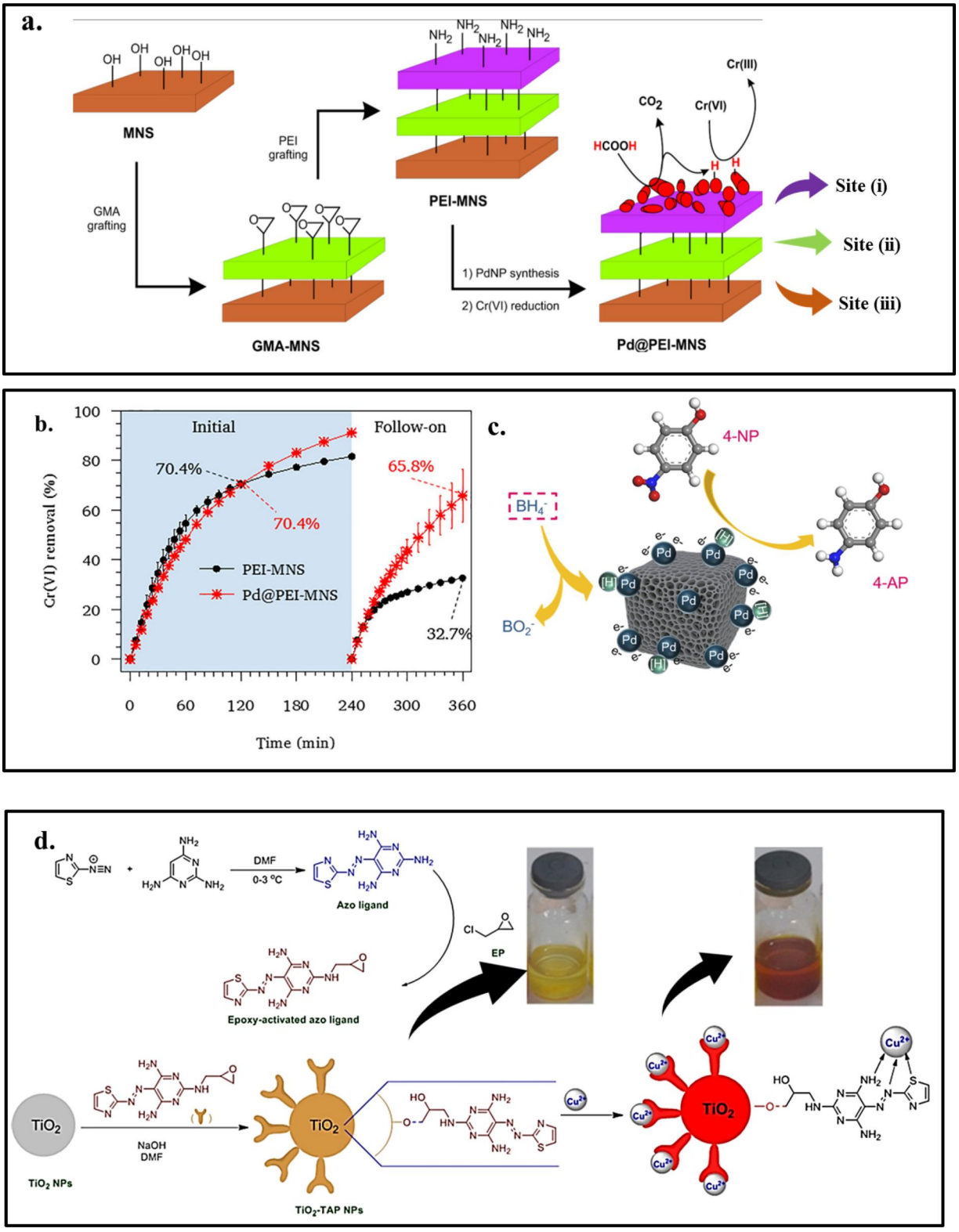

Figure 14. (a) Different sites of the Scaffold Pd@PEI-MNS and (b) comparison graph showing Cr (VI) ions removal by PEI-MNS and Pd@PEI-MNS (Reproduced with permission from Ref. [29]). (c) Reduction of 4-nitrophenol to 4-aminophenol *via* Pd^0(Reproduced with permission from Ref. [217]. (d) Synthesis route of thiazolylazo-pyrimidine (TAP) and simultaneous color change from yellow to red upon anchoring Cu^{2+} by TiO_2-TAP (Adapted with permission from Ref. [34])

The negatively charged and porous surface of the 3-dimensional system was able to attract the organic contaminants like 4-nitrophenol(4-NP) and positively charged Methyleneblue (MB) through surface adsorption and then to reduce both of them in presence of $NaBH_4$. This catalytic hydrogenation continued up to 5 cycles.

Researchers also produced successful results for capturing Cu ions from water using stabilized gold (Au) nanoparticles. Rastogi *et al.* synthesized 4-amino hippuric acid stabilized gold nanoparticles (4-AHA@AuNPs), which showed selective catalytic activity for the determination of Fe^{3+} and Hg^{2+}.[218] These gold nanoparticles produced peroxidase like

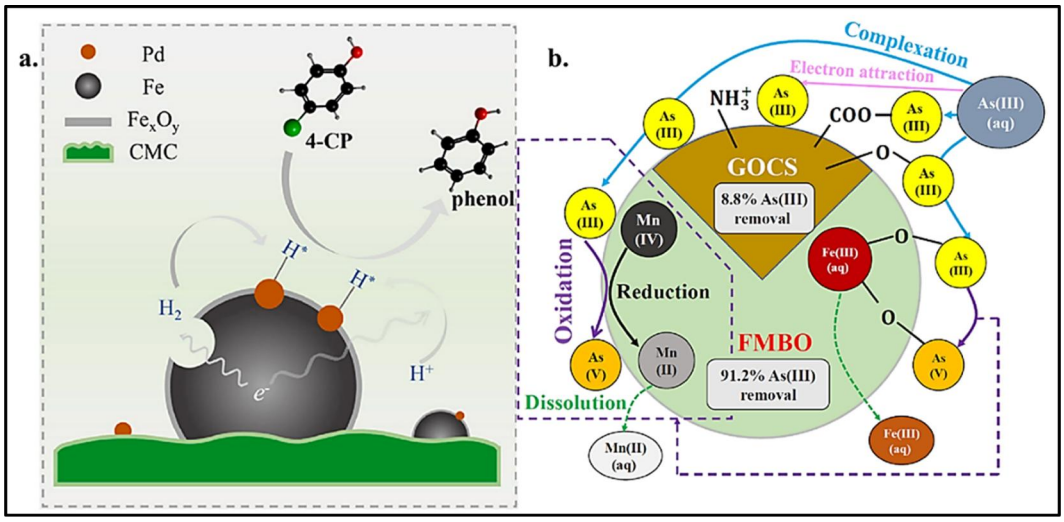

Figure 15. (a) Reduction of 4-chlorophenol to phenol *via* Fe-Pd bimetal coated by chitosan. (b) Adsorption and simultaneous oxidation of As(III) *via* Fe-Mn-GOCS nanocomposite (Adapted with permission from Refs. [41,221]).

activity when injected to the ground water rich in above two ions and generate hydroxyl radicals to detect those ions which prove their potential usability in field scale study. Similarly, another group of people, Ruqya *et al.*, studied the calorimetric detection of Hg^{2+} ions and catalytic reduction of methyl red (MR) by carboxy methyl containing cashew gum modified gold nanoparticles (CMCG-AuNPs) using simple microwave irradiation.[30] CMCG provides stabilization to the generated gold nanoparticles, that was later proved by showing their stability in water for two months without agglomeration. The average size of the particles remained in the range of 12 ± 3 nm whereas, upon binding with Hg^{2+} ions, they form aggregate. The reduction of MR was studied in presence and absence of this catalyst, with the addition of $NaBH_4$ and the outcome was in favor with the catalyst. Within 12 min, there was no change in the absorption peak for the untreated MR, but a drastic decrease in the absorption peak intensity, when MR was treated with catalyst. Ghasemi *et al.* reported a thiazolylazopyrimidine-functionalized TiO_2 nano sensor (TiO_2-TAP) for the effective removal of Cu^{2+} from water sample.[34] The selective removal was detected through colorimetry as the azo ligand produced a stable surface complexation with Cu^{2+} and as a result immediate color change happened from yellow to red due to charge transduction. The average size of the TiO_2 particles lied between 18 and 31 nm whereas, upon surface modification, the size got increased to 29–47 nm with no significant change in shape, but with the increase in the number of cavity sites. The system was applied in real world samples taken from tap water, well water and sea water. Within 1 h of the addition, this system showed 100% Cu^{2+} removal from the water samples (Figure 14d).

Apart from these, The CMC-based bimetallic nanoparticles show better transportation through sands, which was attributed to the higher negative charges on the surface preventing the nanoparticles from interacting with both the sand particles and themselves. Earlier, He *et al.* simultaneously showed how starch and carboxymethylcellulose (CMC) stabilize bimetallic moiety Fe-Pd (palladized iron) nanoparticles for effective dechlorination of the halogenated organic carbons (HOCs) in either soil or ground. Both the starch and CMC provide the bimetallic nanoparticles stability but, the negative charge over the carboxyl groups of CMC provide excellent electrostatic repulsion to the nanoparticles preventing them from getting agglomerated. Moreover, the CMC-stabilized nanoparticles show a higher stability (continuous 9 days dispersibility in water) than the non-stabilized ones (few minutes). In addition, the CMC-stabilized particles showed 2 times more effectiveness for the removal of HOCs than the starch stabilized particles. Also, CMC-stabilized particle size was less (average size 4.3 nm) than the starch-stabilized ones (average size 14.1 nm) which accounts for the higher surface area leading to faster dechlorination.[219,220] Later, Juan *et al.* synthesized the same system for the removal of chlorinated hydrocarbons like 4-chlorophenol. In this work, the group synthesized the bimetallic nanoparticles in one-step rather than the conventional step by step metal reduction which was more advantageous and better yielding (Figure 15a).[221]

Several other scientists further studied the synthesis of bimetallic nanoparticles such as Fe-Ag based composite stabilized *via* chitosan moiety for removal of Biological oxygen demand, Chemical oxygen demand (BOD, COD) and turbidity *via* coagulation/flocculation.[43] Also, a group of researchers synthesized Fe-Mn bimetal system *via* graphene oxide-chitosan (GO-CS) coating for removal of As(III) from water. The mixture of GOCS composites provide the bimetal system a significant support for effective adsorption of As(III) and simultaneous oxidation into As(V) (Figure 15b).[41]

Activated carbon (AC) are one of the most promising low-cost materials which are highly investigated in both *in-situ* and *ex-situ* water treatment. However, the *in-situ* treatment holds some drawback for the only use of AC as the particles possess a stability issue in the increasing ionic strength atmosphere. So, Mackenzie *et al.* studied an effective activated carbon particles impregnated with ZVI colloidal particle having an average size of 800 nm for the halogenated organic hydrocarbon remediation. The main

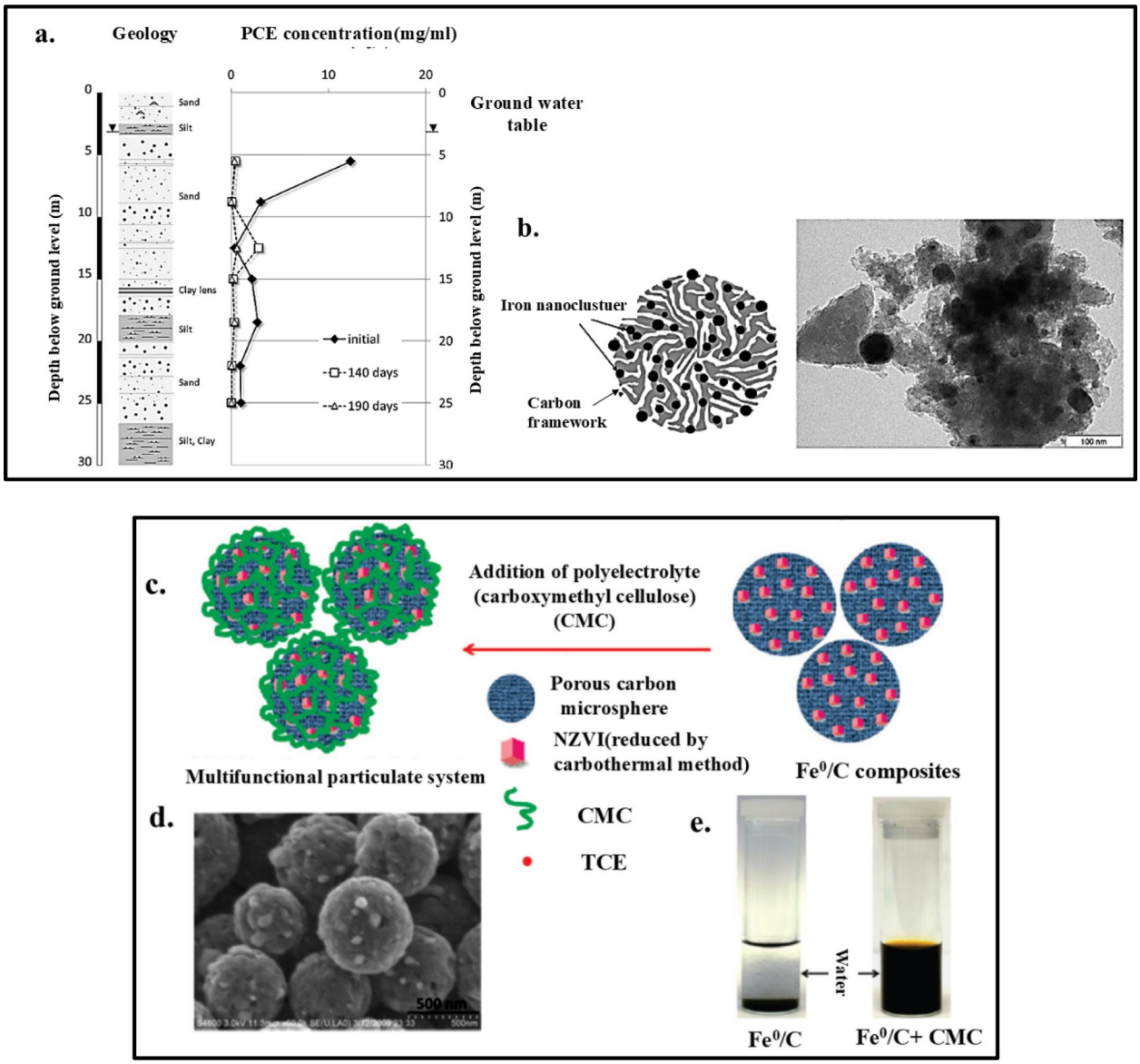

Figure 16. (a) Lateral geological and contamination profile near the injection point at the multi-level monitoring well CMT2. (b) Sketch (left) and TEM (right) images of Fe-AC composites. (Reproduced with permission from Ref. [42]. (c) Schematic diagram of CMC stabilized ZVI/C particles, (d) SEM image of ZVI/C-CMC colloidal particles. (e) Stability of ZVI/C-CMC in water (Adapted with permission from Ref. [223]).

reason for the use of ZVI was to provide a reactive center to the AC, as the AC could only form sorptive barrier inside the aquifer. Moreover, they introduced a polyanionic material such as humic acid to provide the particles more stability while transportation through sands. Later the same group further investigated about the transportability of carbo-iron particles stabilized with CMC.[42,117,222] This colloidal system was tested in a large scale sand column and it was found that initial 20 kg carbon-iron injection helped to reduce the perchloroethylene (PCE) significantly to a certain point but after 10 wk, it again started rising, though remained below the base value. Besides, the second injection led to reduction of the PCE from 19 mg/L to 1.5 µg/L in 200 days upon injecting almost 110 kg of particles (Figure 16a,b).

Similarly, Sunkara *et al.* synthesized ZVI/C based colloidal particles which were further stabilized by CMC. This composite performed the remediation of chlorinated contaminant (Trichloroethane TCE) and showed stability for more than 24 h which was clearly visible in the Figure 16(c–e). The visual image illustrates the stability of the colloidal particles.[223]

Georgi *et al.* investigated the effect of activated carbon colloidal (ACC) particles'suspension and studied the suspension stability by humic acid (HA) and CMC through batch experiments *via* sand column.[118] ACC has an excellent capability to adsorb several hydrophobic organic compounds (HOCs). In this report, they have synthesized and optimized the activity of colloidal ACC with particles size of 800 nm in the aquifer medium. Both the HA and CMC possessed negatively charged surface which can be effectively transported through the negatively charged sand particles *via* electrostatic repulsion. However, HA and CMC generated a homogenous deposition in the column resulting in the creation of uniform artificial sorption layer in terms of colloidal deposition in the sand column, but HA stabilized ACC showed

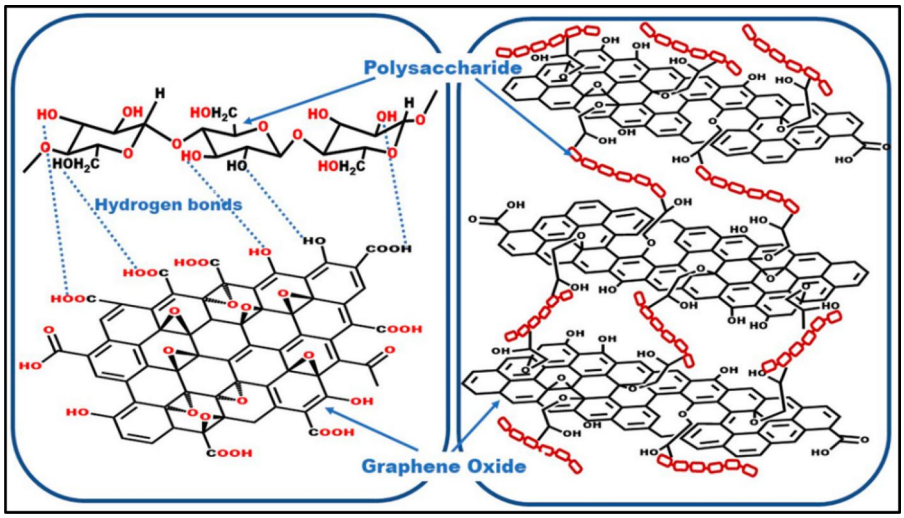

Figure 17. The intermolecular H-bonds between GO and hydroxyl/amino groups of polysaccharides (Adapted from [225]).

less suspension stability than CMC in the hard water environment. Results proved even in lower ACC concentration (5 g/L) and presence of 2 mM Ca^{2+} concentration, HA became ineffective whereas, CMC stabilized ACC achieved the stability in hard water conditions. Even at 11 g/L concentration of ACC was able to sustain 5 mM concentration of Ca^{2+}indicating their promise for the future on-field application of the activated carbon. Another group studied the colloidal activated carbon (CAC) and their stability using polydiallyldimethylammonium chloride (PolyDM) for the treatment of polyfluoroalkyl substances (PFAS). In their study, Guan *et al.* reported that polyDM was positively charged entity which altered the negatively charged CAC and made the overall charge of polyDM-CAC negative. Unlike the previous study where CMC stabilized ACC was negatively charged, this polyDM-CAC had an affinity toward quartz/sand particles *via* electrostatic attraction. This interaction created a high energy barrier which provides the particles to form strong bond with sand particles and prevented the particles to mobilize even if the ionic strength of the surroundings altered.[224] At a low ionic strength (0.1 mM), the polyDM-CAC particles were transported through sand to a particular layer and created a stable sorptive barrier in the regions like coastal area where fluctuations of the ionic strength frequently happens. Apart from these, GO and CNTs play crucial role in remediation of contaminants. GO and CNTs have extensive stability under water unlike the metals which are prone to easy oxidation. Due to presence of hydroxyl groups, GO has tendency to form H-bonds with polysaccharides which further enhance the suspension stability of GO (Figure 17).[225]. However, there are very few literatures reported for polymer modified CNTs for the waste removal from ground water probably due to their high cost; rather CNTs are generally used for membrane-based applications for site-specific waste water treatment.

Unlike the other fields, the discovery of Janus nanoparticles (Jps) could not grasp the interest in scientific community for nearly first 10 years due to absence of efficient methods. Later, with progression in unique fabrication techniques, the particles gained lucrative attention toward materials scientists.[226] Suitably functionalized Jps may behave like surfactant due to presence of their amphiphilicity. This property promotes the particles to stabilize emulsion or foams for an extended period. The Jps have a higher interfacial activity which helps to stabilize multiphasic systems (oil in water) by lowering their interfacial tension,[227] For example, Glaser *et al.* studied the synthesis of Jps having gold in one side and iron oxide on the other and subsequently studied the interfacial activity of Jps in hexane-water interface. To achieve highly effective amphiphilicity, gold compartments were capped with Dodecanethiol (DDS) and Octadecanethiol (OTD). The size of the Jps was found to be very less (14 nm) which were used further for interfacial study in hexane phase and water as a drop phase. The interfacial tension significantly dropped (22.5 mN/m in case for DDT capped gold particles and 18 mN/m for OTD capped) with respect to pure hexane-water mixture which proved the surface-active properties of those tiny biphasic particles (Figure 18a,b).[228]

Recently Ifra *et al.* and Pandey *et al.* synthesized a class of Jps *via* EHDC to produce ZVI encapsulated bicompartmental nanoparticles which were found to produce stable emulsion for 4 months and 1 month, respectively[45,208] (Figure 18c–e). In this former case, surface-initiated ATRP (SIATRP) was carried out for one hour to growpoly(2-dimethyl amino ethyl methacrylate) [PDMAEMA)] brushes from the surface of the bicompartmental spheres containing iron nanoparticles in one hemisphere followed by gold immobilization on the brush modified compartment only. The whole composite particles containing dual metallic nanoparticles were employed for the emulsion stabilization as well as interfacial catalysis to remove both hydrophobic and hydrophilic contaminants from water. Whereas Pandey *et al.* thoughtfully applied Janus nanoparticles inside ground water to deliver the catalytic nanoparticles in controlled manner at targeted zone. Later the same group developed a set of Janus particles composed of biodegradable polymers such as polylactic acid (PLA) and hydroxyl functionalized

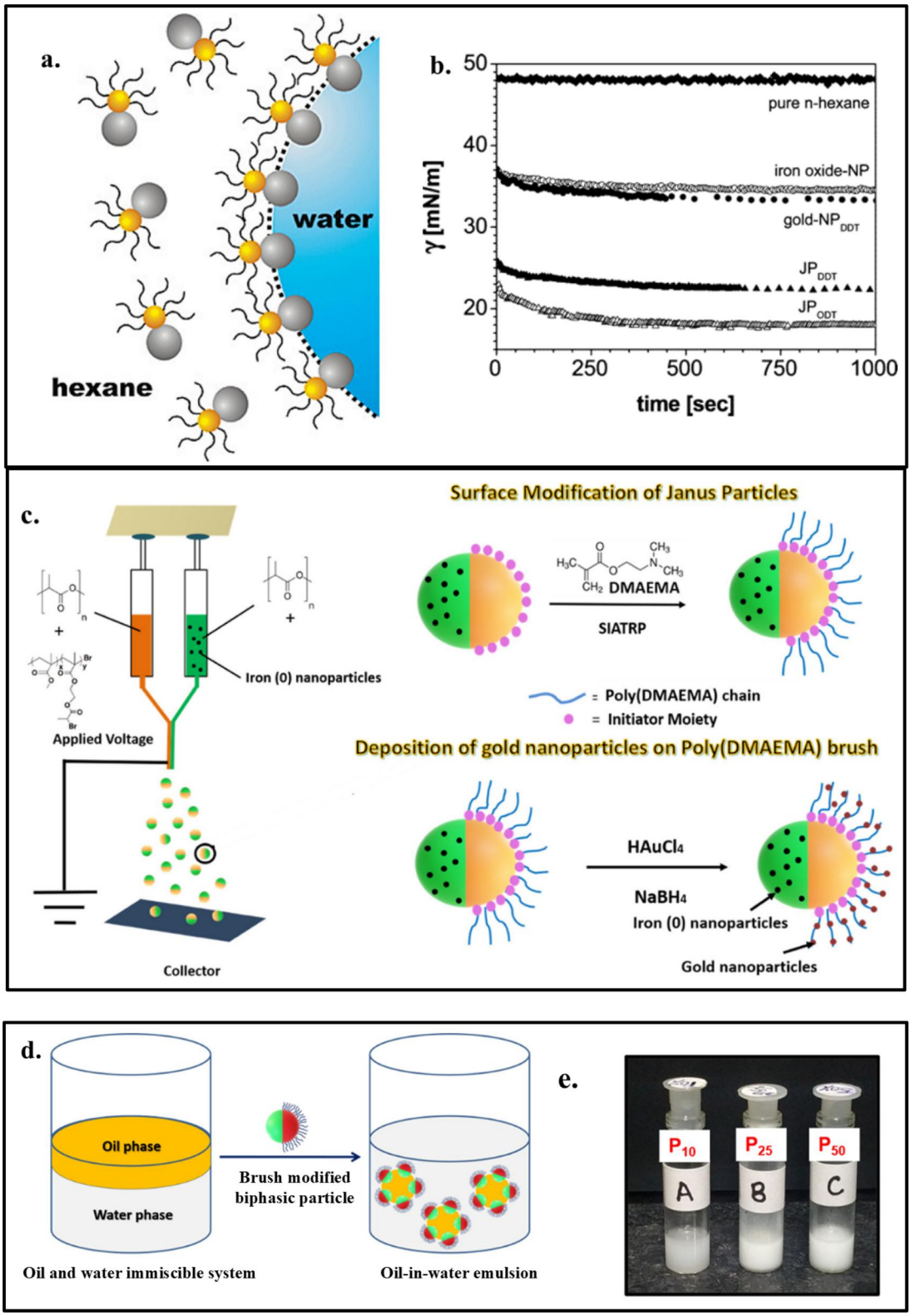

Figure 18. (a)Schematic presentation of the Jps (grey-iron oxide particles and yellow- gold) and (b) Interfacial tension measurement for surface modified Jps. (Adapted with permission from Ref. [228]). (c) and (d) Represents the schematic diagram and formation of the Jps made by Ifra et al. in oil-water interface and (e) emulsion stabilization of the Jps. (Adapted with permission from Ref. [208]). (f) ZVI encapsulated in P1- only PLA (without modification), P2- plasma treated PLA, and P3-both compartments having PLA in one side and tartrate-based polyester in another side which provides the amphiphilicity to the Janus particles. The graph shows the better transportability of the P3 system along sand column (Adapted with the permission from Ref. [229]).

polyester for encapsulating ZVI and performed sand column study in presence and absence of harsh environmental conditions (presence of varying ionic strength). They have found that the ZVI loaded Janus particles provided best result even under harsh conditions due to their enhanced mobility through the sand column (Figure 18f).[45,229]

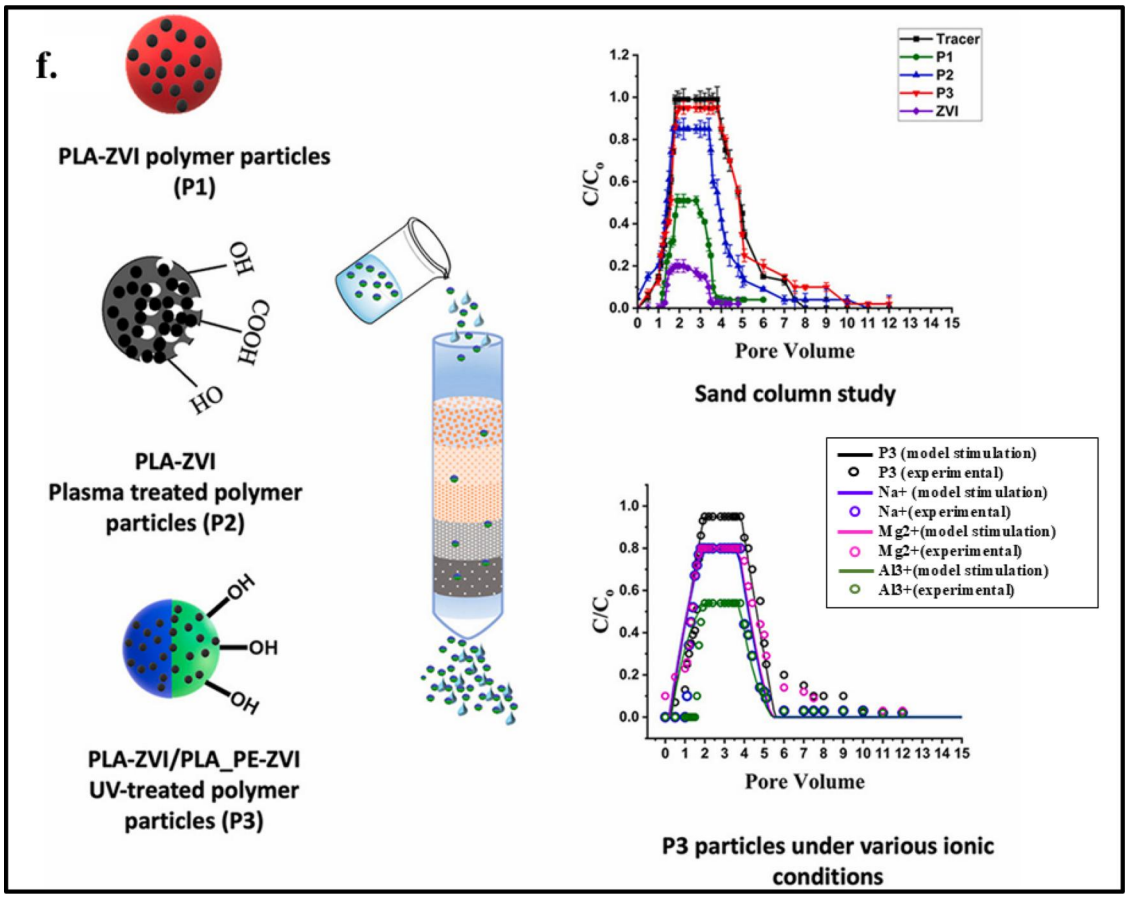

Figure 18. Continued

5. Current challenges of MNPs incorporated colloidal polymeric particles in real-time ground water remediation

Colloidal polymeric metal nanoparticles have garnered significant interest in recent years for *in situ* groundwater remediation, particularly for their ability to target and degrade a wide range of contaminants, including chlorinated solvents, hydrocarbons, and heavy metals. These nanoparticles are entrapped and stabilized with natural or synthetic polymers (e.g., polyacrylic acid, carboxymethyl cellulose, or dextran), exhibiting enhanced colloidal stability and reactivity, allowing for deeper subsurface transport and prolonged activity. Very few patents have been granted in this area, mostly with n-ZVI; such as US patent 20100232883, which describes a method for delivering polymer-coated reactive nanoparticles for groundwater cleanup, and WO2014168728A1 focusing on the use of bare nZVI or polymer-entrapped nZVI, such as calcium-alginate-entrapped nZVI, as environmental remediation agents for removing contaminants like arsenic from aqueous media.[230,231] These innovations have enabled more effective *in situ* treatment strategies, minimizing excavation and reducing long-term remediation costs. Table 4 summarizes about the accepted patents of polymer encapsulated n-ZVI for their application in ground water remediation *in situ*.

These composites are designed to adsorb and degrade chlorinated hydrocarbons such as trichloroethylene (TCE) in contaminated environments.[233] These patents highlight advancements in the development of polymer-stabilized iron nanoparticles for the effective *in situ* dechlorination of NAPLs in contaminated soils and groundwater. However, most of the study still confined in the laboratory. Scaling up colloidal systems remain a significant challenge and requires rigorous optimization at industrial scale. Another complex problem is to prepare water dispersible but cost effective biodegradable colloidal systems which remain stable under varying hydrogeological conditions. Since, industrial applications require field-scale deployment for treating TCE, and PCE plumes, with improved dispersion and contaminant contact provided by the polymeric stabilizer. Also, it is crucial to establish standardized protocols to obtain consistent transport and application of the materials inside ground water for reliable data generation. For example, an industrial zone contaminated with high degree of waste effluent needs well dispersed colloidal particles which remain unperturbed at ionic strength region and deliver the active catalyst at targeted zone. This requires a further comprehensive risk assessment to ensure the secondary pollution generated by the overdose of injected materials. Similarly, varying ionic strength and the temperature fluctuations of the subsurface may alter the conventional release kinetics of the active agents. The available data are yet to meet the requirements for the real-field applications which must be addressed for revolutionary progress in this field. Therefore, judicious research is required in order to refine the procedures for

Table 4. Patented studies for polymer encapsulated metal nanoparticles.

Patents	Metal nanoparticle	Polymer/stabilizer	Applications	Ref.
WO2014168728A1	n-ZVI	Calcium-Alginate	Arsenic removal in groundwater remediation	[230]
US20100232883A1	n-ZVI	Organic polymers	Soil and aquifer remediation (chlorinated solvents)	[231]
US20080190865A1	n-ZVI	Starch, Sodium Carboxymethyl Cellulose (CMC)	*In situ* degradation of chlorinated hydrocarbons in soils, sediments, groundwater	[232]
US20130058724A3	n-ZVI	Carboxymethyl Cellulose (CMC)	Composite materials for adsorption and dechlorination of TCE in groundwater	[233]

synthesizing the colloidal materials, serving the public regulatory issues and meeting the cost effectiveness of the products at industrial scale.

6. Conclusion and future outlook

For the last two decades, there has been a significant development for the miniaturization of the available systems for simplification of ground water remediation. Scientists are working tirelessly to get micron or nano sized particles with tunable functional properties. This metal encapsulated polymeric nano/micro particles can be synthesized easily *via* key synthesis methods like- emulsion solvent evaporation, EHDC, self-assembly, microfluidic etc. Applying pristine nanoparticles in ground water remediation face many challenges including their reproducibility, optimization for large scale production, mobility, water dispersibility, and stability. The metal encapsulation inside the biodegradable, eco-friendly polymers effectively provided solutions for easy transport and increased stability inside the ground water for a significant time. Furthermore, it is very important to understand the mechanism of colloidal particles' transportation through the subsurface region, the stability inside the aquifer, the interaction with contaminants and the contaminants' removal. Innumerable research has been conducted on such metal encapsulated systems, whether it is supported by another metal or inorganic systems or polymers. However, there is very limited research on the biodegradable polymers which can be employed to encapsulate metallic nanoparticles. Though promising results were achieved, mostly these studies remained in laboratory. Future research must focus on rational designing of the colloidal particles and scaling those up in economically favorable ways. In addition, the physicochemical characteristics and a well-accepted mechanism through which the particles interact with the soil while transporting through the subsurface are very rarely discussed in literatures. To establish a strong idea about the surface chemistry and the fate of the particles deep down in the ground water, especially at highly contaminated region, e.g., industrial waste contaminated zone, is vital for future research development. Another crucial factor that future research must address is the transition of the lab-based system to real-world applications, ensuring it does not leave behind any toxic residues in subsurface. If industrially viable, the biodegradable polymer coated nanoparticles would make them the most sustainable water remediation approach as compared to the existing alternatives.

Acknowledgments

The authors are thankful to the Department of Material Science and Engineering (DMSE), Indian Institute of Technology (IIT) Delhi, SERB for the support with grant number SPF/2023/00021 and CRF IIT Delhi for providing financial funds, research facility and characterizations. Author Chandrani Sarkar would like to express her deep gratitude to the Science and Engineering Research Board (SERB), India, for funding her research work under the National Post-Doctoral Fellowship Scheme (Reference No. PDF/2022/000679).

Disclosure statement

The authors declare no conflict of interest.

Funding

This work was supported by the Department of Science and Technology, Ministry of Science and Technology, India

References

[1] Döll, P.; Hoffmann-Dobrev, H.; Portmann, F. T.; Siebert, S.; Eicker, A.; Rodell, M.; Strassberg, G.; Scanlon, B. R. Impact of Water Withdrawals from Groundwater and Surface Water on Continental Water Storage Variations. *J. Geodyn.* **2012**, *59–60*, 143–156. DOI: 10.1016/j.jog.2011.05.001.

[2] Water Facts. | UN-Water, https://www.unwater.org/water-facts. (accessed 27 May 2025).

[3] Alharbi, B. H.; Pasha, M. J.; Alhudhodi, A. H.; Alduwais, A. K. Assessment of Soil Contamination Caused by Underground Fuel Leakage from Selected Gas Stations in Riyadh, Saudi Arabia. *Soil Sediment Contamin.* **2018**, *27*, 674–691. DOI: 10.1080/15320383.2018.1503228.

[4] Mgonja, C. T., Dar es Salaam Institute of Technology. The Consequences of Cracks Formed on the Oil and Gas Pipelines Weld Joints. *IJETT* **2017**, *54*, 223–232. DOI: 10.14445/22315381/IJETT-V54P232.

[5] Hu, J.; Tian, Y.; Teng, H.; Yu, L.; Zheng, M. The Probabilistic Life Time Prediction Model of Oil Pipeline Due to Local Corrosion Crack. *Theor. Appl. Fract. Mech.* **2014**, *70*, 10–18. DOI: 10.1016/j.tafmec.2014.04.002.

[6] Bortone, I.; Erto, A.; Di Nardo, A.; Santonastaso, G. F.; Chianese, S.; Musmarra, D. Pump-and-Treat Configurations with Vertical and Horizontal Wells to Remediate an Aquifer Contaminated by Hexavalent Chromium. *J. Contam. Hydrol.* **2020**, *235*, 103725. DOI: 10.1016/j.jconhyd.2020.103725.

[7] Sahu, D.; Pervez, S.; Karbhal, I.; Tamrakar, A.; Mishra, A.; Verma, S. R.; Deb, M. K.; Ghosh, K. K.; Pervez, Y. F.; Shrivas, K.; Satnami, M. L. Applications of Different Adsorbent Materials for the Removal of Organic and Inorganic Contaminants from Water and Wastewater: A Review. *Desalin. Water Treat.* **2024**, *317*, 100253. DOI: 10.1016/j.dwt.2024.100253.

[8] Satyam, S.; Patra, S. Innovations and Challenges in Adsorption-Based Wastewater Remediation: A Comprehensive

Review. *Heliyon* **2024**, *10*, e29573. DOI: 10.1016/j.heliyon.2024.e29573.

[9] Hashim, M. A.; Mukhopadhyay, S.; Sahu, J. N.; Sengupta, B. Remediation Technologies for Heavy Metal Contaminated Groundwater. *J. Environ. Manage.* **2011**, *92*, 2355–2388. DOI: 10.1016/j.jenvman.2011.06.009.

[10] Romantschuk, M.; Lahti-Leikas, K.; Kontro, M.; Galitskaya, P.; Talvenmäki, H.; Simpanen, S.; Allen, J. A.; Sinkkonen, A. Bioremediation of Contaminated Soil and Groundwater by in Situ Biostimulation. *Front. Microbiol.* **2023**, *14*, 1258148. DOI: 10.3389/fmicb.2023.1258148.

[11] Wei, K. H.; Ma, J.; Xi, B. D.; Yu, M. D.; Cui, J.; Chen, B. L.; Li, Y.; Gu, Q. B.; He, X. S. Recent Progress on in-Situ Chemical Oxidation for the Remediation of Petroleum Contaminated Soil and Groundwater. *J. Hazard. Mater.* **2022**, *432*, 128738. DOI: 10.1016/j.jhazmat.2022.128738.

[12] Wang, W.; Jia, J.; Zhang, B.; Xiao, B.; Yang, H.; Zhang, S.; Gao, X.; Han, Y.; Zhang, S.; Liu, Z.; et al. A Review of Sustained Release Materials for Remediation of Organically Contaminated Groundwater: Material Preparation, Applications and Prospects for Practical Application. *J. Hazard. Mater. Adv.* **2024**, *13*, 100393. DOI: 10.1016/j.hazadv.2023.100393.

[13] Yuan, L.; Wang, K.; Zhao, Q.; Yang, L.; Wang, G.; Jiang, M.; Li, L. An Overview of in Situ Remediation for Groundwater Co-contaminated with Heavy Metals and Petroleum Hydrocarbons. *J. Environ. Manage.* **2024**, *349*, 119342. DOI: 10.1016/j.jenvman.2023.119342.

[14] Kurniawan, T. A.; Lo, W.; Liang, X.; Goh, H. H.; Othman, M. H. D.; Chong, K. K.; Chew, K. W. Remediation Technologies for Contaminated Groundwater Due to Arsenic (As), Mercury (Hg), and/or Fluoride (F): A Critical Review and Way Forward to Contribute to Carbon Neutrality. *Separat. Purific. Tech.* **2023**, *314*, 123474. DOI: 10.1016/j.seppur.2023.123474.

[15] Bagheri, A. Micellar Interaction and Thermodynamic Behavior between Double-Chained Surface Active Ionic Liquid and Conventional Surfactants in Aqueous Solution. *Korean J. Chem. Eng.* **2023**, *40*, 2017–2025. DOI: 10.1007/s11814-023-1469-0.

[16] Sierra, M. B.; Rodríguez, J. L.; Minardi, R. M.; Morini, M. A.; Aicart, E.; Junquera, E.; Schulz, P. C. The Low Concentration Aggregation of Sodium Oleate-Sodium Linoleate Aqueous Mixtures. *Colloid Polym. Sci.* **2010**, *288*, 631–641. DOI: 10.1007/s00396-009-2171-4.

[17] Harwell, J. H.; Sabatini, D. A.; Knox, R. C. Surfactants for Ground Water Remediation. *Colloid. Surface A: Physicochem. Engng. Aspect.* **1999**, *151*, 255–268. DOI: 10.1016/S0927-7757(98)00785-7.

[18] Mnger, F. M.; Littau, C. A. Gemini Surfactants: Synthesis and Properties. *J. Americ. Chem. Societ.* **1991**, *113*, 1451–1452. DOI: 10.1021/ja00004a077

[19] Pensini, E.; Hsiung, C.; Ghazani, S. M.; Marangoni, A. A Zwitterionic Surfactant Concentrates Sulfolane in Floating Foams, to Purify Water. *Colloid. Surf. C: Environ. Aspec.* **2025**, *3*, 100051. DOI: 10.1016/j.colsuc.2024.100051.

[20] Binks, B. P. Particles as Surfactants Similarities and Differences. *Current Opinio. Colloid Interf. Sci.* **2002**, *7*, 21–41. DOI: 10.1016/S1359-0294(02)00008-0.

[21] Shi, Z.; Chen, J.; Liu, J.; Wang, N.; Sun, Z.; Wang, X. Anionic–Nonionic Mixed-Surfactant-Enhanced Remediation of PAH-Contaminated Soil. *Environ. Sci. Pollut. Res. Int.* **2015**, *22*, 12769–12774. DOI: 10.1007/s11356-015-4568-6.

[22] Vuong, N. M. T.; Nguyen, P. T.; Nguyen, T. K. O.; Nguyen, D. B.; Tran, T. M. D.; Oanh, L. T. K.; Nguyen, T. B.; Pham, T. T.; Lin, K. Y. A.; Bui, X. T. Application of Nano Zero-Valent Iron Particles Coated by Carboxymethyl Cellulose for Removal of Congo Red Dye in Aqueous Solution. *Case Stud. Chem. Environ. Eng.* **2023**, *8*, 100469. DOI: 10.1016/j.cscee.2023.100469.

[23] Yu, Q.; Guo, J.; Muhammad, Y.; Li, Q.; Lu, Z.; Yun, J.; Liang, Y. Mechanisms of Enhanced Hexavalent Chromium Removal from Groundwater by Sodium Carboxymethyl Cellulose Stabilized Zerovalent Iron Nanoparticles. *J. Environ. Manage.* **2020**, *276*, 111245. DOI: 10.1016/j.jenvman.2020.111245.

[24] Yang, X.; Yu, S.; Wang, M.; Liu, Q.; Jing, X.; Cai, X. One-Pot Preparations of Cyclodextrin Polymer-Entrapped Nano Zero-Valent Iron for the Removal of p-Nitrophenol in Water. *Chem. Engng. J.* **2022**, *431*, 133370. DOI: 10.1016/j.cej.2021.133370.

[25] Joseph, S.; Mathew, B. Facile Synthesis of Silver Nanoparticles and Their Application in Dye Degradation. *Mater. Sci. Engng. B.* **2015**, *195*, 90–97. DOI: 10.1016/j.mseb.2015.02.007.

[26] Huang, S. H.; Chen, D. H. Rapid Removal of Heavy Metal Cations and Anions from Aqueous Solutions by an Amino-Functionalized Magnetic Nano-Adsorbent. *J. Hazard. Mater.* **2009**, *163*, 174–179. DOI: 10.1016/j.jhazmat.2008.06.075.

[27] Zhou, C.; Zhang, W.; Xia, M.; Zhou, W.; Wan, Q.; Peng, K.; Zou, B. Synthesis of Poly(Acrylic Acid) Coated-Fe3O4 Superparamagnetic Nano-Composites and Their Fast Removal of Dye from Aqueous Solution. *J. Nanosci. Nanotechnol.* **2013**, *13*, 4627–4633. DOI: 10.1166/jnn.2013.6886.

[28] Bibi, A.; Bibi, S.; Abu-Dieyeh, M.; Al-Ghouti, M. A. New Material of Polyacrylic Acid-Modified Graphene Oxide Composite for Phenol Remediation from Synthetic and Real Wastewater. *Environ. Tech. Innov.* **2022**, *27*, 102795. DOI: 10.1016/j.eti.2022.102795.

[29] Moyo, M.; Modise, S. J.; Pakade, V. E. Palladium Nanoparticles Dispersed on Functionalized Macadamia Nutshell Biomass for Formic Acid-Mediated Removal of Chromium(VI) from Aqueous Solution. *Sci. Total Environ.* **2020**, *743*, 140614. DOI: 10.1016/j.scitotenv.2020.140614.

[30] Banu, R.; Gangapuram, B.; Ayodhya, D.; Dadigala, R.; Veerabhadram, G.; Kotu, G. M. Biogenic Synthesis of Carboxymethyl Cashew Gum Modified Gold Nanoparticles and Its Sensitive and Selective Calorimetric Detection of Hg2+ Ions and Catalytic Reduction of Methyl Red. *J. Fluoresc.* **2023**, *33*, 209–221. DOI: 10.1007/s10895-022-03073-3.

[31] Zayed, M. F.; Eisa, W. H.; Hosam, A. E. H. M.; Abou Zeid, A. M. Spectroscopic Investigation of Chitosan-Supported Cu2O/CuO Nanocomposite; a Separable Catalyst for Water-Pollutants Degradation. *J. Alloy. Comp.* **2020**, *835*, 155306. DOI: 10.1016/j.jallcom.2020.155306.

[32] Miller, S. M.; Zimmerman, J. B. Novel, Bio-Based, Photoactive Arsenic Sorbent: TiO2-Impregnated Chitosan Bead. *Water Res.* **2010**, *44*, 5722–5729. DOI: 10.1016/j.watres.2010.05.045.

[33] Wang, Y.; Hu, L.; Zhang, G.; Yan, T.; Yan, L.; Wei, Q.; Du, B. Removal of Pb(II) and Methylene Blue from Aqueous Solution by Magnetic Hydroxyapatite-Immobilized Oxidized Multi-Walled Carbon Nanotubes. *J. Colloid Interf. Sci.* **2017**, *494*, 380–388. DOI: 10.1016/j.jcis.2017.01.105.

[34] Ghasemi, Z.; Mohammadi, A. Sensitive and Selective Colorimetric Detection of Cu (II) in Water Samples by Thiazolylazopyrimidine-Functionalized TiO2 Nanoparticles. *Spectrochim. Acta. A Mol. Biomol. Spectrosc.* **2020**, *239*, 118554. DOI: 10.1016/j.saa.2020.118554.

[35] Gong, T.; Zhou, Y.; Sun, L.; Liang, W.; Yang, J.; Shuang, S.; Dong, C. Effective Adsorption of Phenolic Pollutants from Water Using β-Cyclodextrin Polymer Functionalized Fe_3O_4 Magnetic Nanoparticles. *RSC Adv.* **2016**, *6*, 80955–80963. DOI: 10.1039/C6RA16383A.

[36] Aga-Tagieva, S. E.; Omelyanchik, A. S.; Magomedov, K. E.; Motorzhina, A. V.; Orudzhev, F. F.; Rodionova, V. V.; Levada, E. V. PEGylated Iron-Oxide Nanoparticles: Structural, Magnetic, and Sorption Properties. *Nanotechnol. Russia.* **2023**, *18*, 886–893. DOI: 10.1134/S2635167623600633.

[37] Gorylewski, D.; Tyszczuk-Rotko, K.; Sowa, I.; Wójciak, M. Nanomolar Simultaneous Determination of Cd(II) and Pb(II) Using Composite Carbon Material Based on PEG-Functionalized Magnetic Nanoparticles (PEG-Fe3O4). *Food*

Chem. **2025**, *493*, 145647. DOI: 10.1016/j.foodchem.2025.145647.

[38] Chen, M.; Farooqi, Z. H.; Bolognesi, G.; Vladisavljević, G. T. Microfluidic Fabrication of Monodisperse and Recyclable TiO2-Poly(Ethylene Glycol) Diacrylate Hybrid Microgels for Removal of Methylene Blue from Aqueous Medium. *Langmuir* **2023**, *39*, 18784–18796. DOI: 10.1021/acs.langmuir.3c02276.

[39] Bhattacharjee, S.; Basnet, M.; Tufenkji, N.; Ghoshal, S. Effects of Rhamnolipid and Carboxymethylcellulose Coatings on Reactivity of Palladium-Doped Nanoscale Zerovalent Iron Particles. *Environ. Sci. Technol.* **2016**, *50*, 1812–1820. DOI: 10.1021/acs.est.5b05074.

[40] McCann, C. M.; Peacock, C. L.; Hudson-Edwards, K. A.; Shrimpton, T.; Gray, N. D.; Johnson, K. L. In Situ Arsenic Oxidation and Sorption by a Fe-Mn Binary Oxide Waste in Soil. *J. Hazard. Mater.* **2018**, *342*, 724–731. DOI: 10.1016/j.jhazmat.2017.08.066.

[41] Shan, H.; Mo, H.; Liu, Y.; Zeng, C.; Peng, S.; Zhan, H. As(III) Removal by a Recyclable Granular Adsorbent through Dopping Fe-Mn Binary Oxides into Graphene Oxide Chitosan. *Int. J. Biol. Macromol.* **2023**, *237*, 124184. DOI: 10.1016/j.ijbiomac.2023.124184.

[42] Mackenzie, K.; Bleyl, S.; Kopinke, F. D.; Doose, H.; Bruns, J. Carbo-Iron as Improvement of the Nanoiron Technology: From Laboratory Design to the Field Test. *Sci. Total Environ.* **2016**, *563-564*, 641–648. DOI: 10.1016/j.scitotenv.2015.07.107.

[43] Olajire, A. A.; Bamigbade, L. A. Green Synthesis of Chitosan-Based Iron@Silver Nanocomposite as Adsorbent for Wastewater Treatment. *Water Resour. Indust.* **2021**, *26*, 100158. DOI: 10.1016/j.wri.2021.100158.

[44] Sharma, R. K.; Arora, B.; Sharma, S.; Dutta, S.; Sharma, A.; Yadav, S.; Solanki, K. In Situ Hydroxyl Radical Generation Using the Synergism of the Co–Ni Bimetallic Centres of a Developed Nanocatalyst with Potent Efficiency for Degrading Toxic Water Pollutants. *Mater. Chem. Front.* **2020**, *4*, 605–620. DOI: 10.1039/C9QM00628A.

[45] Pandey, K.; Saha, S. Encapsulation of Zero Valent Iron Nanoparticles in Biodegradable Amphiphilic Janus Particles for Groundwater Remediation. *J. Hazard. Mater.* **2023**, *445*, 130501. DOI: 10.1016/j.jhazmat.2022.130501.

[46] Yu, R.; Shi, Y.; Yang, D.; Liu, Y.; Qu, J.; Yu, Z. Z. Graphene Oxide/Chitosan Aerogel Microspheres with Honeycomb-Cobweb and Radially Oriented Microchannel Structures for Broad-Spectrum and Rapid Adsorption of Water Contaminants. *ACS Appl. Mater. Interf.* **2017**, *9*, 21809–21819. DOI: 10.1021/acsami.7b04655.

[47] Stanisz, M.; Klapiszewski, Ł.; Jesionowski, T. Recent Advances in the Fabrication and Application of Biopolymer-Based Micro- and Nanostructures: A Comprehensive Review. *Chem. Engng. J.* **2020**, *397*, 125409. DOI: 10.1016/j.cej.2020.125409.

[48] Liu, Y.; Wang, J.; Shao, Y.; Deng, R.; Zhu, J.; Yang, Z. Recent Advances in Scalable Synthesis and Performance of Janus Polymer/Inorganic Nanocomposites. *Prog. Mater. Sci.* **2022**, *124*, 100888. DOI: 10.1016/j.pmatsci.2021.100888.

[49] Liang, F.; Liu, B.; Cao, Z.; Yang, Z. Janus Colloids toward Interfacial Engineering. *Langmuir* **2018**, *34*, 4123–4131. DOI: 10.1021/acs.langmuir.7b02308.

[50] Thompson, K. L.; Mable, C. J.; Lane, J. A.; Derry, M. J.; Fielding, L. A.; Armes, S. P. Preparation of Pickering Double Emulsions Using Block Copolymer Worms. *Langmuir* **2015**, *31*, 4137–4144. DOI: 10.1021/acs.langmuir.5b00741.

[51] Yang, S. M.; Kim, S. H.; Lim, J. M.; Yi, G. R. Synthesis and Assembly of Structured Colloidal Particles. *J. Mater. Chem.* **2008**, *18*, 2177–2190. DOI: 10.1039/b716393b.

[52] Venkatesan, J.; Gupta, P. K.; Son, S. E.; Hur, W.; Seong, G. H. Silver-Based Hybrid Nanomaterials: Preparations, Biological, Biomedical, and Environmental Applications. *J. Clust. Sci.* **2023**, *34*, 23–43. DOI: 10.1007/s10876-021-02212-3.

[53] Huang, B.; Xie, Q.; Yang, Z.; Lei, C.; Chen, W.; Tang, X.; Maran, F. Surfactant-Directed Pd-Nanoparticle Assemblies as Efficient Nanoreactors for Water Remediation. *EcoMat* **2020**, *2*, e12046. DOI: 10.1002/eom2.12046.

[54] Kalaiselvi, A.; Roopan, S. M.; Madhumitha, G.; Ramalingam, C.; Elango, G. Synthesis and Characterization of Palladium Nanoparticles Using Catharanthus Roseus Leaf Extract and Its Application in the Photo-Catalytic Degradation. *Spectrochim. Acta. A Mol. Biomol. Spectrosc.* **2015**, *135*, 116–119. DOI: 10.1016/j.saa.2014.07.010.

[55] Chaplin, B. P.; Reinhard, M.; Schneider, W. F.; Schüth, C.; Shapley, J. R.; Strathmann, T. J.; Werth, C. J. Critical Review of Pd-Based Catalytic Treatment of Priority Contaminants in Water. *Environ. Sci. Technol.* **2012**, *46*, 3655–3670. DOI: 10.1021/es204087q.

[56] Ahn, J. Y.; Kim, C.; Jun, S. C.; Hwang, I. Field-Scale Investigation of Nanoscale Zero-Valent Iron (NZVI) Injection Parameters for Enhanced Delivery of NZVI Particles to Groundwater. *Water Res.* **2021**, *202*, 117402. DOI: 10.1016/j.watres.2021.117402.

[57] Edmond, K. V.; Jacobson, T. W. P.; Oh, J. S.; Yi, G. R.; Hollingsworth, A. D.; Sacanna, S.; Pine, D. J. Large-Scale Synthesis of Colloidal Bowl-Shaped Particles. *Soft Matter.* **2021**, *17*, 6176–6181. DOI: 10.1039/d0sm00793e.

[58] Kim, J. W.; Larsen, R. J.; Weitz, D. A. Synthesis of Nonspherical Colloidal Particles with Anisotropic Properties. *J. Am. Chem. Soc.* **2006**, *128*, 14374–14377. DOI: 10.1021/ja065032m.

[59] Hussain, I.; Singh, N. B.; Singh, A.; Singh, H.; Singh, S. C. Green Synthesis of Nanoparticles and Its Potential Application. *Biotechnol. Lett.* **2016**, *38*, 545–560. DOI: 10.1007/s10529-015-2026-7.

[60] Attatsi, I. K.; Nsiah, F. Application of Silver Nanoparticles toward Co(II) and Pb(II) Ions Contaminant Removal in Groundwater. *Appl. Water Sci.* **2020**, *10*, 1–13. DOI: 10.1007/s13201-020-01240-0.

[61] Kassem Agha, M.; Maatouk, B.; Mhanna, R.; El-Dakdouki, M. H. Catalytic Degradation Efficacy of Silver Nanoparticles Fabricated Using Actinidia Deliciosa Peel Extract. *J. Nanomater.* **2024**, 20248813109.

[62] Rando, G.; Sfameni, S.; Galletta, M.; Drommi, D.; Cappello, S.; Plutino, M. R. Functional Nanohybrids and Nanocomposites Development for the Removal of Environmental Pollutants and Bioremediation. *Molecules* **2022**, *27*, 4856. DOI: 10.3390/molecules27154856.

[63] Yin, Z.; Cagnetta, G.; Huang, J. Mechanochemically Sulfidated Zero-Valent Iron as Persulfate Activation Catalyst in Permeable Reactive Barriers for Groundwater remediation: A Feasibility Study. *Chemosphere* **2023**, *311*, 137081. DOI: 10.1016/j.chemosphere.2022.137081.

[64] Giri, S.; Ganguli, S.; Bhattacharya, M. Surface Oxidation of Iron Nanoparticles. *Appl. Surf. Sci.* **2001**, *182*, 345–349. DOI: 10.1016/S0169-4332(01)00446-9.

[65] Mohammadian, S.; Tabani, H.; Boosalik, Z.; Rad, A. A.; Krok, B.; Fritzsche, A.; Khodaei, K.; Meckenstock, R. U. In Situ Remediation of Arsenic-Contaminated Groundwater by Injecting an Iron Oxide Nanoparticle-Based Adsorption Barrier. *Water. (Basel)* **2022**, *14*, 1998. DOI: 10.3390/w14131998.

[66] Luo, J.; Lai, H.; Jin, L.; Yang, Y.; Zhao, L.; Wang, J.; Cheng, D. Synthesis of Novel Magnetic Carboxyl-Functionalized Crosslinked Copolymer Microspheres for Methylene Blue Removal from Water. *Journal of Macromolecular Science, Part A: Pure and Applied Chemistry* **2025**, *62*, 201–211. DOI: 10.1080/10601325.2025.2452883.

[67] Benhalima, T.; Ferfera-Harrar, H.; Saha, N.; Saha, P. Fe3O4 Imbuing Carboxymethyl Cellulose/Dextran Sulfate Nanocomposite Hydrogel Beads: An Effective Adsorbent for Methylene Blue Dye Pollutant. *J. Macromol. Sci. Part A.* **2023**, *60*, 442–461. DOI: 10.1080/10601325.2023.2212731.

[68] Gui, M.; Smuleac, V.; Ormsbee, L. E.; Sedlak, D. L.; Bhattacharyya, D. Iron Oxide Nanoparticle Synthesis in

Aqueous and Membrane Systems for Oxidative Degradation of Trichloroethylene from Water. *J. Nanopart. Res.* **2012**, *14*, 861.

[69] Ma, Y.; Ni, M.; Li, S. Optimization of Malachite Green Removal from Water by TiO2 Nanoparticles under UV Irradiation. *Nanomaterials* **2018**, *8*, 428. DOI: 10.3390/nano8060428.

[70] Chao, C.; Xiangyu, W.; Chang, Y.; Huiling, L. Dechlorination of Disinfection by-Product Monochloroacetic Acid in Drinking Water by Nanoscale Palladized Iron Bimetallic Particle. *J. Environ. Sci.* **2008**, *20*, 945–951. DOI: 10.1016/S1001-0742(08)62191-9.

[71] Tang, C.; Wang, X.; Zhang, Y.; Liu, N.; Hu, X. Corrosion Behaviors and Kinetics of Nanoscale Zero-Valent Iron in Water: A Review. *J. Environ. Sci. (China)* **2024**, *135*, 391–406. DOI: 10.1016/j.jes.2022.12.028.

[72] Zhou, H.; Lv, L.; Ye, M.; Baig, S. A.; Luo, Y.; Chen, J.; Hu, S.; Zhang, H.; Wang, J. Improvement Strategy of Citrate and Biochar Assisted Nano-Palladium/Iron Composite for Effective Dechlorination of 2,4-Dichlorophenol. *Environ. Sci. Pollut. Res. Int.* **2024**, *31*, 34661–34674. DOI: 10.1007/s11356-024-33475-8.

[73] Zhu, N.; Luan, H.; Yuan, S.; Chen, J.; Wu, X.; Wang, L. Effective Dechlorination of HCB by Nanoscale Cu/Fe Particles. *J. Hazard. Mater.* **2010**, *176*, 1101–1105. DOI: 10.1016/j.jhazmat.2009.11.092.

[74] Dabwan, A. H. A.; Kaneco, S.; Katsumata, H.; Suzuki, T.; Egusa, K.; Ohta, K. Simultaneous Removal of Trihalomethanes by Bimetallic Ag/Zn: Kinetics Study. *Front. Chem. Eng. China* **2010**, *4*, 322–327. DOI: 10.1007/s11705-009-0261-y.

[75] Ali, F.; Mehmood, S.; Ashraf, A.; Saleem, A.; Younas, U.; Ahmad, A.; Bhatti, M. P.; Eldesoky, G. E.; Aljuwayid, A. M.; Habila, M. A.; et al. Ag-Cu Embedded SDS Nanoparticles for Efficient Removal of Toxic Organic Dyes from Water Medium. *Ind. Eng. Chem. Res.* **2023**, *62*, 4765–4777. DOI: 10.1021/acs.iecr.2c03460.

[76] Dwivedi, C.; Chaudhary, A.; Srinivasan, S.; Nandi, C. K. Polymer Stabilized Bimetallic Alloy Nanoparticles: Synthesis and Catalytic Application. *Colloid. Interf. Sci. Commun.* **2018**, *24*, 62–67. DOI: 10.1016/j.colcom.2018.04.001.

[77] Tokunaga, S.; Haron, M. J.; Wasay, S. A.; Uchiumi, A.; Wong, K. F.; Laosangthum, K. Removal of Fluoride Ions from Aqueous Solutions by Multivalent Metal Compounds. *Int. J. Environ. Stud.* **1995**, *48*, 17–28. DOI: 10.1080/00207239508710973.

[78] Chinnakoti, P.; Vankayala, R. K.; Chunduri, A. L. A.; Nagappagari, L. R.; Muthukonda, S. V.; Kamisetti, V. Trititanate Nanotubes as Highly Efficient Adsorbent for Fluoride Removal from Water: Adsorption Performance and Uptake Mechanism. *J. Environ. Chem. Eng.* **2016**, *4*, 4754–4768. DOI: 10.1016/j.jece.2016.11.007.

[79] Wang, J.; Xu, W.; Chen, L.; Jia, Y.; Wang, L.; Huang, X. J.; Liu, J. Excellent Fluoride Removal Performance by CeO2-ZrO2 Nanocages in Water Environment. *Chem. Engng. J.* **2013**, *231*, 198–205. DOI: 10.1016/j.cej.2013.07.022.

[80] Biswas, A.; Prathibha, C. Nanocomposite of Ceria and Trititanate Nanotubes as an Efficient Defluoridating Material for Real-Time Groundwater: Synthesis, Regeneration, and Leached Metal Risk Assessment. *ACS Omega.* **2021**, *6*, 31751–31764. DOI: 10.1021/acsomega.1c04424.

[81] Lingamdinne, L. P.; Koduru, J. R.; Karri, R. R. A Comprehensive Review of Applications of Magnetic Graphene Oxide Based Nanocomposites for Sustainable Water Purification. *J. Environ. Manage.* **2019**, *231*, 622–634. DOI: 10.1016/j.jenvman.2018.10.063.

[82] Azam, S. U.; Orlińska, B. Carbon Nanotubes as Advanced Catalysts and Catalytic Supports for the Liquid-Phase Aerobic Oxidation of Hydrocarbons: A Review. *Appl. Catal. A.* **2023**, *668*, 119465. DOI: 10.1016/j.apcata.2023.119465.

[83] Delgado, N.; Capparelli, A.; Navarro, A.; Marino, D. Pharmaceutical Emerging Pollutants Removal from Water Using Powdered Activated Carbon: Study of Kinetics and Adsorption Equilibrium. *J. Environ. Manage.* **2019**, *236*, 301–308. DOI: 10.1016/j.jenvman.2019.01.116.

[84] Su, D.; Maksimova, N. I.; Mestl, G.; Kuznetsov, V. L.; Keller, V.; Schlögl, R.; Keller, N. Oxidative Dehydrogenation of Ethylbenzene to Styrene over Ultra-Dispersed Diamond and Onion-like Carbon. *Carbon. N Y* **2007**, *45*, 2145–2151. DOI: 10.1016/j.carbon.2007.07.005.

[85] Zhang, J.; Liu, X.; Blume, R.; Zhang, A.; Schlögl, R.; Dang, S. S. Surface-Modified Carbon Nanotubes Catalyze Oxidative Dehydrogenation of n-Butane. *Science* **2008**, *322*, 73–77. DOI: 10.1126/science.1161916.

[86] Yang, S.; Li, X.; Zhu, W.; Wang, J.; Descorme, C. Catalytic Activity, Stability and Structure of Multi-Walled Carbon Nanotubes in the Wet Air Oxidation of Phenol. *Carbon. N Y* **2008**, *46*, 445–452. DOI: 10.1016/j.carbon.2007.12.006.

[87] Liao, S.; Peng, F.; Yu, H.; Wang, H. Carbon Nanotubes as Catalyst for the Aerobic Oxidation of Cumene to Cumene Hydroperoxide. *Appl. Catal. A.* **2014**, *478*, 1–8. DOI: 10.1016/j.apcata.2014.03.024.

[88] Luo, J.; Peng, F.; Yu, H.; Wang, H. Selective Liquid Phase Oxidation of Benzyl Alcohol Catalyzed by Carbon Nanotubes. *Chem. Engng. J.* **2012**, *204-206*, 98–106. DOI: 10.1016/j.cej.2012.07.098.

[89] Luo, J.; Peng, F.; Yu, H.; Wang, H.; Zheng, W. Aerobic Liquid-Phase Oxidation of Ethylbenzene to Acetophenone Catalyzed by Carbon Nanotubes. *ChemCatChem* **2013**, *5*, 1578–1586. DOI: 10.1002/cctc.201200603.

[90] Zhao, G.; Li, J.; Ren, X.; Chen, C.; Wang, X. Few-Layered Graphene Oxide Nanosheets as Superior Sorbents for Heavy Metal Ion Pollution Management. *Environ. Sci. Technol.* **2011**, *45*, 10454–10462. DOI: 10.1021/es203439v.

[91] Liu, L.; Liu, S.; Zhang, Q.; Li, C.; Bao, C.; Liu, X.; Xiao, P. Adsorption of Au(III), Pd(II), and Pt(IV) from Aqueous Solution onto Graphene Oxide. *J. Chem. Eng. Data.* **2013**, *58*, 209–216. DOI: 10.1021/je300551c.

[92] Zhao, G.; Ren, X.; Gao, X.; Tan, X.; Li, J.; Chen, C.; Huang, Y.; Wang, X. Removal of Pb(ii) Ions from Aqueous Solutions on Few-Layered Graphene Oxide Nanosheets. *Dalton Trans.* **2011**, *40*, 10945–10952. DOI: 10.1039/c1dt11005e.

[93] Yang, S. T.; Chang, Y.; Wang, H.; Liu, G.; Chen, S.; Wang, Y.; Liu, Y.; Cao, A. Folding/Aggregation of Graphene Oxide and Its Application in Cu2+ Removal. *J. Colloid Interf. Sci.* **2010**, *351*, 122–127. DOI: 10.1016/j.jcis.2010.07.042.

[94] Zhao, Y.; Jafvert, C. T. Environmental Photochemistry of Single Layered Graphene Oxide in Water. *Environ. Sci. Nano.* **2015**, *2*, 136–142. DOI: 10.1039/C4EN00209A.

[95] Matsumoto, Y.; Koinuma, M.; Ida, S.; Hayami, S.; Taniguchi, T.; Hatakeyama, K.; Tateishi, H.; Watanabe, Y.; Amano, S. Photoreaction of Graphene Oxide Nanosheets in Water. *J. Phys. Chem. C.* **2011**, *115*, 19280–19286. DOI: 10.1021/jp206348s.

[96] Wang, B.; Fielding, A. J.; Dryfe, R. A. W. Electron Paramagnetic Resonance as a Structural Tool to Study Graphene Oxide: Potential Dependence of the EPR Response. *J. Phys. Chem. C.* **2019**, *123*, 22556–22563. DOI: 10.1021/acs.jpcc.9b04292.

[97] Arnold, W. A.; Roberts, A. L. Pathways and Kinetics of Chlorinated Ethylene and Chlorinated Acetylene Reaction with Fe(0) Particles. *Environ. Sci. Technol.* **2000**, *34*, 1794–1805. DOI: 10.1021/es990884q.

[98] Elliott, D. W.; Zhang, W. X. Field Assessment of Nanoscale Bimetallic Particles for Groundwater Treatment. *Environ. Sci. Technol.* **2001**, *35*, 4922–4926. DOI: 10.1021/es0108584.

[99] Godvin Sharmila, V.; Kavitha, S.; Rajashankar, K.; Yeom, I. T.; Rajesh Banu, J. Effects of Titanium Dioxide Mediated Dairy Waste Activated Sludge Deflocculation on the Efficiency of Bacterial Disintegration and Cost of Sludge Management. *Bioresour. Technol.* **2015**, *197*, 64–71. DOI: 10.1016/j.biortech.2015.08.038.

[100] Zhou, L.; Zhuang, W. Q.; De Costa, Y.; Xia, S. Potential Effects of Suspended TiO2 Nanoparticles on Activated Sludge Floc Properties in Membrane Bioreactors. *Chemosphere* **2019**, *223*, 148–156. DOI: 10.1016/j.chemosphere.2019.02.042.

[101] Lin, S.; Lu, D.; Liu, Z. Removal of Arsenic Contaminants with Magnetic γ-Fe2O3 Nanoparticles. *Chem. Engng. J.* **2012**, *211-212*, 46–52. DOI: 10.1016/j.cej.2012.09.018.

[102] Luther, S.; Borgfeld, N.; Kim, J.; Parsons, J. G. Removal of Arsenic from Aqueous Solution: A Study of the Effects of pH and Interfering Ions Using Iron Oxide Nanomaterials. *Microchem. J.* **2012**, *101*, 30–36. DOI: 10.1016/j.microc.2011.10.001.

[103] Leiva, E.; Tapia, C.; Rodríguez, C.; Palet, C.; Bastos-Arrieta, J. Highly Efficient Removal of Cu(II) Ions from Acidic Aqueous Solution Using ZnO Nanoparticles as Nano-adsorbents. *Waters (Basel)*. **2021**, *13*, 2960. DOI: 10.3390/w13212960.

[104] Law, C. K. Y.; Kundu, K.; Bonin, L.; Peñacoba-Antona, L.; Bolea-Fernandez, E.; Vanhaecke, F.; Rabaey, K.; Esteve-Núñez, A.; De Gusseme, B.; Boon, N. Electrochemically Assisted Production of Biogenic Palladium Nanoparticles for the Catalytic Removal of Micropollutants in Wastewater Treatment Plants Effluent. *J. Environ. Sci. (China)*. **2023**, *128*, 203–212. DOI: 10.1016/j.jes.2022.08.018.

[105] Chen, L.; Yang, J.; Zeng, X.; Zhang, L.; Yuan, W. Adsorption of Methylene Blue in Water by Reduced Graphene Oxide: Effect of Functional Groups. *Mat. Express.* **2013**, *3*, 281–290. DOI: 10.1166/mex.2013.1130.

[106] Lin, Y.; Jin, X.; Owens, G.; Chen, Z. Simultaneous Removal of Mixed Contaminants Triclosan and Copper by Green Synthesized Bimetallic Iron/Nickel Nanoparticles. *Sci. Total Environ.* **2019**, *695*, 133878. DOI: 10.1016/j.scitotenv.2019.133878.

[107] Singh, N.; Yadav, A.; Das, S.; Debnath, N. Recent Advances in Heavy Metal/Metalloid Ion Treatment from Wastewater Using Nanocomposites and Bionanocomposites. *Front. Nanotechnol.* **2024**, *6*, 1307353. DOI: 10.3389/fnano.2024.1307353.

[108] Nel, A.; Xia, T.; Mädler, L.; Li, N. Toxic Potential of Materials at the Nanolevel. *Science* **2006**, *311*, 622–627. DOI: 10.1126/science.1114397.

[109] Cheng, Y.; Yin, L.; Lin, S.; Wiesner, M.; Bernhardt, E.; Liu, J. Toxicity Reduction of Polymer-Stabilized Silver Nanoparticles by Sunlight. *J. Phys. Chem. C.* **2011**, *115*, 4425–4432. DOI: 10.1021/jp109789j.

[110] Estrada, A. C.; Daniel-da-Silva, A. L.; Leal, C.; Monteiro, C.; Lopes, C. B.; Nogueira, H. I. S.; Lopes, I.; Martins, M. J.; Martins, N. C. T.; Gonçalves, N. P. F.; et al. Colloidal Nanomaterials for Water Quality Improvement and Monitoring. *Front. Chem.* **2023**, *11*, 1209263. DOI: 10.3389/fchem.2022.1011186.

[111] Pandey, K.; Sharma, S.; Saha, S. Advances in Design and Synthesis of Stabilized Zero-Valent Iron Nanoparticles for Groundwater Remediation. *J. Environ. Chem. Eng.* **2022**, *10*, 107993. DOI: 10.1016/j.jece.2022.107993.

[112] Potara, M.; Focsan, M.; Craciun, A. M.; Botiz, I.; Astilean, S. Polymer-Coated Plasmonic Nanoparticles for Environmental Remediation: Synthesis, Functionalization, and Properties. *New Polymer Nanocompos. Environ. Remed.* **2018**, 361–387.

[113] Olawade, D. B.; Wada, O. Z.; Egbewole, B. I.; Fapohunda, O.; Ige, A. O.; Usman, S. O.; Ajisafe, O. Metal and Metal Oxide Nanomaterials for Heavy Metal Remediation: Novel Approaches for Selective, Regenerative, and Scalable Water Treatment. *Front. Nanotechnol.* **2024**, *6*, 1466721. DOI: 10.3389/fnano.2024.1466721.

[114] Kamyab, H.; Chelliapan, S.; Hayder, G.; Yusuf, M.; Taheri, M. M.; Rezania, S.; Hasan, M.; Yadav, K. K.; Khorami, M.; Farajnezhad, M.; Nouri, J. Exploring the Potential of Metal and Metal Oxide Nanomaterials for Sustainable Water and Wastewater Treatment: A Review of Their Antimicrobial Properties. *Chemosphere* **2023**, *335*, 139103. DOI: 10.1016/j.chemosphere.2023.139103.

[115] Elella, M. H. A.; Goda, E. S.; Gab-Allah, M. A.; Hong, S. E.; Lijalem, Y. G.; Yoon, K. R. Biodegradable Polymeric Nanocomposites for Wastewater Treatment. *Engng. Mater.* **2022**, 245–298.

[116] Kamai, T.; Nassar, M. K.; Nelson, K. E.; Ginn, T. R. Colloid Filtration Prediction by Mapping the Correlation-Equation Parameters from Transport Experiments in Porous Media. *Water Resourc. Res.* **2015**, *51*, 8995–9012. DOI: 10.1002/2015WR017403.

[117] Mackenzie, K.; Georgi, A.; Mackenzie, K.; Schierz, A. Colloidal Activated Carbon and CARBO-IRON-Novel Material for in-Situ Groundwater Treatment. *Global Nest J.* **2008**, *10*, 54–61.

[118] Georgi, A.; Schierz, A.; Mackenzie, K.; Kopinke, F. D. Colloidal Activated Carbon for in-Situ Groundwater Remediation—Transport Characteristics and Adsorption of Organic Compounds in Water-Saturated Sediment Columns. *J. Contam. Hydrol.* **2015**, *179*, 76–88. DOI: 10.1016/j.jconhyd.2015.05.002.

[119] Costa, T. B.; Matias, P. M. C.; Sharma, M.; Murtinho, D.; Rosa, D. S.; Valente, A. J. M. Recent Advances on Starch-Based Adsorbents for Heavy Metal and Emerging Pollutant Remediation. *Polymers (Basel).* **2024**, *17*, 15. DOI: 10.3390/polym17010015.

[120] Su, M.; Yin, W.; Liu, L.; Li, P.; Fang, Z.; Fang, Y.; Chiang, P.; Wu, J. Enhanced Cr(VI) Stabilization in Soil by Carboxymethyl Cellulose-Stabilized Nanosized Fe0 (CMC-nFe0) and Mixed Anaerobic Microorganisms. *J. Environ. Manage.* **2020**, *257*, 109951. DOI: 10.1016/j.jenvman.2019.109951.

[121] Alnemari, A. M.; Moustapha, M. E.; Hassan, A. A.; Salah, D. Chitosan Nano-composites Applications for Water Remediation. *Cogent Eng.* **2023**, *10*, 2220498. DOI: 10.1080/23311916.2023.2220498.

[122] Sajjadi, M.; Ahmadpoor, F.; Nasrollahzadeh, M.; Ghafuri, H. Lignin-Derived (Nano)Materials for Environmental Pollution Remediation: Current Challenges and Future Perspectives. *Int. J. Biol. Macromol.* **2021**, *178*, 394–423. DOI: 10.1016/j.ijbiomac.2021.02.165.

[123] Zheng, D.; Wang, K.; Bai, B. A Critical Review of Sodium Alginate-Based Composites in Water Treatment. *Carbohydr. Polym.* **2024**, *331*, 121850. DOI: 10.1016/j.carbpol.2024.121850.

[124] Fouda-Mbanga, B. G.; Tywabi-Ngeva, Z.; Badawy, W. M.; Ebite, C.; Onotu, O. P.; Abogidi, C.; Uzordinma, A. P.; Kaba, S. Green Cyclodextrins-Derivatives for Sustainable Remediation of Pesticides and Heavy Metals: A Review. *J. Mol. Struct.* **2025**, *1328*, 141326. DOI: 10.1016/j.molstruc.2025.141326.

[125] Yadav, N.; Nain, L.; Khare, S. K. Studies on the Degradation and Characterization of a Novel Metal-Free Polylactic Acid Synthesized via Lipase-Catalyzed Polymerization: A Step towards Curing the Environmental Plastic Issue. *Environ. Tech. Innov.* **2021**, *24*, 101845. DOI: 10.1016/j.eti.2021.101845.

[126] Wei, Y. Y.; Sun, X. T.; Xu, Z. R. One-Step Synthesis of Bifunctional PEGDA/TiO2 Composite Film by Photopolymerization for the Removal of Congo Red. *Appl. Surf. Sci.* **2018**, *445*, 437–444. DOI: 10.1016/j.apsusc.2018.03.149.

[127] Su, E.; Okay, O. Hybrid Cross-Linked Poly(2-Acrylamido-2-Methyl-1-Propanesulfonic Acid) Hydrogels with Tunable Viscoelastic, Mechanical and Self-Healing Properties. *React. Funct. Polym.* **2018**, *123*, 70–79. DOI: 10.1016/j.reactfunctpolym.2017.12.009.

[128] Saha, Sampa, Ifra, Fabrication of Topologically Anisotropic Microparticles and Their Surface Modification with pH Responsive Polymer Brush. *Mater Sci Eng C Mater Biol Appl.* **2019**, *104*, 109894. DOI: 10.1016/j.msec.2019.109894.

[129] Shrivastava, S.; Upadhyay, A.; Pradhan, S. S.; Saha, S.; Singh, A. Evolution Kinetics of Stabilizing Pickering Emulsion by Brush-Modified Janus Particles: DPD Simulation and

Experimental Insights. *Langmuir* **2024**, *40*, 13920–13934. DOI: 10.1021/acs.langmuir.4c01083.

[130] Pradhan, S. S.; Saha, S. Advances in Design and Applications of Polymer Brush Modified Anisotropic Particles. *Adv. Colloid. Interf. Sci.* **2022**, *300*, 102580. DOI: 10.1016/j.cis.2021.102580.

[131] Dutta, S.; Shreyash, N.; Satapathy, B. K.; Saha, S. Advances in Design of Polymer Brush Functionalized Inorganic Nanomaterials and Their Applications in Biomedical Arena. *Wiley Interdisciplinary Review. Nanomed. Nanobiotech.* **2023**, *15*, e1861.

[132] Mirza, I.; Saha, S. Biocompatible Anisotropic Polymeric Particles: Synthesis, Characterization, and Biomedical Applications. *ACS Appl. Bio Mater.* **2020**, *3*, 8241–8270. DOI: 10.1021/acsabm.0c01075.

[133] Wu, S.; Guo, W.; Li, B.; Zhou, H.; Meng, H.; Sun, J.; Li, R.; Guo, D.; Zhang, X.; Li, R.; Qu, W. Progress of Polymer-Based Strategies in Fungal Disease Management: Designed for Different Roles. *Front. Cell. Infect. Microbiol.* **2023**, *13*, 1142029. DOI: 10.3389/fcimb.2023.1142029.

[134] Pédrot, M.; Dia, A.; Davranche, M.; Bouhnik-Le Coz, M.; Henin, O.; Gruau, G. Insights into Colloid-Mediated Trace Element Release at the Soil/Water Interface. *J. Colloid Interf. Sci.* **2008**, *325*, 187–197. DOI: 10.1016/j.jcis.2008.05.019.

[135] Sen, T. K.; Khilar, K. C. Review on Subsurface Colloids and Colloid-Associated Contaminant Transport in Saturated Porous Media. *Adv. Colloid Interf. Sci.* **2006**, *119*, 71–96. DOI: 10.1016/j.cis.2005.09.001.

[136] Gavrilescu, M. *The Role of Colloidal Systems in Environmental Protection*. Ed. Fanun, M., Palestine, 2014; pp 363–397.

[137] Albert Pearce, B. E.; Voudrias, E. A.; Whelan, M. P. Dissolution of TCE and TCA Pools in Saturated Subsurface Systems. *J. Environ. Eng.* **1994**, *120*, 1191–1206. DOI: 10.1061/(ASCE)0733-9372(1994)120:5(1191).

[138] Huling, S. G.; Weaver, J. W. Dense Nonaqueous Phase Liquid. Superfund Technology Support Center for Ground Water Ground Water Issue. **1991**.

[139] Verma, K.; Sarkar, C.; Saha, S. Exploration of Biodegradable Polymeric Particles in Agriculture: A Holistic Approach for Sustainable Farming. *Environ. Sci.: Adv.* **2025**, *4*, 409–431.

[140] Spielman-Sun, E.; Boye, K.; Dwivedi, D.; Engel, M.; Thompson, A.; Kumar, N.; Noël, V. A Critical Look at Colloid Generation, Stability, and Transport in Redox-Dynamic Environments: Challenges and Perspectives. *ACS Earth Space Chem.* **2024**, *8*, 630–653. DOI: 10.1021/acsearthspacechem.3c00255.

[141] Bizmark, N.; Ioannidis, M. A. Effects of Ionic Strength on the Colloidal Stability and Interfacial Assembly of Hydrophobic Ethyl Cellulose Nanoparticles. *Langmuir* **2015**, *31*, 9282–9289. DOI: 10.1021/acs.langmuir.5b01857.

[142] Ryan, J. N.; Elimelech, M. Colloid Mobilization and Transport in Groundwater. *Colloid. Surface A Physicochem. Engng. Aspect.* **1996**, *107*, 1–56. DOI: 10.1016/0927-7757(95)03384-X.

[143] Gavrilescu, M. Colloid-Mediated Transport and the Fate of Contaminants in Soils. *Role Colloid. Sys. Environ. Protect.* **2014**, 397–451.

[144] Reihanifar, M.; Takallou, A.; Taheri, M.; Gholizadeh Lonbar, A.; Ahmadi, M.; Sharifi, A. Nanotechnology Advancements in Groundwater Remediation: A Comprehensive Analysis of Current Research and Future Prospects. *Groundwater Sustain. Develop.* **2024**, *27*, 101330. DOI: 10.1016/j.gsd.2024.101330.

[145] Zhang, C.; Chung, J. W.; Priestley, R. D. Dialysis Nanoprecipitation of Polystyrene Nanoparticles. *Macromol. Rapid Commun.* **2012**, *33*, 1798–1803. DOI: 10.1002/marc.201200335.

[146] Huang, Y.; Stonehouse, A.; Abeykoon, C. Encapsulation Methods for Phase Change Materials: A Critical Review. *Int. J. Heat Mass Transf.* **2023**, *200*, 123458. DOI: 10.1016/j.ijheatmasstransfer.2022.123458.

[147] Carpenter, J.; Saharan, V. K. Ultrasonic Assisted Formation and Stability of Mustard Oil in Water Nanoemulsion: Effect of Process Parameters and Their Optimization. *Ultrason. Sonochem.* **2017**, *35*, 422–430. DOI: 10.1016/j.ultsonch.2016.10.021.

[148] Rajendra, P. K. M.; Nidamanuri, B. S. S.; Balan, A. P.; Venkatachalam, S.; Jawahar, N. A Review on Structure, Preparation and Applications of Silk Fibroin-Based Nano-Drug Delivery Systems. *J. Nanopart. Res.* **2022**, *24*. DOI: 10.1007/s11051-022-05526-z.

[149] Wang, Y.; Li, P.; Tran, T. T. D.; Zhang, J.; Kong, L. Manufacturing Techniques and Surface Engineering of Polymer Based Nanoparticles for Targeted Drug Delivery to Cancer. *Nanomaterials* **2016**, *6*, 26. DOI: 10.3390/nano6020026.

[150] Martínez Rivas, C. J.; Tarhini, M.; Badri, W.; Miladi, K.; Greige-Gerges, H.; Nazari, Q. A.; Galindo Rodríguez, S. A.; Román, R. Á.; Fessi, H.; Elaissari, A. Nanoprecipitation Process: From Encapsulation to Drug Delivery. *Int. J. Pharm.* **2017**, *532*, 66–81. DOI: 10.1016/j.ijpharm.2017.08.064.

[151] Legrand, P.; Lesieur, S.; Bochot, A.; Gref, R.; Raatjes, W.; Barratt, G.; Vauthier, C. Influence of Polymer Behaviour in Organic Solution on the Production of Polylactide Nanoparticles by Nanoprecipitation. *Int. J. Pharm.* **2007**, *344*, 33–43. DOI: 10.1016/j.ijpharm.2007.05.054.

[152] Bilati, U.; Allémann, E.; Doelker, E. Development of a Nanoprecipitation Method Intended for the Entrapment of Hydrophilic Drugs into Nanoparticles. *Eur. J. Pharm. Sci.* **2005**, *24*, 67–75. DOI: 10.1016/j.ejps.2004.09.011.

[153] Bazylińska, U.; Lewińska, A.; Lamch, Ł.; Wilk, K. A. Polymeric Nanocapsules and Nanospheres for Encapsulation and Long Sustained Release of Hydrophobic Cyanine-Type Photosensitizer. *Colloid. Surface A Physicochem. Engng. Aspect.* **2014**, *442*, 42–49. DOI: 10.1016/j.colsurfa.2013.02.023.

[154] Plüisch, C. S.; Wittemann, A. Assembly of Nanoparticles into "Colloidal Molecules": Toward Complex and yet Defined Colloids with Exciting Perspectives. In Rahman, M., Asiri, A., Eds. IntechOpen, Bonn, Germany, 2016

[155] Pulingam, T.; Foroozandeh, P.; Chuah, J. A.; Sudesh, K. Exploring Various Techniques for the Chemical and Biological Synthesis of Polymeric Nanoparticles. *Nanomaterials* **2022**, *12*, 576. DOI: 10.3390/nano12030576.

[156] Fruntke, A.; Hülsmann, J.; Skodda, L. H.; Blümbott, B.; Godmann, M.; Koschella, A.; Heinzel, T.; Heinze, T.; Wilke, T. Polysaccharide-Based Nanoparticles Prepared by Dialysis: Novel Drug Delivery Systems for Chemistry Education. *J. Chem. Educ.* **2025**, *102*, 1169–1178. DOI: 10.1021/acs.jchemed.4c00895.

[157] Thompson, K. L.; Williams, M.; Armes, S. P. Colloidosomes: Synthesis, Properties and Applications. *J. Colloid. Interf. Sci.* **2015**, *447*, 217–228. DOI: 10.1016/j.jcis.2014.11.058.

[158] Dinsmore, A. D.; Hsu, M. F.; Nikolaides, M. G.; Marquez, M.; Bausch, A. R.; Weitz, D. A. Colloidosomes: Selectively Permeable Capsules Composed of Colloidal Particles. *Science* **2002**, *298*, 1006–1009. DOI: 10.1126/science.1074868.

[159] Laïb, S.; Routh, A. F. Fabrication of Colloidosomes at Low Temperature for the Encapsulation of Thermally Sensitive Compounds. *J. Colloid Interf. Sci.* **2008**, *317*, 121–129. DOI: 10.1016/j.jcis.2007.09.019.

[160] Hsu, M. F.; Nikolaides, M. G.; Dinsmore, A. D.; Bausch, A. R.; Gordon, V. D.; Chen, X.; Hutchinson, J. W.; Weitz, D. A.; Marquez, M. Self-Assembled Shells Composed of Colloidal Particles: Fabrication and Characterization. *Langmuir* **2005**, *21*, 2963–2970. DOI: 10.1021/la0472394.

[161] Thodikayil, A. T.; Sharma, S.; Saha, S. Engineering Carbohydrate-Based Particles for Biomedical Applications: Strategies to Construct and Modify. *ACS Appl. Bio Mater.* **2021**, *4*, 2907–2940. DOI: 10.1021/acsabm.0c01656.

[162] Sarkar, M.; Upadhyay, A.; Pandey, D.; Sarkar, C.; Saha, S. *Cellulose-Based Biodegradable Polymers: Synthesis, Properties, and Their Applications*. In Saha, S., Sarkar; C., Eds.; Singapore: Springer Nature, 2023; pp 89–114.

[163] Thodikayil, A. T.; Sarkar, C.; Saha. S *Carbohydrate-Based Biodegradable Polymers for Biomedical Applications*. In Saha, S.; Sarkar, C., Eds, Singapore: Springer Nature, 2023; pp 69–88.

[164] Nypelö, T. E.; Carrillo, C. A.; Rojas, O. J. Lignin Supracolloids Synthesized from (W/O) Microemulsions: Use in the Interfacial Stabilization of Pickering Systems and Organic Carriers for Silver Metal. *Soft Matter.* **2015**, *11*, 2046–2054. DOI: 10.1039/c4sm02851a.

[165] Moustafa, M.; Abu-Saied, M. A.; Taha, T.; Elnouby, M.; El-Shafeey, M.; Alshehri, A. G.; Alamri, S.; Shati, A.; Alrumman, S.; Alghamdii, H.; Al-Khatani, M. Chitosan Functionalized AgNPs for Efficient Removal of Imidacloprid Pesticide through a Pressure-Free Design. *Int. J. Biol. Macromol.* **2021**, *168*, 116–123. DOI: 10.1016/j.ijbiomac.2020.12.055.

[166] Dong, Z.; Zhang, F.; Wang, D.; Liu, X.; Jin, J. Polydopamine-Mediated Surface-Functionalization of Graphene Oxide for Heavy Metal Ions Removal. *J. Solid State Chem.* **2015**, *224*, 88–93. DOI: 10.1016/j.jssc.2014.06.030.

[167] Zhu, C.; Zhang, X.; Zhang, Y.; Li, Y.; Wang, P.; Jia, Y.; Liu, J. Ultrasonic-Assisted Synthesis of CdS/Microcrystalline Cellulose Nanocomposites With Enhanced Visible-Light-Driven Photocatalytic Degradation of MB and the Corresponding Mechanism Study. *Front. Chem.* **2022**, *10*, 892680. DOI: 10.3389/fchem.2022.892680.

[168] Angaru, G. K. R.; Choi, Y. L.; Lingamdinne, L. P.; Choi, J. S.; Kim, D. S.; Koduru, J. R.; Yang, J. K.; Chang, Y. Y. Facile Synthesis of Economical Feasible Fly Ash–Based Zeolite–Supported Nano Zerovalent Iron and Nickel Bimetallic Composite for the Potential Removal of Heavy Metals from Industrial Effluents. *Chemosphere* **2021**, *267*, 128889. DOI: 10.1016/j.chemosphere.2020.128889.

[169] Karunaratne, T. N.; Nayanathara, R. M. O.; Navarathna, C. M.; Rodrigo, P. M.; Thirumalai, R. V. K. G.; Pittman, C. U.; Kim, Y.; Mlsna, T.; Zhang, J.; Zhang, X. Pyrolytic Synthesis of Graphene-Encapsulated Zero-Valent Iron Nanoparticles Supported on Biochar for Heavy Metal Removal. *Biochar*. **2022**, *4*, 70. DOI: 10.1007/s42773-022-00196-5.

[170] Angaru, G. K. R.; Lingamdinne, L. P.; Choi, Y. L.; Koduru, J. R.; Yang, J. K.; Chang, Y. Y. Encapsulated Zerovalent Iron/Nickel-Fly Ash Zeolite Foam for Treating Industrial Wastewater Contaminated by Heavy Metals. *Mater. Today Chem.* **2021**, *22*, 100577. DOI: 10.1016/j.mtchem.2021.100577.

[171] Liu, H.; Song, C.; Zhang, L.; Zhang, J.; Wang, H.; Wilkinson, D. P. A Review of Anode Catalysis in the Direct Methanol Fuel Cell. *J. Power Sourc.* **2006**, *155*, 95–110. DOI: 10.1016/j.jpowsour.2006.01.030.

[172] Baek, W.; Chang, H.; Bootharaju, M. S.; Kim, J. H.; Park, S.; Hyeon, T. Recent Advances and Prospects in Colloidal Nanomaterials. *J. American Chemical Society Au* **2021**, *1*, 1849–1859. DOI: 10.1021/jacsau.1c00339.

[173] Aziz, F.; Achaby, M. E.; Lissaneddine, A.; Aziz, K.; Ouazzani, N.; Mamouni, R.; Mandi, L. Composites with Alginate Beads: A Novel Design of Nano-Adsorbents Impregnation for Large-Scale Continuous Flow Wastewater Treatment Pilots. *Saudi J. Biol. Sci.* **2020**, *27*, 2499–2508. DOI: 10.1016/j.sjbs.2019.11.019.

[174] Ng, W. M.; Lim, J. K. Complex Interplay between Colloidal Stability, Transport, Chemical Reactivity and Magnetic Separability of Polyelectrolyte-Functionalized Nanoscale Zero-Valent Iron Particles (nZVI) toward Their Environmental Engineering Application. *Colloid Interf. Sci. Commun.* **2022**, *46*, 100582. DOI: 10.1016/j.colcom.2021.100582.

[175] Kumari, B.; Dutta, S. Integrating Starch Encapsulated Nanoscale Zero-Valent Iron for Better Chromium Removal Performance. *J. Water Process Eng.* **2020**, *37*, 101370. DOI: 10.1016/j.jwpe.2020.101370.

[176] Low, K. P.; Ng, W. M.; Leong, S. S.; Toh, P. Y.; Lim, J. K.; Ng, Q. H.; Lim, C. H.; Teoh, Y. P. Colloidal Stability of Polyelectrolyte-Functionalized Magnetic Nanoparticles: Experimental and Theoretical Studies. *J. Nanopart. Res.* **2024**, *26*,

[177] Sun, Y.; Lei, C.; Khan, E.; Chen, S. S.; Tsang, D. C. W.; Ok, Y. S.; Lin, D.; Feng, Y.; Dong Li, X. Nanoscale Zero-Valent Iron for Metal/Metalloid Removal from Model Hydraulic Fracturing Wastewater. *Chemosphere* **2017**, *176*, 315–323. DOI: 10.1016/j.chemosphere.2017.02.119.

[178] Adusei-Gyamfi, J.; Acha, V. Carriers for Nano Zerovalent Iron (nZVI): Synthesis, Application and Efficiency. *RSC Adv.* **2016**, *6*, 91025–91044. DOI: 10.1039/C6RA16657A.

[179] Gong, Y.; Liu, Y.; Xiong, Z.; Kaback, D.; Zhao, D. Immobilization of Mercury in Field Soil and Sediment Using Carboxymethyl Cellulose Stabilized Iron Sulfide Nanoparticles. *Nanotechnology* **2012**, *23*, 294007. DOI: 10.1088/0957-4484/23/29/294007.

[180] Kim, E. J.; Kim, J. H.; Azad, A. M.; Chang, Y. S. Facile Synthesis and Characterization of Fe/FeS Nanoparticles for Environmental Applications. *ACS Appl. Mater. Interf.* **2011**, *3*, 1457–1462. DOI: 10.1021/am200016v.

[181] Verma, M.; Sarkar, C.; Saha, S. *Surface Modification of Biodegradable Polymers, Materials Horizons: From Nature to Nanomaterials*. In Saha S.; Sarkar C., Eds.; Singapore: Springer Nature, 2023; pp 49–68.

[182] Panda, G.; Sarkar, C.; Saha, S. *Processing of Biodegradable Polymers, Materials Horizons: From Nature to Nanomaterials*. In Saha S.; Sarkar C., Eds.; Singapore: Springer Nature, 2023; pp 27–47.

[183] Berger, S.; Synytska, A.; Ionov, L.; Eichhorn, K. J.; Stamm, M. Stimuli-Responsive Bicomponent Polymer Janus Particles by 'Grafting From'/"Grafting to" Approaches. *Macromolecules* **2008**, *41*, 9669–9676. DOI: 10.1021/ma802089h.

[184] Li, Z.; Fan, Q.; Yin, Y. Colloidal Self-Assembly Approaches to Smart Nanostructured Materials. *Chem. Rev.* **2022**, *122*, 4976–5067. DOI: 10.1021/acs.chemrev.1c00482.

[185] Huang, X.; Liu, W.; Zheng, Z.; Zhang, Y.; Zhao, X.; Li, Z.; Gao, W.; Xie, P.; Pan, Y.; Sun, Q. Efficient Construction of Self-Assembled Starch Colloidosomes for Controlled-Release of Pesticides. *Colloid. Surface. A: Physicochem. Engng. Aspect.* **2024**, *702*, 135107. DOI: 10.1016/j.colsurfa.2024.135107.

[186] Gao, W.; Pei, A.; Feng, X.; Hennessy, C.; Wang, J. Organized Self-Assembly of Janus Micromotors with Hydrophobic Hemispheres. *J. Am. Chem. Soc.* **2013**, *135*, 998–1001. DOI: 10.1021/ja311455k.

[187] Cho, Y. S.; Kim, S. H.; Yi, G. R.; Yang, S. M. Self-Organization of Colloidal Nanospheres Inside Emulsion Droplets: Higher-Order Clusters, Supraparticles, and Supraballs. *Colloid. Surf. A: Physicochem. Engng. Aspect.* **2009**, *345*, 237–245. DOI: 10.1016/j.colsurfa.2009.05.014.

[188] Barry, E.; Dogic, Z. Entropy Driven Self-Assembly of Nonamphiphilic Colloidal Membranes. *Proc. Natl. Acad. Sci. USA.* **2010**, *107*, 10348–10353. DOI: 10.1073/pnas.1000406107.

[189] Oakes, P. W.; Viamontes, J.; Tang, J. X. Growth of Tactoidal Droplets during the First-Order Isotropic to Nematic Phase Transition of F-Actin. *Phys. Rev. E.* **2007**, *75*, 061902. DOI: 10.1103/PhysRevE.75.061902.

[190] Hu, L.; Zhou, S.; Zhang, X.; Shi, C.; Zhang, Y.; Chen, X. Self-Assembly of Polymers and Their Applications in the Fields of Biomedicine and Materials. *Polymers (Basel).* **2024**, *16*, 2097. DOI: 10.3390/polym16152097.

[191] Sacanna, S.; Korpics, M.; Rodriguez, K.; Colón-Meléndez, L.; Kim, S. H.; Pine, D. J.; Yi, G. R. Shaping Colloids for Self-Assembly. *Nat. Commun.* **2013**, *4*, 1688. DOI: 10.1038/ncomms2694.

[192] Gangwar, N.; Gangwar, C.; Sarkar, J. A Review on Template-Assisted Approaches & Self Assembly of Nanomaterials at Liquid/Liquid Interface. *Heliyon* **2024**, *10*, e36810. DOI: 10.1016/j.heliyon.2024.e36810.

[193] Zhang, J.; Luijten, E.; Granick, S. Toward Design Rules of Directional Janus Colloidal Assembly. *Annu. Rev. Phys. Chem.*

2015, *66*, 581–600. DOI: 10.1146/annurev-physchem-040214-121241.

[194] Tang, S. Y.; Shridharan, P.; Sivakumar, M. Impact of Process Parameters in the Generation of Novel Aspirin Nanoemulsions—Comparative Studies between Ultrasound Cavitation and Microfluidizer. *Ultrason. Sonochem.* **2013**, *20*, 485–497. DOI: 10.1016/j.ultsonch.2012.04.005.

[195] Bai, L.; McClements, D. J. Development of Microfluidization Methods for Efficient Production of Concentrated Nanoemulsions: Comparison of Single- and Dual-Channel Microfluidizers. *J. Colloid Interface Sci.* **2016**, *466*, 206–212. DOI: 10.1016/j.jcis.2015.12.039.

[196] Yazdian Kashani, S.; Afzalian, A.; Shirinichi, F.; Keshavarz Moraveji, M. Microfluidics for Core–Shell Drug Carrier Particles: A Review. *RSC Adv.* **2020**, *11*, 229–249. DOI: 10.1039/d0ra08607j.

[197] Nguyen, P. P. T.; An, S.; Jeong, H. H. Microfluidic Formation of Biodegradable PCLDA Microparticles as Sustainable Sorbents for Treatment of Organic Contaminants in Wastewater. *Colloid. Surf. A Physicochem. Engng. Aspect.* **2023**, *656*, 130409. DOI: 10.1016/j.colsurfa.2022.130409.

[198] Othman, R.; Vladisavljević, G. T.; Nagy, Z. K. Preparation of Biodegradable Polymeric Nanoparticles for Pharmaceutical Applications Using Glass Capillary Microfluidics. *Chem. Eng. Sci.* **2015**, *137*, 119–130. DOI: 10.1016/j.ces.2015.06.025.

[199] Lobo, L.; Svereika, A. Coalescence during Emulsification: 2. Role of Small Molecule Surfactants. *J. Colloid Interf. Sci.* **2003**, *261*, 498–507. DOI: 10.1016/S0021-9797(03)00069-9.

[200] Olson, D. W.; White, C. H.; Richter, R. L. Effect of Pressure and Fat Content on Particle Sizes in Microfluidized Milk. *J. Dairy Sci.* **2004**, *87*, 3217–3223. DOI: 10.3168/jds.S0022-0302(04)73457-8.

[201] Jin, S.; Wei, X.; Ren, J.; Jiang, Z.; Abell, C.; Yu, Z. Construction of Core–Shell Microcapsules via Focused Surface Acoustic Wave Microfluidics. *Lab Chip.* **2020**, *20*, 3104–3108. DOI: 10.1039/d0lc00123f.

[202] Lewis, C. L.; Lin, Y.; Yang, C.; Manocchi, A. K.; Yuet, K. P.; Doyle, P. S.; Yi, H. Microfluidic Fabrication of Hydrogel Microparticles Containing Functionalized Viral Nanotemplates. *Langmuir* **2010**, *26*, 13436–13441. DOI: 10.1021/la102446n.

[203] Chen, M.; Bolognesi, G.; Begum, R.; Farooqi, Z. H.; Vladisavljević, G. T. Monodispersed Biodegradable Microparticles with Wrinkled Surface Coated with Silver Nanoparticles for Catalytic Degradation of Organic Toxins. *Emergent Mater.* **2025**, *8*, 1199–1211. DOI: 10.1007/s42247-024-00637-w.

[204] Bhaskar, S.; Pollock, K. M.; Yoshida, M.; Lahann, J. Towards Designer Microparticles: Simultaneous Control of Anisotropv, Shape and Size. *Small* **2010**, *6*, 404–411. DOI: 10.1002/smll.200901306.

[205] Pan, Y.; Zeng, L. Simulation and Validation of Droplet Generation Process for Revealing Three Design Constraints in Electrohydrodynamic Jet Printing. *Micromachines (Basel).* **2019**, *10*, 94. DOI: 10.3390/mi10020094.

[206] Kamal, W.; Li, M.; Sykes, T. C.; Castrejón-Pita, A. A.; Elston, S. J.; Morris, S. M. Drop-on-Demand Electrohydrodynamic Printing of Nematic Liquid Crystals. *Adv. Eng. Mater.* **2024**, *26*, 2400245. DOI: 10.1002/adem.202400245.

[207] Pandey, K.; Saha, S. Stabilization of Iron (0) in Plasma Treated Semi Porous Polylactic Acid Based Particles for In Situ Groundwater Remediation. *J. Environ. Chem. Eng.* **2023**, *11*, 110493. DOI: 10.1016/j.jece.2023.110493.

[208] Ifra, A.; Thattaru, T.; Saha, S. Compositionally Anisotropic Colloidal Surfactant Decorated with Dual Metallic Nanoparticles as a Pickering Emulsion Stabilizer and Their Application in Catalysis. *ACS Appl. Mater. Interf.* **2022**, *14*, 23436–23451. DOI: 10.1021/acsami.2c03255.

[209] Ifra, A.; Singh; Sampa, S. High Adsorption of α-Glucosidase on Polymer Brush-Modified Anisotropic Particles Acquired by Electrospraying: A Combined Experimental and Simulation Study. *ACS Appl. Bio. Mater.* **2021**, *4*, 7431–7444. DOI: 10.1021/acsabm.1c00682.

[210] Bhaskar, S.; Lahann, J. Microstructured Materials Based on Multicompartmental Fibers. *J. Am. Chem. Soc.* **2009**, *131*, 6650–6651. DOI: 10.1021/ja900354b.

[211] Lahann, J. Recent Progress in Nano-biotechnology: Compartmentalized Micro- and Nanoparticles via Electrohydrodynamic Co-Jetting. *Small* **2011**, *7*, 1149–1156. DOI: 10.1002/smll.201002002.

[212] Pandey, K.; Saha, S. Microencapsulated Zero Valent Iron NanoParticles in Polylactic Acid Matrix for in Situ Remediation of Contaminated Water. *J. Environ. Chem. Engng.* **2020**, *8*, 103909. DOI: 10.1016/j.jece.2020.103909.

[213] Hoch, L. B.; Mack, E. J.; Hydutsky, B. W.; Hershman, J. M.; Skluzacek, J. M.; Mallouk, T. E. Carbothermal Synthesis of Carbon-Supported Nanoscale Zero-Valent Iron Particles for the Remediation of Hexavalent Chromium. *Environ. Sci. Technol.* **2008**, *42*, 2600–2605. DOI: 10.1021/es702589u.

[214] Eljamal, R.; Eljamal, O.; Maamoun, I.; Yilmaz, G.; Sugihara, Y. Enhancing the Characteristics and Reactivity of nZVI: Polymers Effect and Mechanisms. *J. Mol. Liq.* **2020**, *315*, 113714. DOI: 10.1016/j.molliq.2020.113714.

[215] Joo, S. H.; Zhao, D. Destruction of Lindane and Atrazine Using Stabilized Iron Nanoparticles under Aerobic and Anaerobic Conditions: Effects of Catalyst and Stabilizer. *Chemosphere* **2008**, *70*, 418–425. DOI: 10.1016/j.chemosphere.2007.06.070.

[216] He, F.; Zhao, D.; Paul, C. Field Assessment of Carboxymethyl Cellulose Stabilized Iron Nanoparticles for In Situ Destruction of Chlorinated Solvents in Source Zones. *Water Res.* **2010**, *44*, 2360–2370. DOI: 10.1016/j.watres.2009.12.041.

[217] Chan, H.; Shi, C.; Wu, Z.; Sun, S.; Zhang, S.; Yu, Z.; He, M.; Chen, G.; Wan, X.; Tian, J. Superhydrophilic Three-Dimensional Porous Spent Coffee Ground Reduced Palladium Nanoparticles for Efficient Catalytic Reduction. *J. Colloid Interf. Sci.* **2022**, *608*, 1414–1421. DOI: 10.1016/j.jcis.2021.10.028.

[218] Rastogi, L.; Ankam, D. P.; Dash, K. Intrinsic Peroxidase-like Activity of 4-Amino Hippuric Acid Reduced/Stabilized Gold Nanoparticles and Its Application in the Selective Determination of Mercury and Iron in Ground Water. *Spectrochim. Acta. A Mol. Biomol. Spectrosc.* **2020**, *228*, 117805. DOI: 10.1016/j.saa.2019.117805.

[219] He, F.; Zhao, D.; Liu, J.; Roberts, C. B. Stabilization of Fe - Pd Nanoparticles with Sodium Carboxymethyl Cellulose for Enhanced Transport and Dechlorination of Trichloroethylene in Soil and Groundwater. *Ind. Eng. Chem. Res.* **2007**, *46*, 29–34. DOI: 10.1021/ie0610896.

[220] He, F.; Zhao, D. Preparation and Characterization of a New Class of Starch-Stabilized Bimetallic Nanoparticles for Degradation of Chlorinated Hydrocarbons in Water. *Environ. Sci. Technol.* **2005**, *39*, 3314–3320. DOI: 10.1021/es048743y.

[221] Qiao, J.; Zhao, Z.; Zhou, Z.; Wu, D. Enhanced Hydrodechlorination of 4-Chlorophenol through Carboxymethylcellulose-Modified Pd/Fe Nanosuspension Synthesized by One-Step Methods. *Chemosphere* **2024**, *356*, 141857. DOI: 10.1016/j.chemosphere.2024.141857.

[222] Kopinke, F. D.; Sühnholz, S.; Georgi, A.; Mackenzie, K. Interaction of Zero-Valent Iron and Carbonaceous Materials for Reduction of DDT. *Chemosphere* **2020**, *253*, 126712. DOI: 10.1016/j.chemosphere.2020.126712.

[223] Sunkara, B.; Zhan, J.; He, J.; McPherson, G. L.; Piringer, G.; John, V. T. Nanoscale Zerovalent Iron Supported on Uniform Carbon Microspheres for the In Situ Remediation of Chlorinated Hydrocarbons. *ACS Appl. Mater. Interf.* **2010**, *2*, 2854–2862. DOI: 10.1021/am1005282.

[224] Guan, X.; Kong, L.; Liu, C.; Fan, D.; Anger, B.; Johnson, W. P.; Lowry, G. V.; Li, G.; Danko, A.; Liu, X. Polymer Coatings Affect Transport and Remobilization of Colloidal Activated Carbon in Saturated Sand Columns: Implications for

In Situ Groundwater Remediation. *Environ. Sci. Technol.* **2024**, *58*, 8531–8541. DOI: 10.1021/acs.est.3c08251.

[225] Saya, L.; Gautam, D.; Malik, V.; Singh, W. R.; Hooda, S. Natural Polysaccharide Based Graphene Oxide Nanocomposites for Removal of Dyes from Wastewater: A Review. *J. Chem. Eng. Data.* **2021**, *66*, 11–37. DOI: 10.1021/acs.jced.0c00743.

[226] Kumar, A.; Park, B. J.; Tu, F.; Lee, D. Amphiphilic Janus Particles at Fluid Interfaces. *Soft Matter* **2013**, *9*, 6604–6617. DOI: 10.1039/c3sm50239b.

[227] Su, H.; Hurd Price, C. A.; Jing, L.; Tian, Q.; Liu, J.; Qian, K. Janus Particles: Design, Preparation, and Biomedical Applications. *Mater. Today. Bio.* **2019**, *4*, 100033. DOI: 10.1016/j.mtbio.2019.100033.

[228] Glaser, N.; Adams, D. J.; Böker, A.; Krausch, G. Janus Particles at Liquid-Liquid Interfaces. *Langmuir* **2006**, *22*, 5227–5229. DOI: 10.1021/la060693i.

[229] Pandey, K.; Verma, D. K.; Singh, A.; Saha, S. Architecture Dependent Transport Behavior of Iron (0) Entrapped Biodegradable Polymeric Particles for Groundwater Remediation. *Chemosphere* **2024**, *357*, 141892. DOI: 10.1016/j.chemosphere.2024.141892.

[230] Bezbaruah, A.; Talal, B. A.; Michael, Q.; Eakalak, K. Calcium-Alginate Entrapped Nanoscale Zero-Valent Iron (nZVI). WO2014168728A1, 2014.

[231] Hoag, G. E.; Collins, J. B.; Varma, R. S.; Mallikarjuna, N. N. U.S. Patent Application for Polymer Coated Nanoparticle Activation of Oxidants for Remediation and Methods of Use Thereof. US7963720B2, 2011.

[232] Zhao, D.; Feng, H. Preparation and Applications of Stabilized Metal Nanoparticles for Dechlorination of Chlorinated Hydrocarbons in Soils, Sediments, and Ground Water. US7887880B2, 2011.

[233] Vijay, J.; Noshir, P.; Gerhard, P.; Zhan, J.; Gary, M. Novel Multifunctional Materials for In-Situ Environmental Remediation of Chlorinated Hydrocarbons. US20130058724A3, 2011.